Douglas Partners
Geotechnics • Environment • Groundwater

Douglas Partners Pty Ltd
ABN 75 053 980 117
96 Hermitage Road
West Ryde NSW 2114
Australia

PO Box 472
West Ryde NSW 1685
Phone (02) 9809 0666
Fax (02) 9809 4095
www.douglaspartners.com.au

MJT:jlb
Project 71235
25 June 2009

BPPL
c/ - TLB Engineers
514 Miller Street
CAMMERAY NSW 2062

Attention: Mr Howard Bersten

email: howard@tlbengineers.com

Dear Sirs

MARINA AT BREAKFAST POINT
CONSOLIDATION SETTLEMENT AND WATER FLOW

1. INTRODUCTION

Following your instructions we have carried out an estimate on the likely consolidation settlement of sediments around the proposed marina and the amount of water that would be expelled from the sediments due to construction of an erosion blanket. We have based our estimates of settlement and water flow on soil classifications given in the URS report which provides generalised descriptions of the bay sediments and some notional engineering properties, probably based upon their engineering experience. Consequently, the estimates outlined below must be considered as approximate only as they have been calculated using parameters derived from experience with similar materials to those described by URS.

2. SOIL CONDITIONS

In carrying out this evaluation Douglas Partners has used the information provided in a report titled '*Environmental Risk Assessment for Sediments Adjacent to the former AGL Mortlake site*' prepared by URS dated 31 May 2006. The report contained a generalised sediment stratigraphy as summarised below.

Table 1 – Sediment Stratigraphy

Depth (m)	Lithology
0.0 – 0.02	Surficial sediments comprising brown green mud with broken shell material
0.02 – 0.1	Grey green estuarine mud
0.1 – 1.5	Black to olive grey marine mud, very soft with traces of fine grained sand
> 1.5	Grey to orange sandy clay, firm with fine sand and dispersed shells

In carrying out our assessment we have assumed that the upper 100 mm of very soft sediments would probably be disturbed during the placement of the Elcomax 1200 geotextile and the 300 mm thick basalt confining layer. This is based on our experience that it is very difficult to

obtain competent samples of this material in any estuarine environment because the material behaves as a high viscosity fluid.

3. ESTIMATED SETTLEMENT AND WATER FLOW

The estimated settlement due to the design load of 3.2 kPa is 5 mm for the firm clay layer which extends to a depth of 1.5 m below river bed level. This is calculated to result in drainage upwards of the interstitial fluids of about 3 L/m^2. It is also calculated that this drainage will occur within a period of about 5 months using an estimated permeability of 1 x 10^{-7} m/sec and a coefficient of consolidation of 4 m^2 / year. Given that the construction period is expected to be of the order of 12 months the displacement of any interstitial fluid should occur within the construction period.

In carrying out the analysis we have ignored the sediments below a depth of 1.5 m. These sediments, based upon the descriptions provided by URS, are much stiffer than the upper sediments and therefore their contribution (if they were to consolidate slightly under the load) is probably negligible compared to the very soft sediments to depths of 1.5 m.

We trust that the above is of assistance but if you have any further questions please contact Fiona MacGregor.

Yours faithfully
DOUGLAS PARTNERS PTY LTD

Reviewed by

Michael J Thom
Principal

Fiona MacGregor
Principal

PlasticsEurope
Association of Plastics Manufacturers

Clarification of Viscosity Measurements of PET

Intrinsic Viscosity and Viscosity number

Both intrinsic viscosity (IV) and viscosity number (VN) measure the viscosity of a polymeric solution. VN is also referred to as coefficient of viscosity (CV). Both IV and VN are related to the average number molecular weight of the polymer.

The polymeric solution is prepared by dissolving the PET polymer in one of several solvents; most commonly a 50/50 by weight mixture of phenol and 1,2-dichlorobenzene is used for PET. The viscosity is determined at constant temperature, usually 25°C.

The Intrinsic Viscosity, usually expressed in dl/g, is defined as:

$$IV = \lim_{c \to 0} \frac{\eta - \eta_0}{c * \eta_0}$$

where:

c concentration of the polymeric solution (in g/dl)

η viscosity of the solution at concentration c

η_0 viscosity of the solvent

Instead of using the definition, for simplicity's sake IV is more commonly determined with the approximate Billmeyer equation:

$$IV = \frac{\eta_{rel} - 1 + 3 * \ln(\eta_{rel})}{4 * c}$$

where:

c concentration of the polymeric solution (in g/dl); usually, a concentration of 0.5 g/dl (i.e., 0.005 g/ml) is used

η_{rel} relative viscosity = t/t_0

t flow time of the solution at concentration c

t_0 flow time of the solvent

The Viscosity Number however, usually expressed in ml/g, is defined as:

$$VN = \frac{t - t_0}{t_0 * c}$$

where:

PlasticsEurope AISBL
Avenue E. Van Nieuwenhuyse 4/3 - B -1160 Brussels - Belgium
Tel (32-2) 675 32 97 - Fax (32-2) 675 39 35
VAT BE 416 155 338 – www.plasticseurope.org

c concentration of the polymeric solution (in g/ml); the International Standard ISO 1628-5 recommends that the concentration should be approximately 0.005 g/ml.
t flow time of the solution at concentration c
t_0 flow time of the solvent

As stated previously the Viscosity Number is identical to the Coefficient of Viscosity.

Whether determining IV by the Billmeyer equation or measuring VN , the flow time of the polymeric solution and of the solvent is measured in an Ubbelhode viscometer (see figure); the thermostatic bath is set at 25°C. The flow time is measured starting when the meniscus passes the initial tally and ending when it reaches the final tally.
While automatic viscometers are generally used, their operational principle is similar to that of the manual viscometer that is shown in the figure.

According to ASTM D2515, D446
Capillary III, diameter 1.83 mm

1	Loading pipe
2	Aspiration
3	Vent
4	Drain
A	Tank for solution
B	Measuring bubble
C	Protection bubble
D	Initial tally
E	Final tally
F	Thermostatic bath

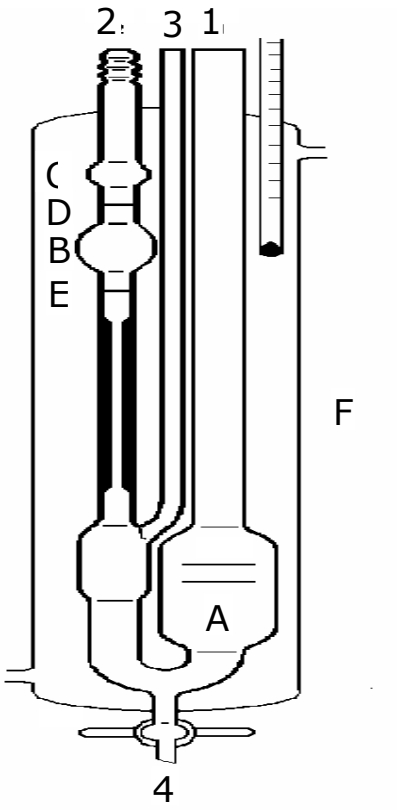

Within Plastics*Europe*, we determined an empirical correlation between IV determined via the Billmeyer equation and VN, as follows for PET:

$$VN = 133.446 * IV - 14.290$$

The following graph shows the trend of VN versus IV for PET, as calculated from this empirical correlation.

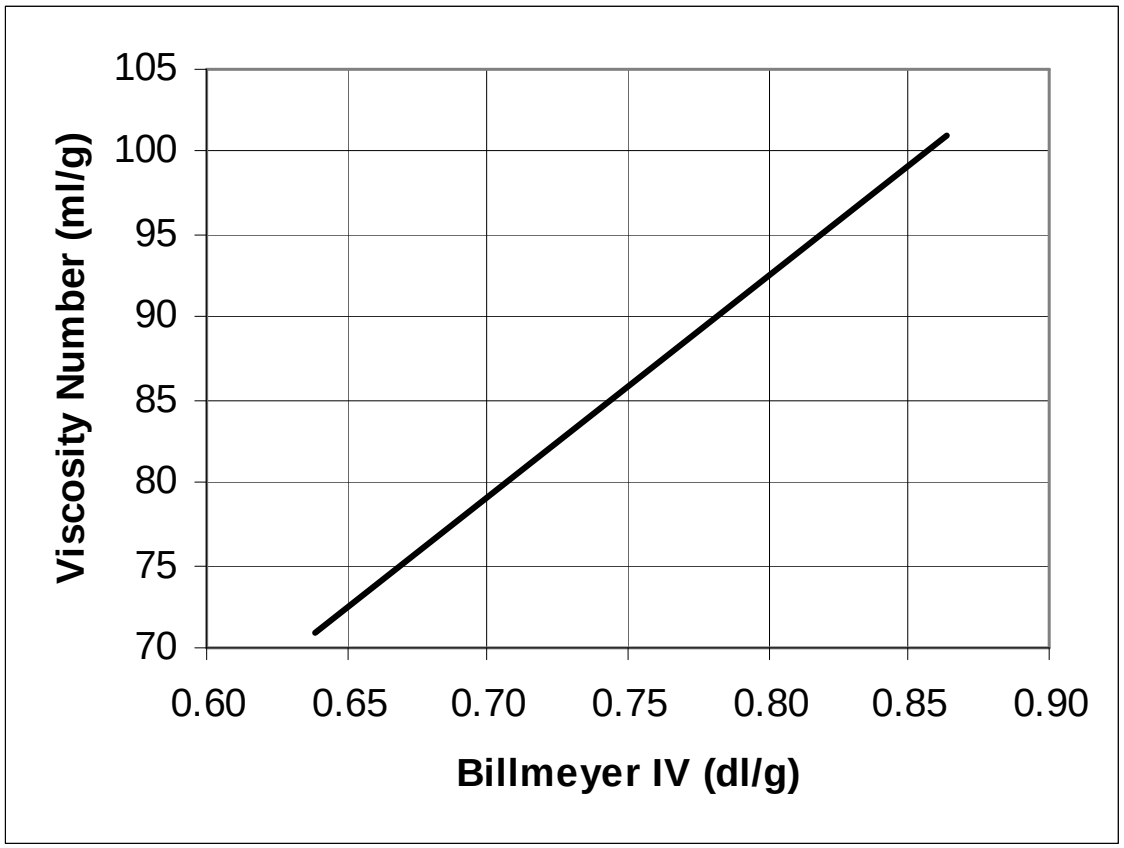

22nd March 2007

Case Study

Coastal

Project: Nerang River Training Walls - Filtration
Date: April 1984 – May 1986
Client: Gold Coast City Council
Location: Surfers Paradise, Queensland

Geofabrics AUSTRALASIA PTY LTD

ELCOMAX® staple fibre geotextile

The Nerang River Training wall project was the first time **Australian made** thick nonwoven needlepunched geotextiles (**ELCOMAX**®) was installed on the Australian continent. Over 75000 m^2 of **ELCOMAX® 1200R** was used to replace a granular filter layer in a hostile marine environment. 2.5 to 5.0 tonne armour rock was placed directly onto the geotextile, which needed to be sufficiently robust to resist damage thereby ensuring long-term filter stability.

Training walls under construction 1985

Today after 17 years service the Nerang River Training Walls, having withstood the extremes of the South Pacific and are a testament to the effectiveness and durability of thick **ELCOMAX®** nonwoven staple fibre geotextiles.

www.geofabrics.com.au

MELBOURNE (03) 8586 9111 Fax: (03) 8586 9186 | SYDNEY (02) 9821 3277 Fax: (02) 9821 3670 | BRISBANE (07) 3279 1588 Fax: (07) 3279 1589 | PERTH (08) 9309 4388 Fax: (08) 9309 4389 | ADELAIDE (08) 8293 3613 Fax: (08) 8293 1306 | NEWCASTLE (02) 4950 5845 Fax: (02) 4950 5895 | HOBART (03) 6273 0511 Fax: (03) 6273 0686 | TOWNSVILLE (07) 4774 8222 Fax: (07) 4774 8655

Technical Enquiries: 1800 4 BIDIM (1800 424 346)

Coastal

Case Study

Project: Filtration – Port Kembla Seawall
Date: 1979/1980
Client: NSW Government
Location: Port Kembla, New South Wales

Geofabrics AUSTRALASIA PTY LTD

ELCOMAX® STAPLE FIBRE GEOTEXTILES

In 1977 the NSW Government decided to construct a new coal loader at Port Kembla near Wollongong. In order to provide additional land for coal stockpiles it was necessary to construct a 1200m long seawall and reclaim the land behind the wall.

The seawall would form an integral part of the new coal loader, containing a roadway and rail mounted stackers servicing half of the total stockpile area. Failure of the seawall would not only lead to extensive damage to the facility, but more importantly, reduce the coal export capacity of the facility.

Hanbars & Rock placed directly on ELCOMAX® geotextile

Installation of ELCOMAX® 1200R

The seawall was constructed within the surf zone, which posed some construction and quality control problems. A unique feature of the design was the use of ELCO**MAX® 1200R & 2000R nonwoven staple fibre geotextiles**. These thick and robust geotextiles allowed 3t armour rock and 15t Hanbars to be placed directly on the geotextile, which was placed on the aggressive core material of blast furnace slag. This translated into considerable savings in material and construction time. Real dollar savings equated to nearly AUD$750,000, over traditional granular filter techniques.

The performance of the ELCO**MAX®** geotextiles in this critical and aggressive application has been impressive, without maintenance, and is now used as a benchmark for subsequent seawall contracts.

www.geofabrics.com.au

MELBOURNE	SYDNEY	BRISBANE	PERTH	ADELAIDE	NEWCASTLE	HOBART	TOWNSVILLE
(03) 8586 9111	(02) 9821 3277	(07) 3279 1588	(08) 9309 4388	(08) 8293 3613	(02) 4950 5845	(03) 6273 0511	(07) 4774 8222
Fax: (03) 8586 9186	Fax: (02) 9821 3670	Fax: (07) 3279 1589	Fax: (08) 9309 4389	Fax: (08) 8293 1306	Fax: (02) 4950 5895	Fax: (03) 6273 0686	Fax: (07) 4774 8655

Technical Enquiries: 1800 4 BIDIM (1800 424 346)

Coastal

Case Study

Project: Filtration Geotextiles – Port of Brisbane
Date: 2004
Client: Port of Brisbane
Location: Fisherman Island, Brisbane

Geofabrics AUSTRALASIA PTY LTD

ELCOMAX® STAPLE FIBRE GEOTEXTILE

Construction of the 4.6km Future Port Expansion (FPE) Seawall off Fisherman Islands is one of the major coastal construction projects in Australia. The alliance contract allowed a number of specialist companies to become actively involved in the search for innovative and practical solutions to many of the complex problems encountered on the Port of Brisbane site.

Soil Filters Australia Pty Ltd attended the contract announcement meeting and thereafter was instrumental in offering the client a number of geosynthetic-related options/solutions at a very early stage of the investigation/design process. The company's pedigree as the oldest geotextile manufacturer in Australia, with products engineered specifically for coastal and marine applications, made its input into the design of the geotextile filtration layer invaluable.

The company provided technical support based on experience on similar projects such as the Nerang River training walls and the Port Kembla sea wall, while providing both standard and customised, ELCO**MAX**® non-woven staple geotextiles for site-specific testing. The quality assurance plan, which forms part of the company's ISO 9001:2000 certification, submitted as part of the tender process, gave the client confidence in the consistency and quality of the product proposed.

The final construction methodology required the fabrication of large panels of geotextile. This fabrication was carried out in Soil Filters' purpose-built 2,000m^2, sewing and fabrication department. Extensive testing of the seam strengths and pullout webbing was carried out in order to optimise seam efficiencies and ensure no site failures occurred. 140 panels, each 40m x 32m (180 320m^2) ELCO**MAX**® 1200R and 40,000m^2 ELCO**MAX**® 600R have been supplied to the project to date.

The key to the successful design, manufacture and installation of the filtration geotextile on the FPE Seawall Alliance contract was the close cooperation and working relationship between client, consultant, contractor and supplier. Soil Filters Australia is proud to have been part of this prestigious project.

www.geofabrics.com.au

MELBOURNE	SYDNEY	BRISBANE	PERTH	ADELAIDE	NEWCASTLE	HOBART	TOWNSVILLE
(03) 8586 9111	(02) 9821 3277	(07) 3279 1588	(08) 9309 4388	(08) 8293 3613	(02) 4950 5845	(03) 6273 0511	(07) 4774 8222
Fax: (03) 8586 9186	Fax: (02) 9821 3670	Fax: (07) 3279 1589	Fax: (08) 9309 4389	Fax: (08) 8293 1306	Fax: (02) 4950 5895	Fax: (03) 6273 0686	Fax: (07) 4774 8655

Technical Enquiries: 1800 4 BIDIM (1800 424 346)

Geotextiles Under Rock Armour

A number of factors should be considered when designing the geotextile for this application, these are as follows:-

1. Survivability
2. Permeability
3. Abrasion resistance

1. Survivability

This is the most important criterion because if the geotextile is ruptured during the placement of the covering rock fines rapidly leach through these damaged areas, which results in slumping of the rock armour and embankment instability. In areas where high stream velocity and wave action can occur the loss of fines through the geotextile can be significant.

Trials were carried by the Port of Brisbane in April 2003, the trials were undertaken to asses the suitability of various geotextiles to be used beneath rock armouring in a bund wall. In this trial 200kg rocks were dropped onto a geotextile placed on a sandy base from 1.5 and 3m. Initially the Port of Brisbane specified a 1050g/m^2 product but we felt that a 1200g/m^2 product would be better and supplied the 1200g/m^2 product to show the increased survivability that can be achieved when using a the heavier product.

The test

The 1050g/m^2 product was damaged during 1.5 and 3m drops, see examples below.

1.5m Drop

3m Drop

The 1200g/m^2 product was slightly damaged during the 3m drop, see the only damage below.

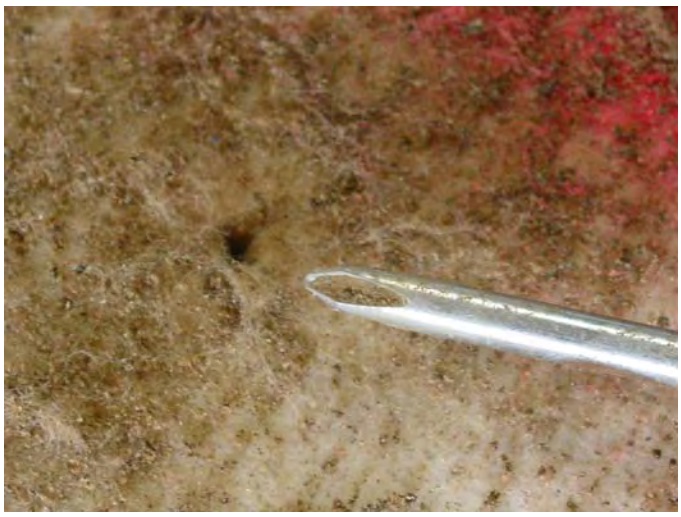

These trials convinced the Port of Brisbane to use the 1200g/m^2 product (Terrafix 1200R).

An important factor to note when designing for survivability is that strength alone is not a good indication of survivability, the combination of strength, mass and elongation determines the survivability of the geotextile. For example the survivability of high strength low elongation geotextiles were analysed during the tests above and a 800kN x 100kN product with and elongation of <15% was severely damaged during 1.5m and 3m drops.

800Kn x 100kN woven geotextile – 1.5m drop height

2. Permeability

Permeability rather than through flow of a geotextile should always be specified so that the client can be sure that the geotextile specified is compatible with the subgrade material. A rule of thumb to use is that the geotextile permeability should be 10 times greater than the soil permeability, this allows for the inevitable reduction in permeability of the geotextile due to the build up of fine material, on the interface or within the geotextile, over time.

A simple chart is available to assess the permeability of the subgrade soil based on the d_{15} of the soil.

3. Abrasion Resistance

Due to the voids that are likely to occur between 2 000kg rock, abrasion of the geotextile will be an important factor. In order to be assured of the long term stability and filtration characteristics of the geotextile the geotextile should retain at least 70% of it initial strength after having undergone an abrasion test.

The recommend abrasion test which best mimics actual field conditions is the German Rotating Drum test method, see attachment for detailed test method.

Use of geotextiles to overcome challenging conditions at the seawall project in Port of Brisbane

Ameratunga, J.
Coffey Geosciences Pty Ltd, Brisbane, Australia. ameratunga@coffey.com.au

Boyle, P.J.
Port of Brisbane Corporation, Brisbane, Australia. Peter.Boyle@portbris.com.au

Loke, K.H.
Polyfelt Asia, Kuala Lumpur, Malaysia. lokekh@polyfelt.com.my

Hornsey, W.
Soil Filters Australia Pty Ltd, Gold Coast, Australia. whornsey@soilfilters.com.au

Strevens, M.
Leighton Contractors Pty Ltd, Brisbane, Australia. Matt.Strevens@leicon.com.au

Keywords: Brisbane, geotechnical, geotextile, marine conditions, soft clay

ABSTRACT: Stage 1 of the Future Port Expansion (FPE) Project located at the Port of Brisbane, Fisherman Islands involved the design and construction of a 4.6 km long seawall. The Seawall up to 8 m high, was constructed in waters up to 6 m deep and extends 1.8 km into Moreton Bay from shore. The factors which significantly impacted its design and construction, included the weak and deep soft clay subsoil profile, potential issues related to settlement, instability and loss of materials due to seabed penetration, marine conditions, and environmental concerns due to the proximity of the sensitive Moreton Bay Marine Park. High strength geotextiles up to 850 kN/m were used to overcome stability issues related to weak marine clay at the seabed and a filtration geotextile was used to protect the sand pancake below the rock bund. Damage trials were conducted on the selected geotextiles to assess the potential for damage from rock placement and trafficking.

1 INTRODUCTION

The Port of Brisbane is located at the mouth of the Brisbane River at Fisherman Islands in Brisbane. The Port land has seen rapid development due to increased Port activities and this growth is expected to continue for the next 25 years and beyond. The Future Port Expansion (FPE) Project will provide the land to cater for the increased demand in the future.

The ultimate objective of the FPE Project is to allow the Port to reclaim and develop an additional 230 ha of port land including extending the current quayline by a further 1800 m. The reclamation will be carried out using channel maintenance dredging materials. The first stage of this process was the construction of a 4.6 km long and up to 8 m high seawall to encompass the area so that reclamation could be carried out in an environmentally friendly and controlled manner.

The client used an Alliance delivery mechanism to deliver Stage 1 of the project because of the significant geotechnical, environmental and construction risks and constraints associated with the project. These included, highly variable soft clays extending over 30 m below the seabed on the eastern wall alignment, the close proximity of the Moreton Bay Marine Park, varying water depths, wind and expected sea conditions during construction.

Preliminary designs indicated the consistency of the marine clay at seabed level to be generally too weak to support high embankments unless the ground was improved or the construction staged allowing the clay to gain some strength. Most options were not feasible due to uncertainties on the effectiveness of the method, time constraints and/or associated costs. The use of a high strength geotextile was ultimately assessed to be the most cost effective and least risk solution.

A rock embankment placed on a high strength geotextile laid on the seabed was the design adopted where the seabed is shallow (1 m below low water). However in the deeper areas (3.5 m below low water), a wide sand pancake was included in the design because of weaker subsoil conditions (see design section for East Bund in Figure 1). The rock bund forming the upper part of the seawall was then placed on this sand pancake. During construction an appropriate filtration geotextile was selected to cover and contain the sand to prevent losses from the effects of tides and waves. Damage trials were conducted on the selected geotextiles to assess whether significant damage would occur during the placement of the rock and construction trafficking above and what allowance should be made for these effects.

2 SITE CONDITIONS

Based on the published geology map of Brisbane (1:100,000 scale), the site is underlain by Quaternary marine deposits consisting of "fluvial lithofeldspathic sublabile sand and muddy sand".

The main geological formations across the project site can be summarized as Holocene deposits overlying Pleistocene deposits, which in turn overlie the Petrie Formation, which consists of basalt bedrock. The Holocene alluvial deposit consists of two sub-layers with the upper layer generally between 0 to 4 m thick, comprising mainly sands with interlayered soft clays and silts. The lower layer comprises very soft to firm compressible clay generally normally consolidated from about 3 m depth below the seabed.

Along the East Bund, the soft clay at shallow depth is weak, having undrained shear strength values of 3 to 5 kPa, increasing towards the shoreline. The thickness of the layer varies from about 8 m to 30 m along the alignment.

3 GEOTEXTILE DAMAGE TRIALS

At the initial stages of the design, risk assessments were carried out. Damage to high strength geotextiles during rock placement and trafficking was identified as a significant hazard. However, it was recognized that downrating the basal geotextile strength, was an acceptable way to treat such issues in the design. Theoretical formulae were available to assess the requirements of a geotextile but not to assess the damage factors. There were also no documented experiences on damage due to trafficking on rock placed on a geotextile. Also of great concern was the potential for damage of the filtration fabric, because of the potential consequences if sand was sucked out by the tides leading to collapse of the rockwall above and consequent major failures.

From the outset it was decided to carry out a set of field trials to assess these effects using typical rockcore and armour materials to be used on the project.

3.1 *Basal High Strength Geotextile*

Although trials were conducted on several products only the trials conducted on the materials of the successful tenderer are discussed in this paper. The geotextiles tested were Maccaferri Rock WX200 (200 kN/m) & WX800 (800 kN/m) manufactured by Polyfelt Asia and supplied via Maccaferri Brisbane.

The trials were conducted in one of the reclamation paddocks filled with dredged mud capped off with a 2 m thick sand base. Dynamic Cone Penetrometer testing conducted to assess the strength variation of the base generally indicated medium dense conditions.

The geotextile was supplied 4 m wide, which was stitched together to form a panel of about 12 m x 12 m. Two types of seams (J – Seam and a Butterfly Seam) were used to make an additional check on the effects on seams.

To hold the geotextile in place immediately after placement, smaller rock was placed as a weight along the edges of the test panel. Another issue of concern was the effect of larger rock falling on ballast rock placed to keep the geofabric in place on the seafloor. To simulate this and assess possible damage, a row of smaller rock was placed along the centreline parallel to the warp direction.

The panel was divided into 4 equal cells so that the seams were running along the centerlines of the cells. The trials were conducted using maximum 300 mm rock core with varying the number of drops and/or drop height. The two drop heights employed were 1.5 m and 3.0 m. The latter was used only as an assessment of the worst case scenario as generally the drop height employed during actual construction was always less than 1.5 m. Even the 1.5 m drop is somewhat conservative because in the Project part of the drop would be cushioned by water buoyancy.

On completion, rock core was carefully removed from the geofabric by hand after the bulk was removed by excavator bucket to assess, measure and photograph the damage prior to quantifying the damage. To assess the effect of construction vehicle movement, the removed rockcore was placed over the geofabric to form an access track wide enough for a 45 T excavator to travel. The length of the access track was about 5 m and the height was 1.0 m. This track was then subjected to 16 passes of the excavator moving parallel to the weft direction. The number of passes used was excessive compared to actual conditions during construction.

For the basal geotextile, the damage was calculated as a ratio of the width of damaged section over the total width of the panel or cell. Random parallel lines were drawn and the assessment for each line was assessed and only the worst case is summarized in Table 1.

The results indicated that:

- Except for an outlier, the damage factor varied between 1.2 and 1.8.
- WX800 showed better resistance than WX200.
- Tracking damage is more significant than damage created by rockcore drops.
- WX200 was significantly damaged by the tracking trial.

Table 1 – Summary of damage factors (Basal Geotextile)

Test Locn.	Drop	Factor Worst Case	Remarks
M200/1	2 x 1500	1.7	J Seam
M200/2	1500	2.4	J Seam
M200/3	1500	1.4	Test over ballast
M200/4	1500	1.6	B Seam
M200/5	3000	1.8	B Seam
M200	Tracking	60-70% of test section damaged	
M800/1	1500	1.3	
M800/2	1500	1.2	Test over ballast
M800/3	1500	1.2	B Seam
M800/4	1500	1.4	B Seam
M800/5	3000	1.5	J Seam
M800	Tracking	1.8	

Based on the test results it was decided as a minimum to use geotextiles whose strength is at least double the 200 kN/m strength. A constant damage factor of 1.7 was used for all grades of geotextile between 400 kN/m and 850 kN/m used on the project.

3.2 *Filtration Geotextile*

The client was very concerned about the effects of rock placement and trafficking on the filtration geotextile covering the cohesionless white sand. Therefore the damage trials carried out on the filtration geotextile were more extensive. The geotextile trialed was a 1200 g/m^2 nonwoven staple fibre material (Terrafix 1200R) supplied by Soil Filters Australia.

As the filtration geotextile is placed over a sand pancake at and below the low tide level and the rock was to be placed and not dropped, only trafficking trials were conducted. The geotextile was anchored to an area of moist, loose to medium dense white sand in a reclamation paddock and 0.3 t armour rock placed (by excavator) over the geotextile to varying heights. The rock surface was divided into 4 sections, each approximately 4 m square, so that several trials could be conducted.

The results of a series of trials conducted with a 30 T excavator are summarized in Table 2.

Table 2 – Summary of damage factors of trials T1 to T7

No.	**Material cover and no. of passes**	**No. of fabric punctures**
T1	0.3 m of fine sand – 6 passes	Nil
T2	no cover - 6 plus 1 slight screw of tracks	Nil
T3	1.0 m of fine core – 12 passes	1 *100 mm tear[#]
T4	0.35 m of 60/40 mm crushed aggregate – 6 passes	Nil
T5	1.2 m of 0.35 t armour rock over 0.3 m of fine sand – 12 passes	Nil
T6	0.9/1.0 m of 0.35 t armour rock – 12 passes	1*75 mm tear[#] and 6 tears (20-30 mm)
T7	0.3 m crushed concrete 75 mm - passes	Nil

(# Damage assessed to be by bucket on uncovering test panel)

There were numerous indentations which were also recorded but not included in the above table. The presence of indentations indicated the significantly high strain the geotextile could withstand without rupture.

Further trials T8 to T10 were conducted with a 45 T excavator using previously tracked panels (T8 & T10) and a new panel (T9). The results summarized in Table 3 indicate that the damage from the 45 T excavator was greater than that from the 30 T. Also the damage on re-used geotextile was greater.

Table 3 – Summary of damage factors of trials T8 to T10

Trial No.	Material description	No. of passes	No. of fabric punctures (tear width)
T8	1.1 m of armour rock	12 plus 3 track screws	3 (50-75 mm)
T9	1.0 m of core rock	12 plus 3 track screws	6 (10-50 mm)
T10	1.1 m of armour rock	12 plus 3 track screws	12 (10-150 mm)

For trials T11 to T13, 1.0 m of core rock (T11) and 1.0m of armour rock (T12 & T13) were placed over new fabric and subjected to 12 passes of a 30 T excavator plus 4 track screws on T11 and 6 on T12 and T13. No punctures were observed in T11 and only two tears, maximum 25 and 75 mm, were observed on each T12 and T13 panels respectively.

Subsequent to Trial T11, approximately 0.3 m thick layer of core rock was placed on the previously trafficked geotextile and was subjected to the following at the same location:

- Full downward pressure of excavator bucket
- Four free thumps of the bucket
- Bucket screwing causing all rock to move.

The above actions produced only two (2) small (30 mm) punctures indicating the robust nature of the geotextile used.

4 GEOTEXTILE PLACEMENT FROM THE BARGE

On the Project, a ‘multipurpose’ barge was used for laying both geotextiles and for placing the sand through a spreader system. A flat-top barge, 53 m x 17 m, was modified for the Project (see Figure 2). The unloaded barge has a draft of 0.6 m.

In general the barge consisted of 3 zones:

- The high strength geotextile deployment zone on the port side of the barge.
- The ballast storage and loading zone on the starboard side of the barge, later used for the deployment of the filtration geotextiles.

- The barge controls, facilities, power and hydraulic systems running along the centre of the barge.

A tug was used to move the barge from the load out facility to site where it assisted in setting anchors. The barge positioned and moved itself once set with the hydraulic winches. At the completion of an anchor set, the tug would assist in retrieving the anchors and returning the barge to the load out facility.

Geotextiles were stitched offsite using a J seam into panels up to 42 m wide and 100 m long. The basal geotextile was rolled over in front of the barge and under as shown in Figure 2 with the initial panel done by divers. To avoid geotextile folding transversely 12 mm reinforcement bars were attached to the geotextile with cable ties at 10 m spacing to hold the geotextile tight. Ballast was placed to hold the geotextile in place on the seabed.

The filtration geotextile was required to cover the sand and separate the sand from rock above to minimize sand losses due to wave action. The filtration geotextiles were stitched together using a pray seam stitch to panels of size 32 m x 40 m and transported to the site. The filtration geotextile panels were placed on top of the sand straight off the starboard side of the barge (the area previously used as ballast storage during the placement of the high strength geotextile) as the sand was placed from the sand spreader (attached to the starboard side of the barge). To minimize the risk of the geotextile moving, rock was placed to cover the fabric at the crest (using land-based methods) as soon as practical.

5 CONCLUDING REMARKS

Geotextile damage trials were conducted to assess the damage due to rock placement and due to construction trafficking. The damage factors calculated were successfully used in the design of the high strength geotextiles. The trials conducted to assess the damage on filtration geotextiles due to construction trafficking indicated that the damage was minimal if 1200 R geotextile was used and the excavator weight was limited to 30 T as long as a 800 mm minimum height of rock cover is used before construction traffic is allowed to traffick it.

The FPE Seawall Project Stage 1 was designed based on the results of the trials conducted and the construction was successfully completed in March 2005 (Figure 2).

ACKNOWLEDGEMENTS

The assistance given by Alliance participants including Port of Brisbane Corporation (Client), Leighton Contractors (Contractor), WBM Oceanics (Hydraulics Consultant), Coffey Geosciences (Geotechnical Consultant) and Parsons Brinckerhoff Australia (Civil Consultant) is gratefully acknowledged.

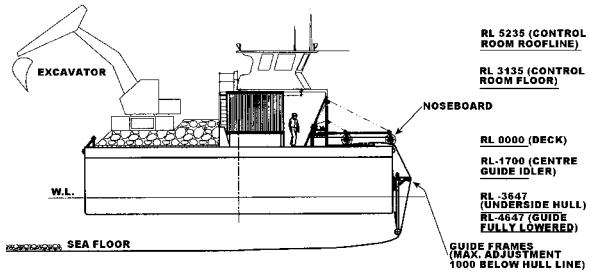

Figure 2 Placement of High Strength Basal Geotextile

Figure 3. Completed Seawall

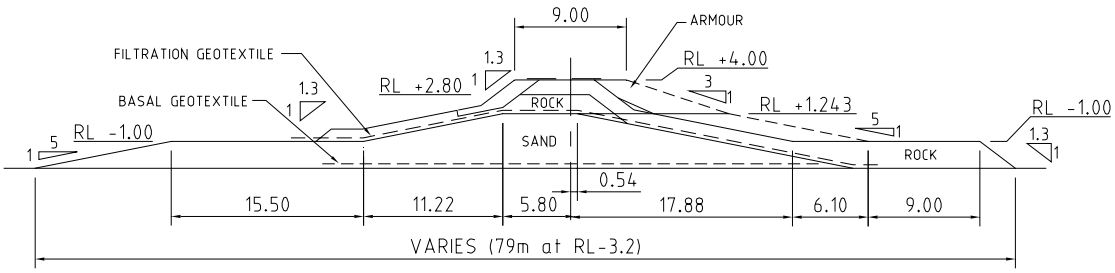

Figure 1. Typical Section on East Bund

Geosynthetics

San Diego Bay gets an underwater facelift

Geotextile cap is a key to this novel seafloor remediation project.

Geosynthetics | October 2006

By Sarah O'Connor, Michael Whelan and Ron Bygness

Overview

This project included aquatic remediation of a former shipyard area consisting of approximately 3,500 tons of underwater demolition, 35,000 yds.^{3} of dredging of contaminated material with upland disposal, and placement of a new structural cap consisting of layers of geotextiles, sand, gravel, and armor rock to contain the remaining contaminated sediments.

The specified work also included debris removal, demolition of shipways, repair and reconstruction of a 1,200-ft.-long seawall, repair and retrofitting of a 180-ft.-long mole pier, construction of rock revetment, wave berm, maintenance dredging of approximately 41,000 yds.^{3} of material with offshore disposal, and other related items of work as specified.

Environmental remediation

Beginning in the 1880s, the Campbell Shipyard site—adjacent to the under-construction Hilton San Diego Convention Center Hotel in downtown San Diego—was used for industrial activities including shipbuilding, the manufacturing of bulk petroleum, and gas waste disposal. Consequently, extensive environmental remediation has been required to clean up the site for development.

In the first phase of remediation, the Port treated or removed more than 80,000 yds.^{3} of contaminated soil from the upland portion of the project site. During the current and final phase of remediation, 9.2 acres of waterside sediment was capped with 5 feet of geotextiles, sand, gravel, and rock. Included in the capping phase are 1.6 acres of mitigation area to replace eelgrass habitat lost by the project.

Campbell Shipyard site

The Campbell Shipyard operated actively near the corner of 8th and Harbor Drive in San Diego from 1910 until 1999. Also located in this area were a manufactured gas plant waste facility and a bulk petroleum distribution facility.

In the late 1990s the shipyard's lease expired and was not renewed. In 2003, the port completed an extensive cleanup of the land, including the removal of thousands of cubic yards of contaminated soil.

However, waterside cleanup proved more difficult.

When the basin was tested, it was determined that interminable dredging and properly disposing of all of the hazardous material would cost too much. Instead, a cap was designed and placed over the sediment to separate the contaminated material from the marine environment: a 5-ft.-thick cap—2 ft. of sand, 1 ft. of gravel, and 2 ft. of armored rock.

The Port is now completing remediation and capping at this site. This remedial activity is being performed in accordance with a 1995 Cleanup and Abatement Order issued by the Regional Water Quality Control Board (RWQCB) and an agreement with the RWQCB under the Polanco site redevelopment statute. This remedial activity included:

- On-site chemical stabilization of 30,000 yds.^{3} of petroleum-contaminated soil (completed December 2001).
- Excavation and off-site disposal of 30,000 yds.^{3} of benzene-contaminated soil associated with a manufactured gas waste impoundment (completed July 2003).

Site preparation, geotextile installation

Prior to installation of the geotextile layer on the seafloor, the contractor removed material, including debris, rocks, and remnants of other piles exposed at subgrade that could damage the geotextile during placement or while applying the armor-rock cap, revetment cap, or habitat cap that would follow on top of the geotextile layer.

Dredging of specific areas of the site's impaired sediment was completed in the summer of 2006 in preparation for the capping procedures. The project was a subaqueous geotextile, sand, gravel, and rock cap over a 9.2-acre area. This cap included a 1.6-acre habitat area. The cap will isolate the site's impaired sediment from environmental receptors and allow for the site's continued use for navigation.

The geotextile layer was applied following completed dredging operations. Following consulting assistance with the contractor and port engineer, the selection of a suitable geotextile as well as help with the installation of the geotextile for this project was undertaken.

HP770 PET geotextile was used for this portion of the layered capping. This geotextile is a polyester/polypropylene fabric with a specific gravity of 1.07. It is woven from high-tenacity, long-chain polymers composed of at least 95% by weight polyesters that form a stable network such that the filaments retain their dimensional stability relative to each other including selvages. It does sink, albeit slowly.

To aid in the deployment and accurate placement of the fabric on the seafloor, the contractor attached #4 rebar encased in PVC pipe with capped ends. The rebar was attached perpendicular to the fabric about every 10 yards prior to being rolled off a floating sectional barge into the water.

Cap installation

The installation of the geotextile layer occurred in a submerged marine environment. This work involved the use of derrick/sectional barges and divers.

Placement constraints included:

1. The geotextile placement involved working from a floating, sectional, deployment barge.
2. The contractor could not anchor the barge with spuds within the capping areas.
3. Penetration of the subgrade during placement of the geotextile cap within the armored cap, revetment cap, and habitat cap areas was not allowed.

Engineered cap

The largest portion of the capped area is an engineered cap designed for permanent isolation of remaining environmental pollutants in bay sediments.

The engineered cap is composed of a geotextile overlaid by 2 ft. of sand for isolation of pollutants in existing sediments; a 1-ft. layer of well-graded, gravelly aggregate material to act as a filter layer between the overlying armor stone and the underlying sand, while also protecting against bioturbation; and then a final layer of 2 ft. of armoring stone to protect against erosive forces that may be imposed on the capping system.

Additional foundation support, in selected areas overlaying unconsolidated bay sediments at the edge of the cap, was strengthened by placement of a layer of "dumped rock foundation."

Habitat cap

The habitat cap is a 1.6-acre eelgrass environment. The design of the habitat cap includes a base layer of sand overlaid by a geotextile layer and topped by a final layer of 2 ft. of sediments with grain sizes ranging from medium to coarse sand to provide a suitable substrate to support the overlying eelgrass habitat.

The function of the geotextile is as a separation layer to help isolate any underlying residual environmental pollutants and to protect against bioturbation into the underlying sediment.

Another structural element is a rock containment berm to protect and enhance the stability of the entire cap system.

Costs

Implementation of these cleanup and abatement actions, including installation of an appropriate capping system to isolate sediments containing residual shipyard waste, has cost approximately $16 million.

To date, a total of more than $72 million has been spent on the entire project area, including: demolition, dredging, and disposal; all land and bay environmental cleanup, disposal, and capping; site preparation, and construction of a 2,000-vehicle parking facility to accommodate further development.

Sarah O'Connor, Sr. Civil/Environmental Engineer with Triumph Geo-Synthetics; Michael Whelan, P.E. with Anchor Environmental; and Ron Bygness, editor of *Geosynthetics*, contributed to this article.

Prep and staging using an I-beam: To establish the start of a fabric run on the seafloor, the geotextile was attached to an I-beam. Photo courtesy of Triumph Geo-Synthetics.

The positioning of the fabric was established with a global positioning system, monitored by the field superintendent and the crane operator. Photo courtesy of Triumph Geo-Synthetics.

Rebar and prep/staging | The rebar was encased in PVC pipe capped at both ends. Photo courtesy of Triumph Geo-Synthetics.

Rebar and prep/staging | The rebar was attached approximately every 10 yards along the length of the fabric to help in deploying fabric into the water and to aid in positioning the fabric on the seafloor. Photo courtesy of Triumph Geo-Synthetics.

Rebar and prep/staging | The rebar was attached approximately every 10 yards along the length of the fabric to help in deploying fabric into the water and to aid in positioning the fabric on the seafloor. Photo courtesy of Triumph Geo-Synthetics.

Rebar process | The rebar was attached onto the fabric using zipties approximately every 10 yards along the width of the entire length of the 900-ft.-long geotextile roll. Photo courtesy of Triumph Geo-Synthetics.

Rebar process | Workers attached rebar across the full width of the 45-ft.-wide, 900-ft.-long roll of geotextile fabric. Photo courtesy of Triumph Geo-Synthetics.

The geotextile fabric floats into the water. Photo courtesy of Triumph Geo-Synthetics.

Deployment | The rolls of fabric were unfurled and floated into the bay from the deck of an 80-ft. x 60-ft. sectional barge. Photo courtesy of Triumph Geo-Synthetics.

The seam of the fabric—3 15-ft.-wide fabric panels were sewn together to get the desired width of 45 ft. It was folded and rolled prior to shipping. The fabric rolls were attached to a 50-ft.-long spool. Photo courtesy of Triumph Geo-Synthetics.

Crane with ball/anchor | When the derrick barge is moved, these 15-ft.-high anchors also have to be repositioned. Photo courtesy of Triumph Geo-Synthetics.

Project Highlights

Project title: Sediment remediation and aquatic enhancement at the former Campbell Shipyard site

Location: San Diego Bay; San Diego, Calif.

Start date September 2005

Completion date: 1st quarter, 2007

Owner: San Diego Unified Port District
Project Manager: Mahmoud Akhavain

Contractor: Traylor Pacific
Project Manager: Calvin Casey
Project Engineer: Mohamad Ramlawi
Marine Superintendent: Ed Adair

Designer: Anchor Environmental LLC

Geosynthetics: Mirafi HP770 PET fabric, installed to help create a cap over the bay floor of the former Campbell Shipyard site on San Diego Bay, installed from a derrick barge and floating deployment platform

Suppliers/consultants: Blaylock Engineering Group, Everest International Consultants, Merkel & Associates, Ninyo & Moore, Terracosta Consulting Group, and Triumph Geo-Synthetics Inc.

Comments

There are not yet any comments.

Standards Australia
Information in fields should be filled in if known or left as is.

Geotextiles—Methods of test

Part Title:	**Determination of abrasion resistance—Rotating drum method**
Designation:	**AS 3706.16—2010**
Part Number:	**2**
AustralianORJoint:	**Australian**
Owner:	**STANDARDS AUSTRALIA**
Creation Date:	
Revision Date:	
Committee Number:	**CE/20**
Committee Title:	**GEOSYNTHETICS**
Subcommittee Number:	
Subcommittee Title:	
Project Manager:	
WP Operator:	
Project Ref:	**CE/020-0060**
Project Number:	**CE/020-0060**
Combined Procedure?:	YES
Committee Doc No.:	**CE/020-0060-580**
Supersedes Committee Doc No.:	**CE/020-0060-551**
Stage:	**PUBLICATION**
Issue Date:	
Introductory Note:	
Dual Number and Year:	
Parent Publication Title:	
"Known-as" Title:	
Date Approved:	
Date Approved by SNZ	
Publication Date:	
Supersedes Standard No:	
Committee Reps:	**Association of Consulting Engineers Australia** **Monash University** **International Geosynthetics Society** **Technical Textiles and Nonwovens Association** **Australian Geomechanics Society** **Australian Industry Group** **CSIRO** **Australian Water Association** **Australian Wool Testing Authority** **AUSTROADS** **Department of Main Roads Queensland** **Commerce Queensland** **Waste Management Association of Australia**

Additional Interests:
DR Number: **DR 99289**
History:
ISBN: **0 7337 2942 8**
WP ID Number: **13480.CDR**
Amendment No.:
Amdt Published Date:
Standard Published Year:
CS Code:
Synopsis PublicComment
Synopsis Publication
Synopsis Draft for Comment

This document was prepared using template Newdraft032.dot
Last re 2/02/2011 10:10:00 AM

Australian Standard™

AS 3706.2

Geotextiles—Methods of test

Method 2: Determination of abrasion resistance—Rotating drum method

METHOD

1 SCOPE

This Standard sets out the method for determining the abrasion resistance properties of geotextiles in wet conditions using the rotating drum method.

2 APPLICATION

This method is applicable to all types of geotextiles.

3 REFERENCED DOCUMENTS

The following documents are referred to in this Standard:

AS	
2193	Methods for calibration and grading of force-measuring systems of testing machines
3704	Geotextiles—Glossary of terms
3706	Geotextiles—Methods of test
3706.1	Method 1 General requirements, sampling, conditioning, basic physical properties, and statistical analysis
3706.2	Determination of tensile properties—Wide-strip method
ASTM	
C131	Resistance to degradation of small coarse size aggregate by abrasion and impact in the los angeles machine
BAW	
3.11	Abrasion resistance

4 PRINCIPLE

The test method simulates abrasion on geotextiles in exposed applications, caused by the movement of sand coral and gravel against the geotextile, under wave action. After exposure the mean tensile strength in machine and cross machine direction is compared with the control specimens. The percent strength retained is calculated.

Various tensile properties of the test specimen are recorded.

5 DEFINITIONS

For the purpose of this Standard, the definitions given in AS 3704 apply.

6 APPARATUS AND REAGENTS

The following apparatus and reagents are required:

(a) An hexagonal steel drum apparatus with six removable abrasion, driven by a central horizontal shaft. The direction of rotation can be changed and the number of revolutions per minute and the total number of revolutions can be set as required.
The machine shall comply with the following criteria:

Drum diameter - 700mm
Rotation speed - 1300 revolutions per hour
Abrasion Plates - 6 (allowing 250mm x 500mm exposed geotextile surface)

(b) 16 litres of water

(c) Abrasive material as follows:

5kg - 8/11mm angular high quality basalt chippings

3kg – 3/5mm angular high quality basalt chippings

(d) Constant-rate-of-extension (CRE) tensile testing machine complying with the requirements for a Grade B machine in accordance with AS 2193, and having an extension rate of 20 mm/mm.

The machine should have an autographic recorder with adequate pen response or an interfaced computer to properly record the force extension curve.

For machines with no autographic recorder, appropriate measuring instruments are required to allow readings of the applied force and the corresponding extension at a number of points up to failure.

The jaws of the machine shall be not less than 10 mm wider than the width of the test specimen and shall prevent the test specimen slipping. They shall also not damage the test specimen.

NOTES:

1 Flat plate type jaws, often supplemented by small G-clamps placed at X_1 and X_2, as shown in Figure 1, have been found to hold most wide strip specimens satisfactorily.

2 Flat plate pneumatic/hydraulic type jaws of appropriate size have also been found to be suitable.

(e) Area-measuring device, such as an integrating accessory to the tensile testing machine or a planimeter.

(f) Water bath maintained at a temperature of 20 ±2°C.

7 PREPARATION OF TEST SPECIMENS

7.1 Sampling

A minimum of 12 test specimens shall be sampled in accordance with AS 3706.1.

The specimens shall be cut as follows:

(a) A minimum of six specimens with the larger dimension in the machine direction.

(b) A minimum of six specimens with the larger dimension in the cross-machine direction.

7.2 Size of specimen

Each specimen shall be prepared so that it is 270 mm wide and 520mm long. This will allow clamping in the test apparatus and sampling for testing in accordance with AS3706.2 shuch that

7.3 Conditioning

The specimens shall be conditioned wet, in accordance with AS 3706.1.

7.4 Marking

No marking for specimen identification purpose shall be made within or at the boundary of the exposed surface of any specimen.

FIGURE 1 CLAMPING DEVICE

8 TEST CONDITIONS

The test atmosphere shall be in accordance with AS 3706.1.

Specimens shall be tested in the tensile testing machine within 20 min after their removal from the water bath.

9 PROCEDURE

The procedure shall be as follows:

(a) Attach geotextiles to inside face of removable abrasion plates, ensure weakest direction is aligned with direction of rotation. Clamp abrasion plates down onto rotating drum frame, ensure watertight seals are in place. Pour the following water - gravel mixture into the drum:

Water		- 16 litres
Basalt	(8-12mm)	- 5kg
Basalt	(3-5mm)	- 3kg

(b) Set the rotation speed at 1300 revolutions per hour

(c) Rotate drum for 5000 revolutions in one direction then reverse for a further 5000 revolutions, this procedure is repeated until a total of 40 000 revolutions has been achieved. After completion of the first 40 000 revolutions the material in the drum is removed and a fresh charge of the mixture above is added, the procedure is then repeated for a further 40 000 revolutions.

The samples are then removed from the apparatus, cleaned carefully and dried.

10 REPORT

The following information shall be reported:

(a) The number of this Australian Standard i.e. AS 3706.16.

(i) Sampling and testing information as follows:

(ii) Name of testing authority and client.

(iii) Identification of batch or order represented by the sample.

(iv) The date or dates of sampling and testing.

(v) Number of specimens tested.

(vi) The nominal mass per unit area, of the sample.

(vii) Conditioning of specimens.

(viii) The test environment (standard or non-standard, define non standard conditions).

(ix) Make and model of tensile testing machine.

(b) Representative values for the machine direction and cross-machine direction as applicable:

(i) Yield tensile strength and elongation at yield force.

(ii) Ultimate tensile strength and elongation at ultimate force.

(iii) Offset tensile modulus and offset elongation.

(iv) Where determined and as required, other measures of wide-strip tensile behaviour as follows:

(A) Peak tensile strength and elongation at peak force.

(B) Breaking tensile strength and elongation at break.

(C) Characteristic strength and elongation at peak force.

(D) Initial tensile modulus.

(E) Ten percent secant tensile modulus.

(F) Other tangent or secant tensile moduli as requested.

(G) Toughness.

(c) Individual values as follows:

(i) Individual test results, calculated values, and graphical information for each test and each property.

(ii) Detailed information about any result that is considered to be abnormal.

(d) Any modifications of procedure.

(e) Details of rejected results, including the reasons for the non-inclusion of rejected results in the assessment of the representative values.

NOTES

This Australian Standard was prepared by Technical Committee CE/20, Geosynthetics. It was approved on behalf of the Council of Standards Australia on 3 December 1999 and published on 28 February 2000.

The following interests are represented on Committee CE/20:

Association of Consulting Engineers Australia
Monash University
International Geosynthetics Society
Technical Textiles and Nonwovens Association
Australian Geomechanics Society
Australian Industry Group
CSIRO
Australian Water Association
Australian Wool Testing Authority
AUSTROADS
Department of Main Roads Queensland
Commerce Queensland
Waste Management Association of Australia

Keeping Standards up-to-date

Standards are living documents which reflect progress in science, technology and systems. To maintain their currency, all Standards are periodically reviewed, and new editions are published. Between editions, amendments may be issued. Standards may also be withdrawn. It is important that readers assure themselves they are using a current Standard, which should include any amendments which may have been published since the Standard was purchased.

Detailed information about Standards can be found visiting the Standards Australia web site at www.standards.com.au and looking up the relevant Standard in the on-line catalogue.

Alternatively, the printed Catalogue provides information current at 1 January each year, and the monthly magazine, *The Australian Standard*, has a full listing of revisions and amendments published each month.

We also welcome suggestions for the improvement in our Standards, and especially encourage readers to notify us immediately of any apparent inaccuracies or ambiguities. Contact us via email at mail@standards.com.au, or write to the Chief Executive, Standards Australia International Ltd, PO Box 1055, Strathfield, NSW 2135.

This Standard was issued in draft form for comment as DR 99289.

Published by Standards Australia International Ltd
PO Box 1055, Strathfield, NSW 2135, Australia

ISBN 0 7337 2942 8 Printed in Australia

COMPARISON OF FATIGUE DATA FOR POLYESTER AND WIRE ROPES RELEVANT TO DEEPWATER MOORINGS

Stephen J Banfield*, John F Flory**, John W S Hearle*, Martin S Overington*

* Tension Technology International Ltd
16 Milnthorpe Road, Eastbourne
Sussex, BN20 7NR, UK

** Tension Technology International Inc
4 Tower Lane, Morristown
NJ 07960, USA

ABSTRACT

Polyester ropes are now established in deepwater moorings, but more research is needed to understand long-term durability and to optimise systems.

Three categories of rope failures – environmental, surface damage, and structural – are not considered to be likely problems for deepwater polyester moorings which are properly designed and used. Fatigue of fibres in the rope is thus the concern of this paper. The fatigue mechanisms of interest are creep tensile fatigue, compression fatigue and internal abrasion.

Laboratory test data on potential fibre fatigue mechanisms is reviewed with reference to typical mooring system service conditions. For a 20 year life, a typical mooring might experience 60 million cycles, mostly due to small waves. The occasional severe cycling which might be experienced during storm conditions will cause little fatigue damage.

Tensile fatigue and creep rupture will not occur in polyester fibres at the applicable low loads. Hysteresis heating is not significant for strain amplitudes less than $\pm$0.5%, but might be a problem with the larger amplitudes which might occur in shallow water moorings. Internal abrasion might begin to take effect after millions of cycles. Axial compression fatigue might occur after a large number of cycles in rope elements that go into compression, even though the rope as a whole remains under tension.

Existing fatigue data on large spliced ropes is compared with data for steel wire rope given in API 2SK. The demonstrated polyester rope fatigue life is at least as good as spiral strand and better than multi-strand steel wire rope.

Computer modelling of rope performance is discussed. Under conditions designed to demonstrate fatigue mechanisms, the model shows an early drop in strength due to hysteresis heating and a second drop as some yarns fail in axial compression fatigue. After a very large number of cycles, internal abrasion takes effect and finally creep rupture occurs.

The general conclusions are that, polyester ropes are suitable for deepwater moorings for expected lifetimes of 20 years and that their potential fatigue performance is at least as good as spiral strand steel wire rope at loads representative for FPS mooring. But more research may be needed to identify and quantify active fatigue mechanisms to enable engineers of mooring systems to satisfy regulatory bodies and certification authorities.

Keywords: POLYESTER ROPE FATIGUE MOORINGS DURABILITY

INTRODUCTION

The use of polyester ropes to moor floating production platforms in deep water has now passed from initial research studies into actual use. Petrobras has installed several systems in depths up to 1500 meters in the Campos Basin. Confidence needed for their future use in the Northern North Sea, North Atlantic, Gulf of Mexico and elsewhere is being gained by a number of completed, current and proposed Joint Industry Studies. The technology needed for employing polyester ropes in deepwater mooring appears to be well established. However, further research is needed in order to increase understanding of long-term durability for permanent moorings, to optimise designs, to reduce conservatively imposed “safety factors”, and to reduce costs.

Two aspects are of particular concern. The first is the effective stiffness, or more appropriately the total nonlinear load- extension relation, as it depends on mean load, cyclic loading range and prior history of

the rope. This information is needed as input to mooring analysis programs, which, in addition to determining peak loads and offsets, are used to compute the loading history expected in a given installation during its lifetime. It is thus indirectly related to the second concern, which is the subject of this paper, namely the durability of "permanent" moorings.

The possible causes of rope failures were identified by Parsey (1982) in a paper on fatigue of SPM mooring hawsers and by Hearle and Parsey (1982). Flory, Parsey, and Banfield (1990) updated the listing. Causes of failures were categorised as: environmental; surface wear; tensile and structural failures (such as tensile overload or torque effects); and fatigue.

Corrosion due to sea-water is a potential hazard for steel. The analogous effect for polyester fibres is hydrolysis, but this is not a practical problem. Long times at relatively high temperatures are needed to cause appreciable strength loss due to hydrolisis. Studies by Burgoyne and Merii (1993) extrapolate to a 10% loss in strength after 6000 years at 0^oC, 200 years at 20^oC and 10 years at 40^oC. Polyester has excellent resistance to UV-degradation, so that it is a suitable jacket material for ropes of more susceptible fibres. Other environmental effects, such as microbiological attack, are not expected causes of failure in polyester ropes. However, the long term durability of fibre finishes is an unknown, which needs addressing.

Ropes can be damaged by cutting and by abrasion against external objects, particularly care is needed during installation where contact with rollers or work wires can cause damage. There are no recorded instances of fishbite in large ropes and this mode of damage has generally been ruled out. In locations where fishbite has been prevalent in small buoy mooring ropes, this aspect may need further attention.

Low-twist fibre ropes, which are used for deepwater moorings in order to optimise tensile strength, need tough braided or plastic jackets in order to avoid sensitivity to external abrasion. However, provided unduly careless handling is avoided, external damage should not be a problem. In a properly designed mooring, tensile overload should not occur. Other causes of structural disturbance, such as severe twisting or bending, should be avoided.

This leaves the effect of lifetime cyclic loading on the fibres comprising the main internal structure of the rope as the principal mechanism to be considered. Fatigue due to transverse crack growth under cyclic loading, as occurs in steel, is not a failure mechanism in polyester fibres. However, there are other effects of cyclic loading on fibres, which are not relevant to steel wires but are referred to as fatigue. These will be reviewed in the next section before presenting the analysis of data on ropes themselves, which is the main purpose of this paper.

FIBRE FATIGUE

The great variety of fibre failure forms have been covered by Hearle et al (1998). Five "fatigue" effects, in addition to structural fatigue, have been noted as relevant to ropes.

Tensile fatigue is a mechanism found by Hearle and Bunsell (1971) when nylon fibres are cycled down to zero load. An initial transverse crack turns under the influence of shear forces and runs at an angle of about 10^o across the fibre. In polyester, the effects are less severe because the cracks run almost parallel to the yarn surface. Tests by Oudet et al (1984) on tyre-cord polyester fibres, which are similar in this context to the marine grades used for deepwater moorings, gave a median fatigue life of 10^5 cycles and a range of 1½ decades when cycled between zero load and 70% of break load. A 10% reduction in peak load increased the median to 10^6 cycles. Contrary to earlier studies, these tests showed tensile fatigue up to 20% minimum load at 70% maximum. Typical deepwater loading histories will not approach these peak loads and thus, it is the considered view of the authors that the chance of tensile fibre fatigue failure is negligible.

Hysteresis heating is listed as a cyclic fatigue effect. It is not a problem of current interest in deepwater moorings, but should be addressed for shallow moorings, which might experience high strain amplitudes. In other applications, when ropes are subject to severe cyclic loading, it can cause melting. The heating is partly caused by energy dissipation due to hysteresis within fibres and partly to friction between fibres. A rise in temperature reduces the strength of polyester fibres and thus increases the susceptibility to other fatigue mechanisms. The fibre loss factor has been shown by Bosman (1996) to be proportional to cyclic amplitude. The results of tests on large polyester ropes in a Joint Industry Study, as reported by Banfield and Hearle (1998), show that the temperature rise becomes substantial at cyclic strain amplitudes greater than $\pm$0.5% extension, but is small ($< 5^oC$) for amplitudes less than $\pm$0.5% extension. It takes about 1 hour for half the temperature rise to occur. Cyclic load amplitude of about $\pm$15% of break load corresponds to extension amplitude of $\pm$0.5% for polyester ropes, and this condition is not likely to be exceeded for significant times in deepwater moorings.

Creep rupture occurs under both static and cyclic loading. For constant cyclic load amplitude, the conservative estimate, which is supported by experiment, is to use the peak load as equivalent to the static load. The appropriate summation for variable cyclic loads has not been properly worked out. Short periods of high loading under storm

conditions should not have a major effect, so that it would be reasonable to calculate creep rupture times on the basis of an "average peak load". Creep rupture is a cause for concern in HMPE and, to a less extent, in nylon. But for polyester it is estimated that it would take many thousands of years at 50% of break load to produce creep rupture. Modelling studies by Hearle et al (1993) show that creep rupture would be the final cause of failure after a rope had been weakened due to other fatigue effects.

Internal abrasion is a serious problem in highly twisted nylon ropes under moderate cyclic loading in wet conditions. The damage is less in low-twist ropes, due to the reduced relative fibre movement during cyclic loading, and it is much less in polyester than in nylon, especially for rope yarns with a suitable marine finish. Tests carried out with large cyclic stroke amplitudes on a laboratory yarn-on-yarn abrasion machine in Fibre Tethers 2000 (1995) showed lifetimes up to more than 300,000 cycles for polyester yarns.

Axial compression fatigue is caused by repeated bending of individual fibres when they are allowed to relax while tightly constrained within the structure of a rope. Aramid fibres are particularly vulnerable to axial compression fatigue. In laboratory tests conducted as part of Tethers 2000, aramid yarns lost approximately 50% of their strength after 1000 compression cycles.

This closely corresponds to the results of the Aker Omega (1993) cyclic load tests on very large aramid ropes, in which axial compression fatigue caused failures in splices within several thousand cycles. The trough cyclic load was 10% in some of these tests. But due to unequal load sharing among the strands in splices, some strands went into compression, and when these few strands failed due to axial compression, the structure of the splice was upset causing complete failure of the rope.

Flory (1996) discussed how axial compression fatigue is not likely to be a problem in polyester rope. Because polyester yarn has a lower modulus than aramid, unequal load distribution is much less likely to take place between fibres, yarns, and strands. Because polyester yarn has a lower friction coefficient than aramid, the fibres and yarns are less likely to become tightly bound within the rope structure, such that unequal load distribution can place them into axial compression as the rope relaxes.

And many more compression cycles are required to induce axial compression fatigue in polyester fibres than in aramid fibres. In the Tethers 2000 JIP, using the same laboratory test method as for aramid yarns, polyester yarn retained 97% strength after 100,000 cycles and 78% strength after 500,000 cycles.

Thus it is not necessary to take the same precautions against allowing polyester ropes to relax as must be taken with aramid ropes. From Phase ψψA (1994) studies it was found that polyester ropes can experience many thousands of very low trough load cycles or even complete relaxation without significant strength loss.

Axial compression fatigue differs from traditional "crack-propagation" forms of fatigue in that it is regressive instead of progressive. Thus axial compression fatigue does not lead directly to complete failure of the rope. However, there is a possibility that moderate strength loss due to axial compression can initiate or intensify some other failure mechanism.

A deepwater polyester rope mooring system can be designed and operated so as to maintain an adequate minimum tension on the lines in normal conditions. The tension may drop to lower values for limited periods of storm conditions, as long as this is not allowed for an excessive number of cycles. The deliberately conservative EDG (1998) recommendation for polyester ropes is that the tension should not drop below 5% of break load for more than 100,000 cycles, but note above that this only caused a 3% strength loss in polyester yarns.

In summary, it can be said that studies of fibre and yarn fatigue mechanisms give no reason to expect failures in polyester lines, designed to current standards and planned lifetimes. The fundamental science indicates that the performance of polyester ropes will be at least as good as steel ropes, and due to the absence of corrosion and of metal fatigue, polyester rope performance should be appreciably better. After longer periods, axial compression fatigue might fail some yarns and increase the load on others, but it is not apt to directly cause failure in well designed ropes. Ultimately, after millions of cycles, internal abrasion is the mechanism which appears most likely to cause loss of strength in polyester ropes.

FATIGUE CONDITIONS

Before reviewing the fatigue data on ropes, consider the loading conditions which might be used in testing in order to give a reasonable relation to conditions expected in operation. Note that 20 years at wave frequency generates about 60 million cycles. Extreme storm conditions can give cyclic loads up to ±15% of break load, but the limited number of cycles at these levels will cause little fatigue damage. It is the continuous cycling due to millions of small waves, which give much smaller cyclic load ranges, that has the potential to cause real fatigue damage. Further work is needed to establish a standard fatigue test procedure for comparative purposes or, if necessary, the criteria for customised fatigue testing of lines intended for particular installations. The ideal would seem to be a stochastic loading pattern related to

predictions of loading in use.

There are two other complicating factors in fatigue testing.

Firstly, the nominal break strength quoted for a rope may be less than its real break strength. When required to supply a rope with a guaranteed break load, manufacturers will adopt varying degrees of conservatism to ensure meeting the specification. Paradoxically, the use of a conservative estimate of break load makes the fatigue response appear better. A mean load or load range based on a given percentage of a conservatively stated break strength, will be a smaller force than the same percentage of a higher actual break strength. Consequently, the actual fatigue-loading test conditions based on a conservative break strength will be less severe.

Secondly, metal fatigue test data is commonly plotted against cyclic range, because it has a greater effect than mean load. In fibre ropes, some mechanisms are less dependent on load range. Creep is strongly influenced by sustained maximum load. Axial compression fatigue is determined mainly by low values of minimum load. Fatigue data should be obtained and plotted in terms of two variables. The most obvious choices are *either* mean and range *or* maximum and minimum. As apparent above, there is also a question as to whether load values or strain values are most appropriate.

ROPE FATIGUE DATA

It is not surprising that there is no authoritative set of data on rope fatigue properties, given the complications mentioned in the last section, the variety of fibre types and rope constructions, the heavy and specialised test equipment needed, and the high cost of testing. Never-the-less, in the following we attempt to analyse the available data and compare it with the fatigue curves for steel chain and wire rope given in API 2SK (1997).

The fatigue life and residual strength data reviewed here is taken from a full analysis of available synthetic fibre rope strength and stiffness data being conducted by TTI. This review is restricted to ropes of 5 tonne and higher Minimum Break Strength (MBS) in parallel yarn, parallel strand and wire-rope constructions, which are the types applicable for deepwater mooring lines. For the following reasons, the review is restricted to spliced lines:

$ Only spliced lines have been validated for fibre ropes over 500 tonnes actual break strength.
$ In general spliced terminations give a higher mean strength than other terminations, with similar variability.
$ Fatigue performance of spliced ropes is somewhat inferior to that of resin-socketed ropes, which means that the predictions will be conservative for ropes with properly designed resin sockets.
$ Confidential developments by TTI confirm that improvements in strength and reliability over previous state-of-the art splices can now be made available.

The results are plotted in Fig 1a and 1b along with the API fatigue design curves.

In Fig. 1a, the Load Range is on a normal scale abscissa, while in Fig. 1b the Load Range is on a log scale as it is in the original API figure. When a straight line on a log-log plot is replotted on a semi-log plot, it becomes a curve, as depicted in Fig. 1a. These API wire rope curves are truncated at 60% load in Fig. 1a, and in Fig. 1b they are truncated at 1.75.

In each figure, a straight line has been fitted by regression analysis through the polyester rope data, indicated by the solid squares and triangles. This is the upper full line in each figure. Note that these lines are not equivalent, one having been derived on a semi-log basis and the other on a log-log basis.

During the regression analysis for each figure, the standard deviation for the data was also determined. The lower full line in each figure represents the “Mean - 2 Sigma” for all of the analyzed data. Note that the variation in these polyester rope fatigue data is most likely caused by including data from several different rope constructions and many different manufacturers and test programs together in the statistical analysis. It does not represent the expected scatter of fatigue performance for a single given type of rope from one rope maker. Thus it presents a very conservative estimate of the minimum cycles-to-failure for good-quality polyester ropes.

In Fig. 1a, the polyester “Mean – 2 Sigma” line is above the API six-strand wire rope curve for most of the range, and it is essentially the same as the API spiral-strand curve in the mid range of interest. In Fig. 1 b, this polyester line is above the API wire rope lines throughout the lower load ranges. The data points with a “+” sign to the right of the symbol are run outs.

The mean regression fit for the fibre rope data is

Range (%MBS) = - 12.4331*log cycles +109.4622

and the corresponding lower bound (-2 sigma) fit is

Range (%MBS) = -12.4331*log cycles + 90.1357

These regressions have been conducted with the same dependent and independent variables as Parsey (1982). However, a comparison of regression results is beyond the scope of this paper and would deserve a separate study.

Much of the available polyester rope fatigue data are for tests in which the rope was cycled a limited number of times and then loaded to break in order to determine residual strength. These residual strength data are plotted here in Fig. 2. All of the residual strengths are over 100%, meaning that the residual strengths were greater than the original MBS, assigned by the manufacturer. Note that several of these tests extended to one million (10^6)load cycles or more. In comparison, NEL tests (1992) on 70mm six strand wire rope to 50% of life (231,000 cycles at 20% mean ∀ 12.5% load range) gave a measured 15% strength reduction.

This high residual strength phenomena is not unusual. The break strength of synthetic fibre ropes generally increases during initial cycling, as the splices set and the rope structure becomes better balanced and aligned. In the case of these data, which are based on MBS, it probably also reflects the conservatism of MBS values quoted by rope manufacturers.

COMPUTER MODELLING OF ROPE FATIGUE

The OP*TTI*-ROPE programs, which are described by Hearle et al (1993, 1995) derive from work by TTI for the US Navy. OP *TTI*-ROPE includes procedures for computing the progressive loss of strength and eventual failure of fibre ropes. The input to the programs consists of:

- load-elongation properties of constituent yarns
- rope construction geometry
- creep rupture parameter
- energy dissipation factor
- two constants to give shift of breakpoint with temperature
- rate-of-internal abrasion parameter
- number of cycles to yarn failure in axial compression
- cyclic loading range and frequency

A typical prediction is shown in Fig 3, where the values of the parameters have been chosen to bring in the several fatigue mechanisms. There are two small steps in the retained strength: an initial drop as the rope heats up to an equilibrium temperature; and a second drop when yarns under axial compression reach the failure limit. Internal abrasion causes a slow decrease in strength, which leads to a rapid drop at the end when the effective fraction of break load becomes large enough to cause creep. Final failure occurs when the residual break load, adjusted for creep rupture, matches the maximum imposed load.

The OP*TTI*-ROPE program is useful for exploring the way in which fatigue might lead to loss of strength in ropes. We are not aware of similar programs for steel wire ropes. The problem for actual prediction is a lack of the necessary quantitative knowledge of fibre properties. Reasonable estimates can be made for the creep and heating parameters in polyester ropes, or tests can be made to determine them. At present, there is no confirmed method of applying the results of fibre tests for the abrasion and axial compression parameters to the prediction of rope performance. A possible way forward, as proposed by TTI and NEL for a durability JIP, is to determine the incidence of these mechanisms in test ropes. The results could then be used as inputs to programs intended to determine the effects of changes from the test ropes and conditions.

DISCUSSION

This paper has demonstrated that the fatigue performance of large good-quality polyester ropes can be expected to be as good as that of the wire ropes now used in offshore moorings.

However, further testing and research may be needed to confirm and demonstrate this to the full satisfaction of potential mooring system designers and users, classification societies and regulatory authorities.

One school of thought is that polyester ropes will not be accepted for offshore moorings until it is demonstrated that they can be used for 20 years without failure.

In the absence of 20 years of field experience, this can be done by cyclic load testing using a realistic mean load and amplitude on a full-size specimen of a particular rope design. But it might take nearly 20 years of laboratory testing to reach the 60 million cycles needed to represent 20 years of mooring service. There may be ways to perform such testing in a reasonable length of time and at a reasonable cost but these are yet to be demonstrated .

An alternative testing approach is to conduct a number of tests on “standard” polyester ropes at higher mean loads or amplitudes. This would be similar to the effort used develop the API 2SK steel wire rope fatigue design curves, which are well accepted for design purposes by the industry. These design curves were compiled from a number of sources. The principal work was done in the wire-rope joint industry project, reported by Noble Denton (1991), in which the available wire rope fatigue data was evaluated and further testing was performed to

gain additional confidence.

The TTI/NEL rope durability study has a similar objective to evaluate available synthetic fibre rope data and provide additional fatigue life data. Like the wire rope study, this joint industry project will investigate both large ropes and smaller model ropes representative of those polyester ropes which are now being considered for offshore moorings. This will be the first such testing to employ a stochastic spectrum simulating actual mooring load conditions.

But unlike wire ropes, polyester ropes are not yet "standardized". Thus conducting extensive testing on one or several specific rope designs is not sufficient to demonstrate the performance of all other polyester ropes.

The mechanical properties of high-quality polyester yarns are similar. But different proprietary fibre finishes are used on these yarns to impart special abrasion-resistance and low-friction characteristics which are very important for rope performance. Rope constructions and terminations also differ. Existing designs are being improved and new designs are still being developed. Thus "standardization" at this time would favor certain fibre producers and ropemakers and would inhibit the development of better ropes.

The new ABS Guide (1999) recognizes this. It allows consideration of any viable rope design. It requires that the manufacturer document the rope design details, test prototype ropes, and establish quality control procedures in order to ensure that the rope supplied is the same as the tested prototype.

To demonstrate minimum fatigue performance, ABS requires a test in which the rope is cycled about a mean tension of 30% of mean wet break strength with an amplitude of 10%. If the rope survives 600,000 cycles, the synthetic rope fatigue properties are classified as equivalent to spiral-strand wire as given in API 2SK (1997). If the rope survives 100,000 cycles, ABS classifies the synthetic rope fatigue properties as equivalent to multi-strand wire. ABS then permits the applicable API fatigue design procedures to be used for the tested polyester rope design.

This fatigue test practice is sufficient to certify the initial installation of a polyester rope mooring system. But it may still be necessary to reverify and recertify the rope while it is in service.

One suggested practice is to periodically conduct break tests on short rope specimens removed from the mooring. Such break testing demonstrate the rope residual strength. But this does not demonstrate the remaining service life of that rope. Some forms of rope deterioration develop slowly but accelerate just before ultimate failure: 100% residual strength does not guarantee another year of service. Thus ABS may require that these short rope specimens be subjected to the same fatigue test as was used before installation. This will periodically demonstrate residual fatigue life, which is much more reassuring.

An alternative to extensive rope fatigue testing is to scientifically identify the principal mechanism(s) which cause rope deterioration and failure; to study these through testing of fibres, yarns, rope components, or small rope models; and then to use these findings in computer models to simulate and predict the performance of the full size ropes.

Ironically, because polyester ropes perform so well, there is not yet sufficient information on the nature, extent and rate of the potential polyester rope deterioration mechanisms to carry out such a study.

As this paper is being written, the authors are carrying out laboratory tests and pathological examinations of the near-full-sized polyester ropes which were recently retrieved after two years in the DeepStar TLM in the Gulf of Mexico. Ropes from the proposed TTI/NEL rope durability JIP will also be examined in detail to identify and quantify signs of any deterioration. If any found, these efforts will reveal the principal failure mechanism(s) in polyester ropes.

Computer models which simulate the fatigue performance of several different types of synthetic rope are now available. Once the principal failure mechanisms are known and quantified, it will be possible to use these models to perform a simulation of 20 years fatigue in only a few days. The effects of service variables, such as mean load, amplitude and period, can readily be investigated. And the effects of variations in polyester fibre properties and rope structure on rope fatigue life can be investigated without having to construct actual ropes.

Furthermore, it will then be possible to perform a complete fatigue performance of each leg of a mooring system using realistic load histories for the entire service life before installing the system, and then to reperform this analysis using real load histories while the system is in service. When this can be done, it should not be necessary to remove and test sample ropes from deepwater mooring systems to reverify fatigue life.

CONCLUSIONS

There is now sufficient information to justify the use of good-quality polyester rope in deepwater offshore moorings. Such ropes can be expected to have fatigue performance at least as good as that of typical wire rope. This conclusion is based on examination of the basic polyester fibre properties, performance analysis by computer of low-twist-construction ropes, evaluation of available fatigue test

data on small and large ropes, and consideration of present field service information.

But the fatigue performance of polyester ropes depends upon the fibre quality, the rope construction, and the termination design as well as on the cyclic load history. Thus further laboratory testing may be needed to quantify the effects of the many variables and to provide additional design information for a particular polyester rope design and a particular mooring installation.

It should not be necessary to perform 20 years of fatigue testing before beginning to use polyester ropes in actual mooring systems. A simple fatigue test can be performed to demonstrate that a particular polyester rope has performance equivalent to that of the wire ropes now being used. And this performance can then be reverified by periodically removing samples of rope from service and performing further testing to demonstrate remaining fatigue life.

In the near future, it should be possible to use computer models to simulate synthetic fibre rope testing and field performance. Such computer simulations require an understanding of the principal fatigue mechanisms of polyester ropes, but this knowledge may soon be available from several present joint industry projects. Computer simulations will be much quicker, easier, and more economical than laboratory testing.

REFERENCES

API 2SK (1997) Recommended practice for design and analysis of stationkeeping systems for floating structures, 2nd edition, American Petroleum Institute.

S.J. Banfield and J.W.S. Hearle (1998) Comparative performance of fibre ropes for deepwater moorings, OMAE, Lisbon.

R.L. Bosman (1996) On the origin of heat build-up in polyester ropes, OCEANS 1996 Conference.

A.R. Bunsell and J.W.S. Hearle (1971) A mechanism of fatigue failure in nylon fibres, J.Mater. Sci., 6, 1303-1311.

C.J. Burgoyne and A.L. Merii (1993) Hydrolysis tests on polyester yarns, University of Cambridge, Department of Engineering Technical Report, CUED/D Struct/TR. 138.

Prediction of Wire Rope Endurance for Mooring Offshore Structures, Final Report 1991, JIP managed by Noble Denton.

Phase ψψA (1994), Axial Compression Studies, JIP Tethers 2000 Final Report, Noble Denton Europe Ltd, Tension Technology Int. Ltd and National Engineering Laboratory.

Prediction of Wire Rope Endurance for Mooring Offshore Structures JIP, Partial Life Fatigue and Residual Strength of Six Strand Wire Rope, NEL report 011/92, April 1992.

EDG (1998) Noble Denton Europe and Tension Technology International: Engineers Design Guide for Deepwater Fibre Moorings, Oilfield Publications.

Fibre Tethers 2000 (1995) Joint Industry Study: High Technology Fibres for Deepwater Tethers, NDE/NEL/TTI, Noble Denton Report L17317/NDE/rws, February 10, 1995, with additions June 20,1995.

... ABS Guide For Synthetic Ropes in Offshore Mooring Applications, American Bureau of Shipping, New York, 1999.

... Deep Water Aramid Mooring Line Joint Industry Joint Industry Project, Phase 2 Final Report", Aker Omega, Houston, 1993.

J.F. Flory, "Avoiding Fibre Axial Compression Fatigue in the Design and Use of Tension Members", Proc. Oceans '96 Conferenct, MTS/IEEE, Piscataway, NJ, 1996.

J.F. Flory, M.R. Parsey and S.J. Banfield, "Factors Affecting Life of Synthetic Fibre Ropes in Marine Service" MTS '90 Conference Proceedings, Marine Technology Society, Washington, DC, 1990, Vol 2, pgs 281 - 286

J.W.S. Hearle, R.E. Hobbs, M.S. Overington and S.J. Banfield (1995) Modelling axial compression fatigue in fibre ropes, Proc. 5th ISOPE, 377-383.

J.W.S. Hearle, B. Lomas and W.D. Cooke (1998) Atlas of Fibre Fracture and Damage to Textiles, Woodhead Publishing, Cambridge.

J.W.S. Hearle and M. Miraftab (1991) The flex fatigue of polyamide and polyester fibres, J. Materials Sci., 26, 2861-2867.

J.W.S. Hearle and M.R. Parsey (1983) Fatigue failures in marine ropes and their relation to fibre fatigue, Int. Conf. On Fatigue in Polymers, PRI, London.

J.W.S. Hearle, M.R. Parsey, M.S. Overington and S.J. Banfield (1993) Modelling the long-term fatigue performance of fibre ropes, Proc. 3rd ISOPE Conference, Vol II, 377-383.

R.E. Hobbs, M.S. Overington, J.W.S. Hearle and S.J. Banfield (1995) Element buckling within ropes and cables, Marinflex Conference, University College, London.

Ch. Oudet and A.R. Bunsell (1984) Structural changes in polyester fibres during fatigue, J. Appl. Polymer Sci., 29, 4363-4376.

M.R. Parsey (1982) Fatigue of SPM mooring hawsers, OTC 4307.

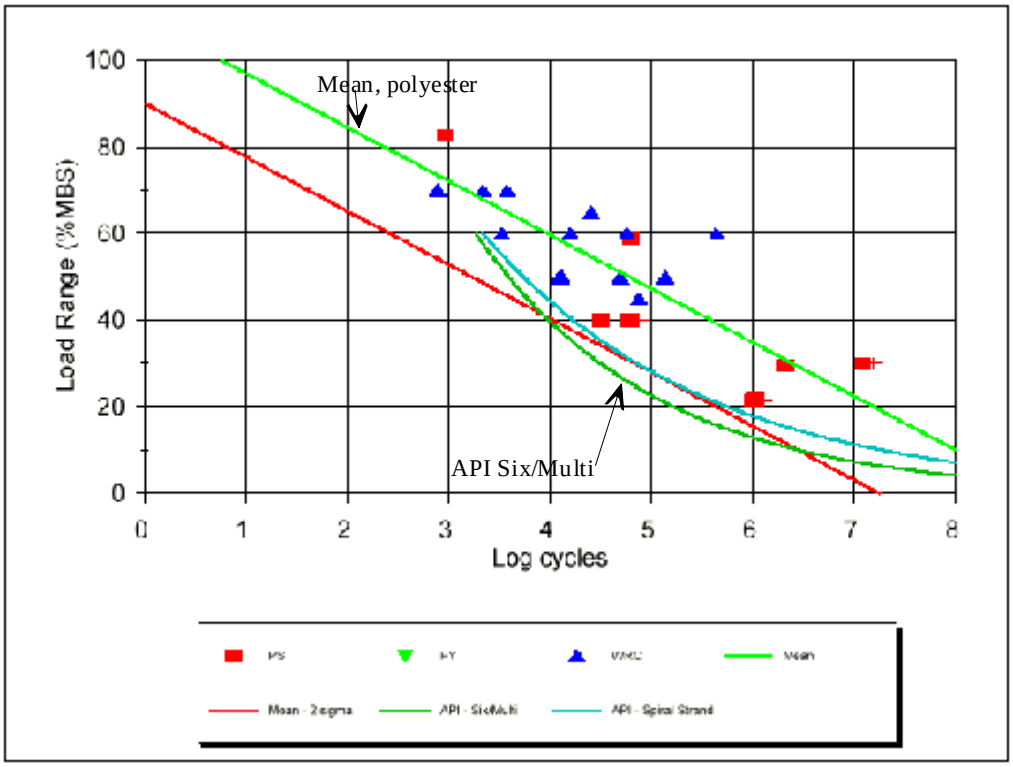

Figure 1a Cycles to Failure, Polyester Data vs. API Wire Rope Design Curve
Load Range on Normal Scale

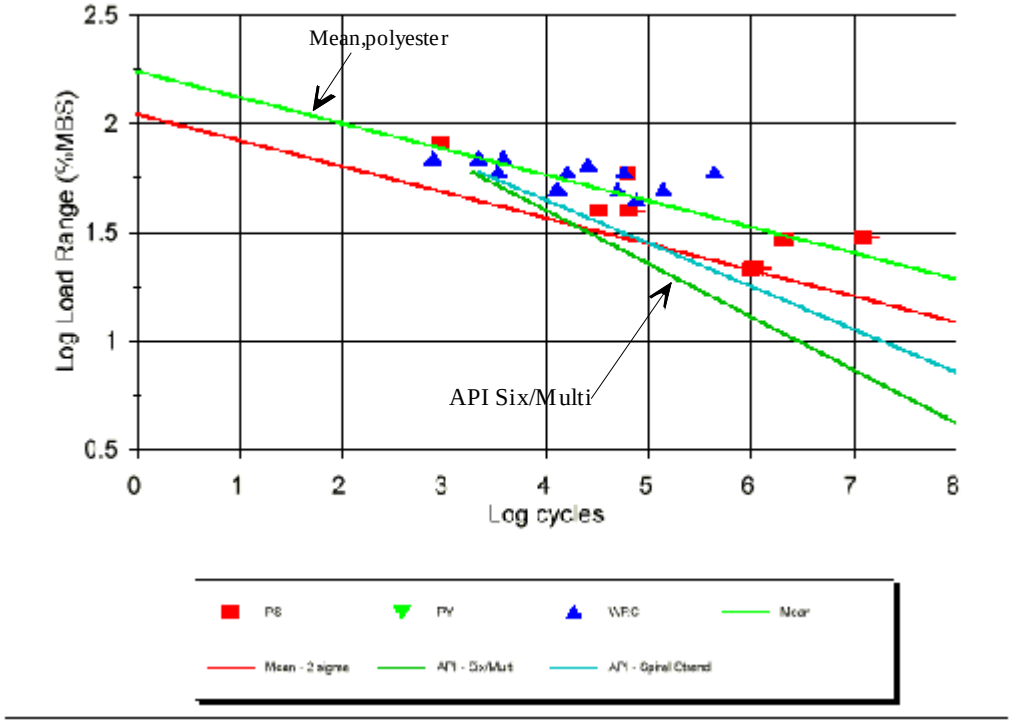

Figure 1b Cycles to Failure, Polyester Data vs. API Wire Rope Design Curve
Load Range on Log Scale

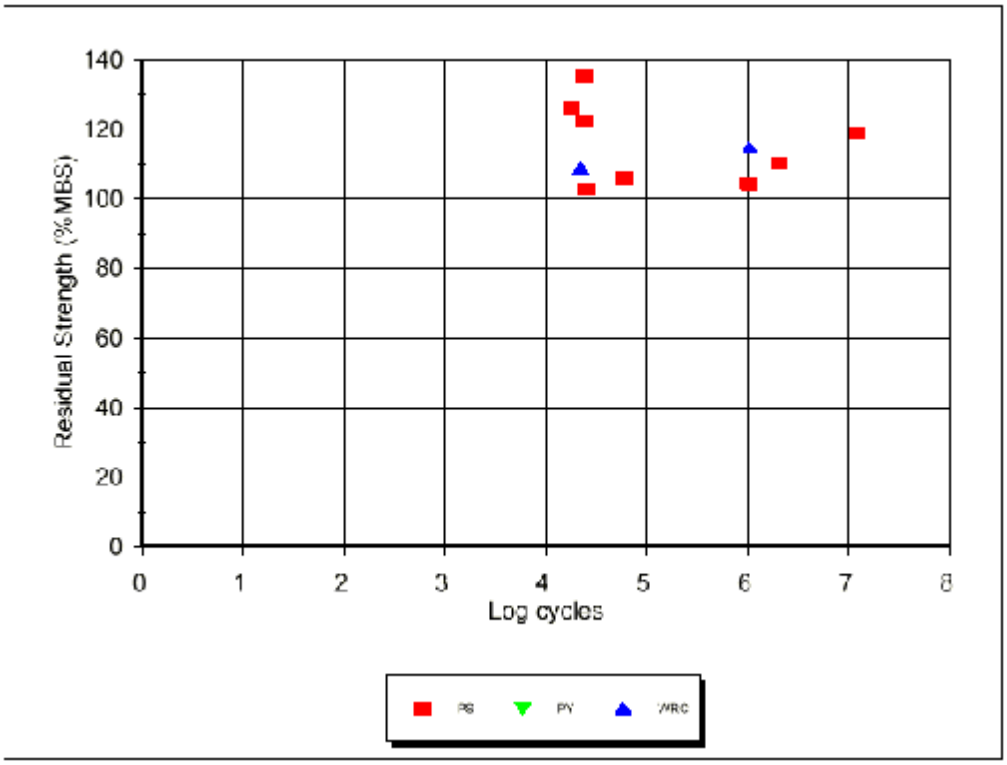

Figure 2 Residual Strength After Cycling, Polyester Rope Data

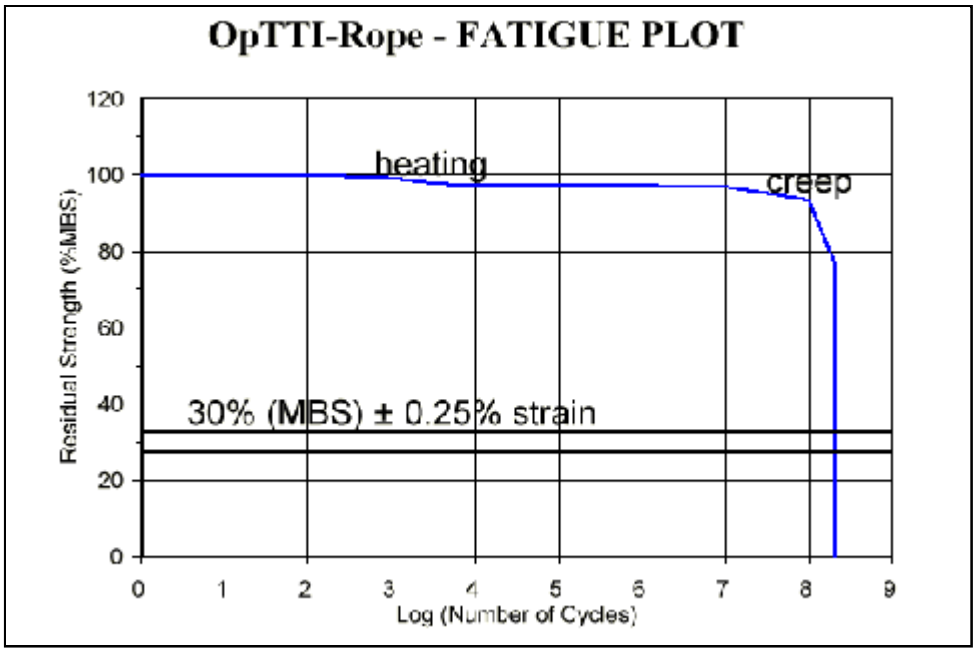

Figure 3 Residual Strength vs. Applied Cycles, Modelling Simulation Using OpTTI-Rope Computer Program

Geotextiles and Geomembranes 1 (1984) 119–141

Geotextiles in Coastal Engineering—25 Years Experience

G. Heerten

Naue Fasertechnik, Gewerbestrasse 2, d 4992 Espelkamp-Fiestel, Federal Republic of Germany

ABSTRACT

During the use of geotextiles in coastal engineering for over 25 years many construction methods have been improved or have been made more economical. Sometimes completely new solutions for coastal engineering problems can be recommended. This paper gives information about the long-term behaviour of geotextiles in coastal engineering and the minimum requirements for their application. Some case studies show the necessity of careful geotextile selection, considering the special requirements of the application, the harsh coastal engineering environment and the rough building practice found in all fields of hydraulic engineering.

1. INTRODUCTION

Coastal engineering was the starting point for the use of synthetic fabrics in geotechnics in the 1950s. Pioneers of coastal engineering first used synthetic fabrics to form huge sand bags for building groins and closing dikes. Based on the advantages of these fabrics (low weight, high strength, long-term resistance) woven and, more recently, nonwoven fabrics have been of growing use in coastal engineering and, latterly, in waterway engineering, dam construction, road construction, railroad construction, tunnelling—all fields of geotechnical engineering.

In the 25 years of geotextile application development many tests and investigations have been carried out and many construction and design

Geotextiles and Geomembranes 0266-1144/84/$03.00

methods have changed owing to the growth in experience. Today we have the expertise for the successful use of geotextiles in design and construction in coastal engineering applications. The objective of this paper is to disseminate the fundamental principles for the successful use of geotextiles in coastal engineering.

2. THE GEOTEXTILE SCENE IN COASTAL ENGINEERING

The following examples give a rough idea of geotextile applications in coastal engineering today:

(i) filters in erosion control structures as revetments of seadikes (Fig. 1), seawalls or bottom protection structures, e.g. of sluices or storm surge barriers (Fig. 2);
(ii) separator in the foundation of groins and breakwaters (Fig. 3);
(iii) fabric forms for sand filled bags or tubes as construction elements of groins and dikes (Fig. 4);
(iv) flexible scour protection mats at different offshore and coastal structures.

Usually, in design drawings of coastal structures, a geotextile is only a line of black ink labelled 'geotextile' or 'synthetic filter cloth'. But when selecting a suitable fabric for a special coastal engineering application the engineer has to learn that various types of fabrics are offered; woven, nonwoven and combinations, produced from different polymers.

The properties of these fabrics are very different, influenced by the polymer properties and by the manufacturing process. Unfortunately there exists a lot of different testing methods used by the manufacturer to

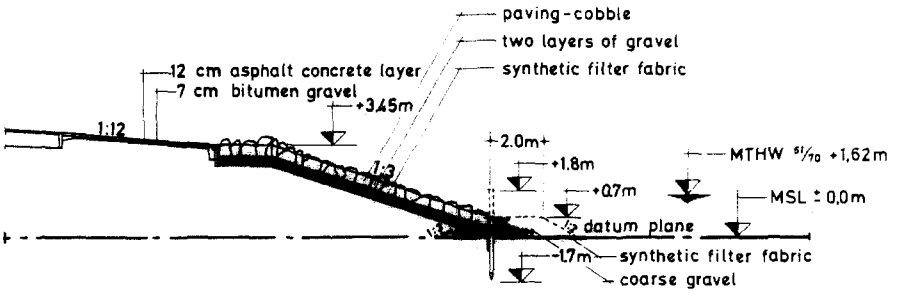

Fig. 1. Cross-section of revetment of a seadike without foreland (Northfrisian Coast).

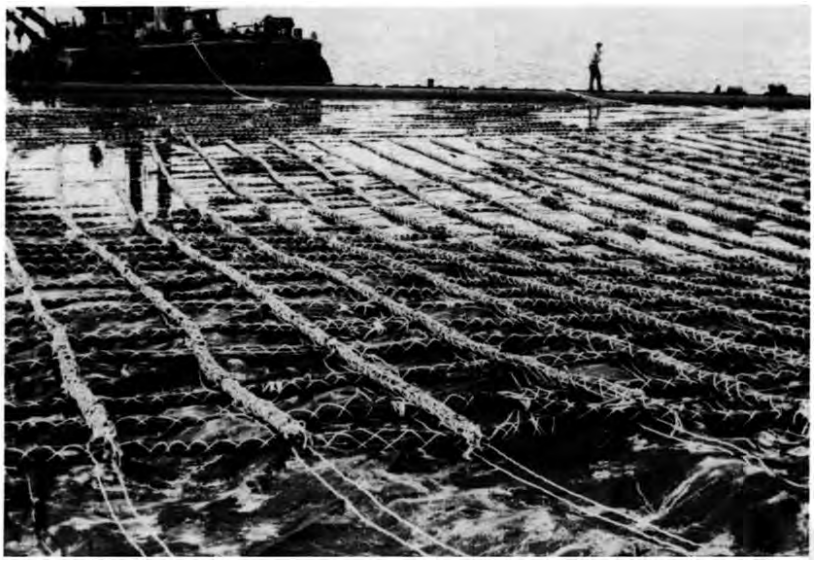

Fig. 2. Willow-fascine mattress for bottom protection.

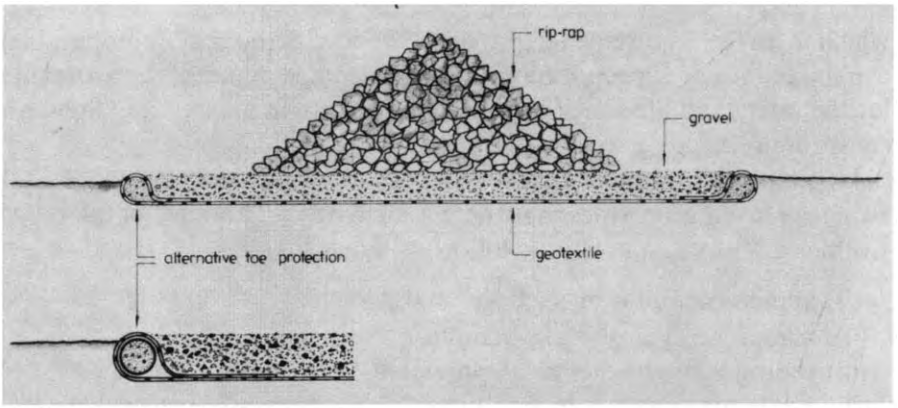

Fig. 3. Foundation of a groin on top of a geotextile.

estimate the properties of the fabrics. Therefore product data of different fabrics are not comparable in many cases. An optimal fabric selection is often difficult and sometimes impossible.

The engineer using geotextiles has to compare the geotextile properties and the requirements of the structure given by design rules or other standards or recommendations. Only if there are two or more fabrics

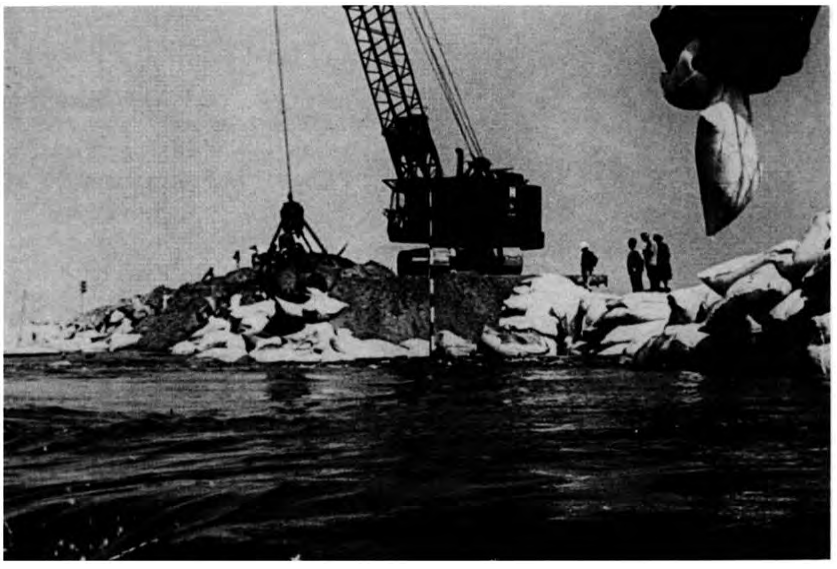

Fig. 4. Closing a dike with huge sand bags.

which meet the requirements (provided the test methods are comparable) can the economic aspects be considered. The importance of the geotextile for the safety and life-time of the whole structure in most cases allows no compromise relating to fabric properties.

In addition it should be borne in mind when designing a coastal structure using geotextiles that there is currently an absence of quantitative design information in the following areas:[1]

(i) admissible uplift or suction forces;
(ii) resistance against wave action;
(iii) sliding against soils to be protected;
(iv) water movement into and out of the soil mass being protected;
(v) general system permeability.

If an improper choice of fabric or system is made in any of these areas, failure could result. Coastal engineering demands the use of heavy weight fabrics of high robustness and permeability.

The following properties are important for geotextiles in coastal engineering:

(i) high filtering efficiency (soil-tightness *and* permeability);

(ii) high robustness for a safe installation (good resistance to puncture and to tear; sufficient stress/strain behaviour for the given installation method);
(iii) sufficient long-term resistance to UV-degradation and to the marine environment;
(iv) high friction resistance with soil (on slopes).

Geotextile application in the harsh environment of coastal engineering is somewhat more of a challenge than the fabric uses in many other applications. An unsuccessful installation can often be seen within a short period of time by irregular deformation of the structure or total damage.

Extensive damage occurred, for example, to the bottom protection structure of a storm surge barrier at the Northfrisian coast, West Germany, after some years of service. After intensive investigations it could be shown that damage was not caused by insufficient long-term resistance of the polyamide multifilament woven fabric (200 g/m^2) but probably by unexpected instability problems in the armour layer and damage caused during construction by heavy bulldozers and excavators running on the gravel layers above the fabric. This example also underlines the demand for heavy weight fabrics in coastal engineering.

3. LONG-TERM EXPERIENCE WITH FABRICS

3.1. Field investigations

To extend knowledge about applications and long-term behaviour of geotextiles in coastal engineering a special research programme was carried out at the Franzius Institute for Hydraulic Research and Coastal Engineering of the University of Hanover.[2,3]

The field investigations on coastal structures mentioned before were the most important part of the research programme. At 13 locations on the North Sea coast of the German Bight sampling operations were carried out and samples of 39 fabrics were taken.

Sixteen samples of revetments of seadikes were dug up and 23 samples of woven fabrics were taken from sand bags and sand filled tubes.

Figure 5 gives an impression of the sampling operation on a seadike

Fig. 5. Sampling operations at the seadike revetment.

revetment at the Dithmarscher Bight on the North Frisian coast. In Fig. 6 a nonwoven fabric is shown after removal of the cover layers of the revetment.

An example of the application of sand filled tubes as stabilizing elements in a beach feeding area is found on the Isle of Langeoog.

From the sandbags and sand filled tubes two different samples could be taken, one of the weathered upper side and one of the protected bottom side. Thus it is possible to obtain information about the influence of weathering on the long-term resistance of the fabrics.

An important result of the investigations on seadike revetments is the registrated extensive filling of the coarse gravel layers with sand and mud particles. Owing to the filling of the coarse layers with sand and mud the boundary layer of fabric and subsoil was protected against dynamic wave attack. This situation also gave stability in revetment sections with fabrics of a larger opening size than expected.

Additional investigations led to the conviction that the sand and mud particles in the coarse layers came mostly from the sea side of the construction and not from the bottom side. Some significant profile changes with a flatter slope of some revetment sections were perhaps caused by soil-liquefaction under wave impact but certainly not by a soil washout through the filter-fabrics.

Fig. 6. Needle-punched nonwoven fabric after removing the revetment cover layers.

3.2. Results for long-term resistance

A usual method for obtaining information about the long-term resistance of synthetics is a comparison of tensile strength of the new and of the aged material. The strength testing procedure used corresponds to the conventional textile strip tests such as the German standard DIN 53857. Samples of multifilament woven fabrics and needle-punched nonwovens of polyester, polyamide and polypropylene as well as samples of tape-fabrics of polyethylene and polypropylene were investigated. Figures 7 and 8 show the average values of residual strength for the different polymers investigated for both weathered fabrics and protected fabrics.

It can be seen that the residual strength of weathered tape-fabrics of polyethylene or polypropylene as base material is higher than the residual strength of multifilament fabrics of polyester, polyamide and polypropylene. Comparable results are given for protection against ultraviolet irradiation but nevertheless, in general, the decrease in residual strength is significantly larger under weathered conditions.

From the interpretation of these results we have to consider that fibre fineness is of great influence in the long-term resistance of fabrics. Therefore the good results of the tape-fabrics, produced from relatively

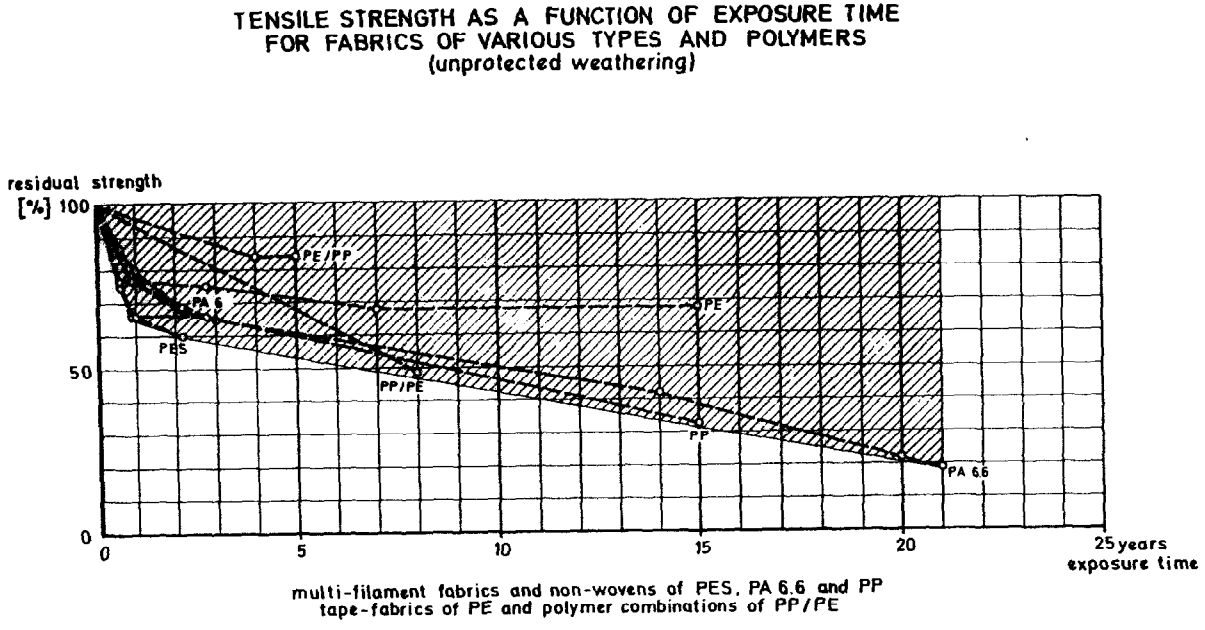

Fig. 7. Decrease of fabric strength, fabrics being unprotected by cover layers. PE, polyethylene; PP, polypropylene; PA 6, polyamide 6 (Perlon); PES, polyester.

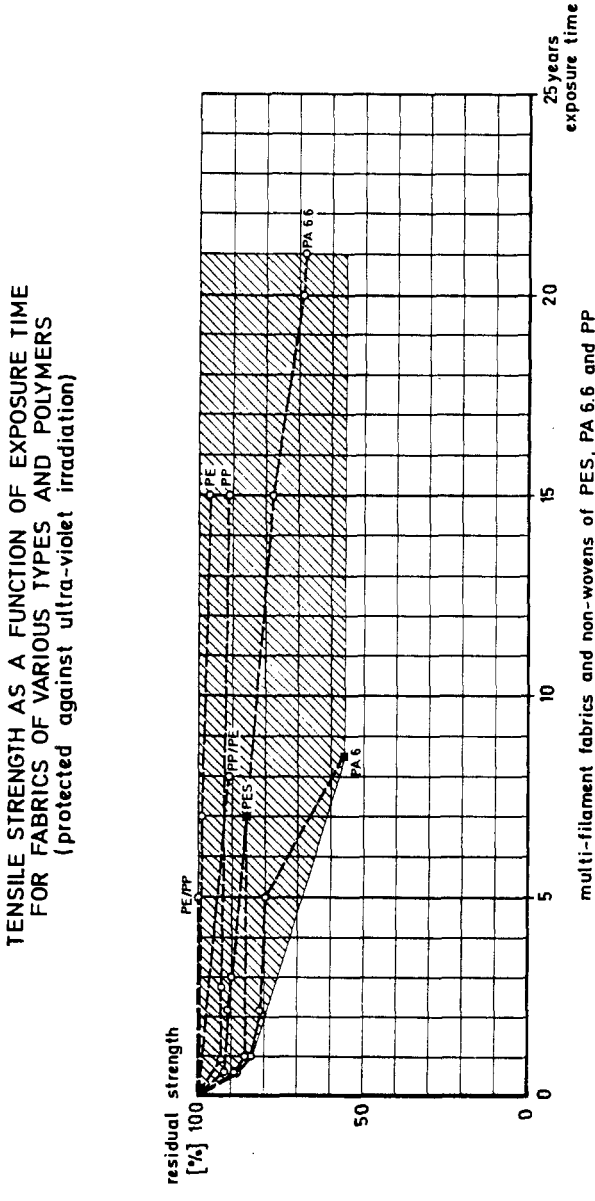

Fig. 8. Decrease of fabric strength, fabrics being protected by cover layers. PE, polyethylene; PP, polypropylene; PA 6, polyamide 6 (Perlon); PES, polyester.

thick tape-threads, is not surprising. The fibre fineness of the tape-threads is a few hundred dtex whereas the fibre fineness of filaments is only 5 to 10 dtex. In addition we have to consider that the results determined from samples in the saltwater region could be influenced by many parameters, such as suspended load of the seawater; duration of tidal flow; covering of the fabrics by mud, seawater, micro-organisms or rubble and the temporary variations in these coverings; drifting wood; ice; shipping and tourists. Most of the parameters only influenced the sections with unprotected weathering such as the upper sides of the sand filled tubes in beach feeding areas. Synthetic filter-fabrics in revetments protected by several cover layers are less endangered but it is important to ensure that there is no damage to the fabrics during construction.

Finally we can say that the most important parameters influencing the long-term resistance of fabrics in the saltwater region of the North Sea coast are ultraviolet irradiation and the raw material and fibre fineness of the fabric. Ageing by biological and chemical damage is of very low importance, but attention must be paid to ensure that there is no damage to fabrics during construction.

3.3. Results of long-term filtering

After geotextile and armour layer(s) have been carefully installed the successful service life of the structure depends mainly on the filtration properties of the fabric. The traditionally used filter materials such as sand and gravel are designed from the well known filtration rules, e.g. from Terzaghi or the US Corps of Engineers.[5] From this a relation between the diameters of the soil particles of the subsoil and the filter layer is found. In many cases the filter on fine soils has to be built up from two or more separate filter layers. Limited by the accuracy of installation techniques in underground construction work with heavy machines such as excavators and bulldozers, the thickness of these filter layers has to be 20 cm minimum. This minimum thickness is not given by the filtration rules mentioned above but is found from experience in underground construction work. Wittmann[4] showed that the thickness of a filter layer affects its performance. Many of the filter layers designed by the given filtration rules would fail, not having the thickness of 'filtration length' of about 20 cm minimum. A filter layer of soil particles does not work as a thin sieve but as a filtration body with a given pore size distribution built up from all the soil particles of the filter layer and the incorporated subsoil

particles. The interaction of the original subsoil and the soil particles of the filter layer is very important for forming a stable, long-term working filter layer.

In discussing the filtration properties of geotextiles we have to distinguish between the properties of woven and nonwoven fabrics. The filtration properties of woven fabrics are given by the mesh size or the fabric openings. The woven geotextile acts as a thin sieve. The filter conditions could be stable, with nearly all soil particles being larger than the mesh size, or unstable, with nearly all soil particles being smaller than the mesh size. Unstable conditions are often found on subsoil in the range from silty sands to clay and are found in most polders.

The filtration properties of nonwoven geotextiles are influenced by the fibre size, the fabric weight and thickness. Thermal bonded nonwoven fabrics are relatively thin and act almost as a woven fabric with irregular openings. Needle-punched nonwoven fabrics are considerably thicker than all other types of geotextiles. Owing to the needle-punching process the void volume of needle-punched geotextiles is about 85% or more. The filter conditions are comparable to soil-filter conditions. The interaction of fibres and soil particles forms a stable, long-term working filter layer. The author's own investigations have confirmed these conditions.[2,3] In Fig. 9 some data for virgin nonwoven fabrics (porosity n, permeability k_n) and for the dug-up fabrics (pore space clogged by soil, remaining porosity n', remaining permeability k'_n) are given.

The estimated permeability of the clogged geotextiles remained 5 to 12 times higher than the measured soil permeability, which is in the range of $k \sim 1{\cdot}0$ to $5{\cdot}0 \times 10^{-5}$ m/s. The remaining porosity of n' (0·32 to 0·74) guarantees an adequate long-term permeability. In contrast to these results, for most of the investigated woven fabrics a lower permeability, compared to that measured in the soil, was estimated.

The water permeability of woven geotextiles is often reduced significantly by the openings in the mesh becoming blocked by a grain particle. $k_{\text{geotextile}}/k_{\text{soil}}$ permeability ratios of 0·16 to 1·8 have been established for samples which have been dug up from the seadike revetments. The given results underline the advantageous filtration properties of needle-punched nonwoven geotextiles.

The tests on the needle-punched nonwovens which had been dug up showed additionally that these products are not compressed in contact with fine soils and sands as a result of spontaneous grain/fibre/grain contacts by an amount in proportion to the load placed on them, but

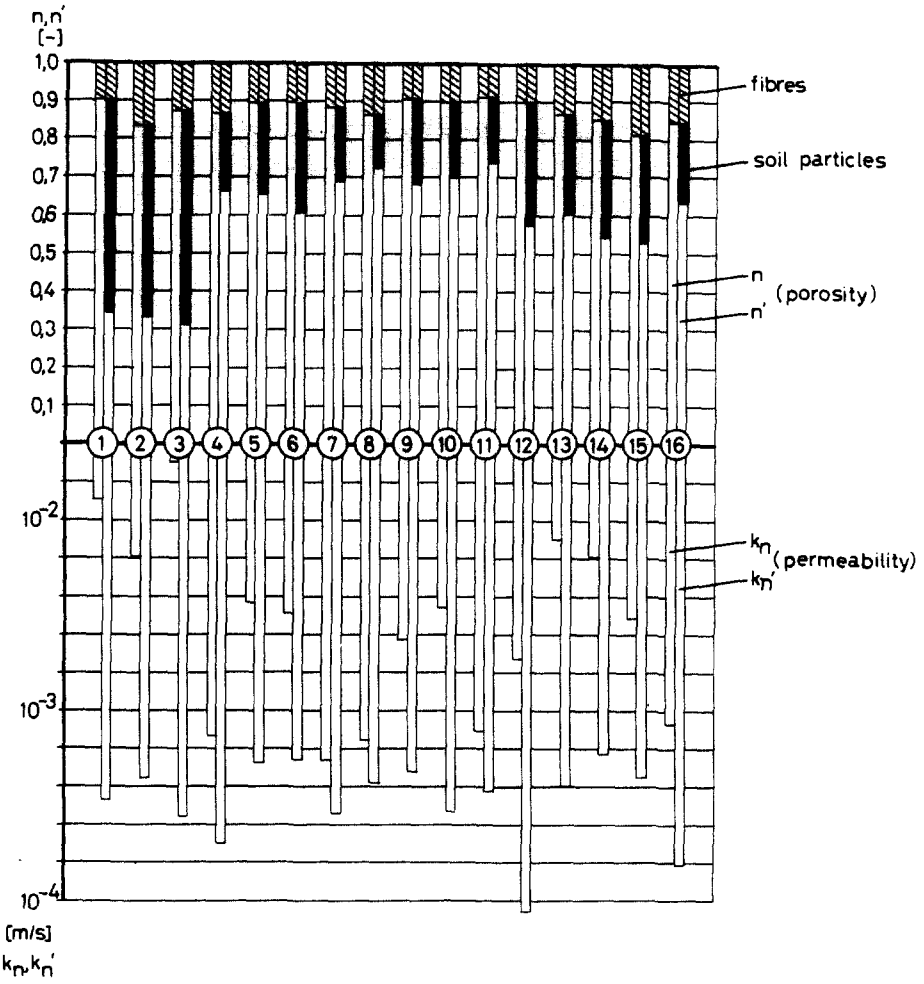

Fig. 9. Clogging of voids volume and permeability decrease of dug-up needle-punched nonwoven geotextiles, samples 1–16.

instead maintain their manufactured filter thickness. This initially unexpected form of behaviour was even demonstrated in the case of needled nonwovens which had been dug up from 4·5 m high road embankments.

The properties which characterize the filtering properties of geotextiles are the 'effective opening width' D_w, and the water permeability coefficients k_v (vertical to the plane of the geotextile) and k_H (in the plane of the geotextile). The appropriate test equipment for the determination of the

filter parameters of geotextiles is to be found in the Franzius Institute for Hydraulic Research and Coastal Engineering at the University of Hanover.

The ancillary technical conditions for the tests are described in the literature.[3] D_w required is given by filtration rules as a function of the particle distribution curve of the soil and the load conditions. The filtration rules for the sand-tightness of geotextiles on noncohesive soils are determined as follows (C_u = uniformity d_{60}/d_{10} where d is the soil particle diameter):

static load conditions, $C_u \geqq 5$:

$$D_w < 10\ d_{50}$$
$$\text{and } D_w \leqq d_{90}$$

static load conditions, $C_u < 5$:

$$D_w < 2{\cdot}5\ d_{50}$$
$$\text{and } D_w \leqq d_{90}$$

dynamic load conditions:

$$D_w < d_{50}$$

Since, as a result of their efficient cohesion, fine-grained soils with $d_{50} < 0{\cdot}06$ mm behave more favourably than coarse-grained ones in terms of their mechanical filtering stability, comparatively larger widths of opening may be accepted with geotextiles so that the following rule for the design of geotextile filters for the full range of loading situations can be approved:

$$D_w < 10 \cdot d_{50} \text{ and } D_w \leqq d_{90} \text{ and } D_w < 0{\cdot}1 \text{ mm}$$

The value $D_w < 0{\cdot}1$ mm is comparable with the values quoted by the US Corps of Engineers, which approves a filter grain diameter of $d_{15} = 0{\cdot}4$ mm for plastic and semi-plastic clays.[5] In the case of a semi-compacted bedding of the filter earth, this corresponds to a pore diameter of:

$$\frac{d_{15}}{4} = 0{\cdot}1 \text{ mm}$$

Static load conditions are given by laminar flow including the change of flow direction. Dynamic load conditions are given by high turbulent flow, wave attack or pumping phenomenon. In a second step the

hydraulic conditions have to be controlled by estimating the permeability-reduction factor as described by Heerten.[2,3] By this the interaction of soil and geotextile is considered and hydraulic over-pressures in a revetment construction are prevented. To avoid permeability problems the use of thick needle-punched nonwoven geotextiles could be recommended in relation to the results of the investigations on dug-up fabrics.

4. EXAMPLES OF GEOTEXTILE APPLICATION

In the following sections three examples of the uses of geotextiles in coastal engineering are described. The case studies are only highlights of some geotextile applications in coastal engineering, showing the different requirements in construction and the different fabric selection.

4.1. Oosterschelde storm surge barrier—filter mattress

The closing of the Veerse Gat, Haringvliet (Fig. 10), Brouwershavense Gat and Oosterschelde shortens the coastline of the Netherlands by 700 km. At present, as the last part of the giant 'Delta Project' the Oosterschelde storm surge barrier is under construction. This consists of monolithic prefabricated piers, the seabed between them being raised by a sill construction of quarry stone and threshold beams. The piers, the sill

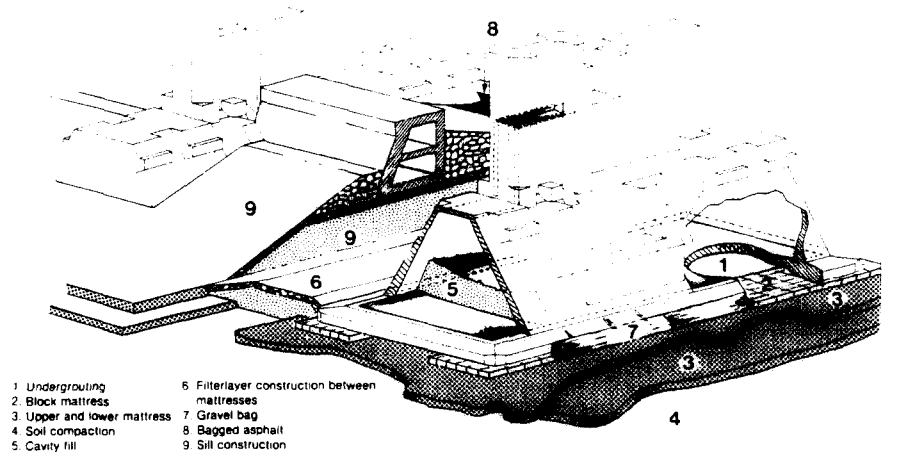

Fig. 10. Oosterschelde storm surge barrier: sill and pier construction.[6]

and the beams together form the frame within which steel sliding gates can be raised and lowered.

After removing bed soils by dredging and replacing with better quality sand the seabed was compacted to a depth of up to 15 m. In the base on which the concrete piers have been placed, an extra layer has been added in the form of a prefabricated filter mattress because no settlement due to any loss of material can be tolerated under the piers (Fig. 10). Two kinds of mats have been placed on the seabed:

—a base mat measuring 200 × 42 m with a thickness of 36 cm;
—an upper mat of 60 × 32 m, also 36 cm thick.

Both mats (Fig. 11), approximately 700 000 m^2, are being manufactured in a purpose built factory and are wound on to a floating cylinder and, after towing into position, are submerged by a special pontoon. Thus under each of the 66 piers (up to now 8 piers have been placed with very good results) there will be two mats: the lower one will be the filter mat proper, intended to keep the sand in place, while the purpose of the second one will be to distribute the weight of the pier and to protect the lower mat. The filter mattress has been designed in accordance with the filter rules for granular materials. Each layer should be physically impermeable to the layer below (soil-tightness), although water is able to pass through freely. To hold the fine Oosterschelde sand in place a filter must be composed of a layer of sand (grain size 0·3 to 2 mm), a layer of fine gravel (2 to 8 mm) and a layer of gravel (8 to 40 mm). These grain sizes are not resistant to the current velocities in the Oosterschelde estuary. For placing these layers it was decided to prefabricate a filter mattress on-shore by packing the granular materials into a system of geotextiles.

The development of mat design, production, transportation and installation has demanded large-scale research on geotextiles.[7,8] To fulfil the design requirements (strength of 800 kN/m in longitudinal direction and 80 kN/m in widthwise direction) a woven polypropylene fabric has

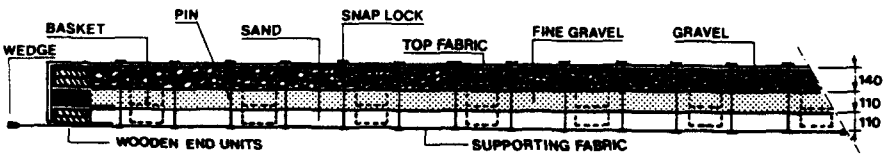

Fig. 11. Oosterschelde storm surge barrier: filter mattress construction (dimensions in mm).[6]

been developed which is reinforced lengthways with 2·7 mm diameter steel wires and which has a fabric weight of 4400 g/m^2. This *supporting fabric* has to take the stresses and strains during winding onto the cylinder and installation. In order to meet the sand-tightness requirement a heat bonded polypropylene nonwoven fabric is placed on top of the supporting fabric. The heat bonded nonwoven is also used as a *separator* between the sand and fine gravel. Between fine gravel and gravel a woven fabric composed of polyethylene monofilaments has to be used to fulfil the permeability requirement. These fabrics are also used for the vertical dividers which are inserted in the mattress to prevent the granular filter material from shifting in the longitudinal direction and to guarantee the mattress thickness during winding and sinking operations. U-shaped baskets are turned inwards to enclose the nonwoven or woven fabric.

The *top fabric* is the outer cover of the filter mattress. For following the curve of the winding-up cylinder the fabric has to meet high strain requirements and, in addition, a permeability to water which corresponds to that of the upper gravel layer. The woven fabric developed is composed of polyamide warp yarns and polyester weft yarns. It can take 25% strain in the longitudinal direction with a strength of 100 kN/m and at the same time 15% strain in the width direction with a strength of 80 kN/m.

Steel pins are used as vertical joints between the supporting fabric and the top fabric to consolidate the sand and gravel layers together into a compact mattress.

4.2. Port Kembla seawall, Australia

In June 1977 the New South Wales government decided to construct a new coal loader at Port Kembla, approximatley 90 km south of Sydney. To provide additional land for coal stockpiles it was necessary to construct a 1200 m long seawall, fronting the Pacific Ocean, in water depths up to 2 m below low water and to reclaim the stockpile area behind the wall. The seawall is part of an embankment containing a roadway and rail mounted stackers servicing half of the total stockpile area. The integrity of the seawall is important in the seawall design and construction as damage or settlement will affect the operation of the stackers. The seawall design must include consideration of a water level change of 4·0 m, including wave set-up, a design breaking wave height of 5·5 m and a scouring depth at the toe of 2·0 m. Two preliminary seawall

designs were prepared with 12 t hanbars and 7 t dolosse as alternate primary armour layers. Both designs included heavy needle-punched nonwoven geotextiles replacing standard filter material. Some construction details are given in Fig. 12.

The stability of the seawall depended on the integrity of the toe of the structure. The difficult construction requirement of excavating a toe within the surf zone where there were large quantities of mobile sand, and the impossibility of satisfactorily placing conventional filter material, led to the adoption of a synthetic filter cloth material. Materials were subject to extensive field tests to ensure that a suitably robust cloth was available to withstand placement and movement of sub-armour (1·5 to 3·0 t rocks) and primary armour (15 t hanbars) without damage to the cloth. On the slack fill slope under the 1·5 to 3·0 t rocks a needle-punched nonwoven fabric produced from polyester fibres with a weight of 1200 g/m^2 has proved its robustness against this heavy stone dumping operation (Fig. 13). Lighter geotextiles are punctured and destroyed during field tests.

On the slope of the toe excavation directly under the 15 t hanbars a needle-punched nonwoven geotextile with a weight of 2000 g/m^2 was selected as a suitable fabric for this special application. Potential problems associated with the placement of the nonwoven fabric in the toe excavation and securement before overlying material was placed, were recognized. A concrete block filter mat was designed as a method of holding the geotextile in position until rock and armour units were placed. The prefabricated block mat consisted of 25 × 670 kg concrete blocks laced together with polyester ropes (see Fig. 12).

On achieving the design section for the toe trench, the dragline laid the concrete block filter mat from the toe of the trench back to the working platform, the geotextile was tied back to prevent excess movement in the waves, rock sub-armour was placed on the landward end of the filter cloth, and hanbars were placed in the toe trench. This operation had to be carried out in the one construction sequence so that sand did not move onto the filter cloth before the placement of the armour and the sub-armour. Each concrete block filter mat was overlaid on the previous mat with a 1·5 m overlap.

Although the concrete block filter mats weighed approximately 18 t in all, and acted as huge sails in strong winds, they could be positioned in winds up to 25 knots (Fig. 14). The adoption of the concrete block mats with heavy nonwoven geotextiles in lieu of rock resulted in a total saving of approximately $600,000 over the 1200 m length of wall.

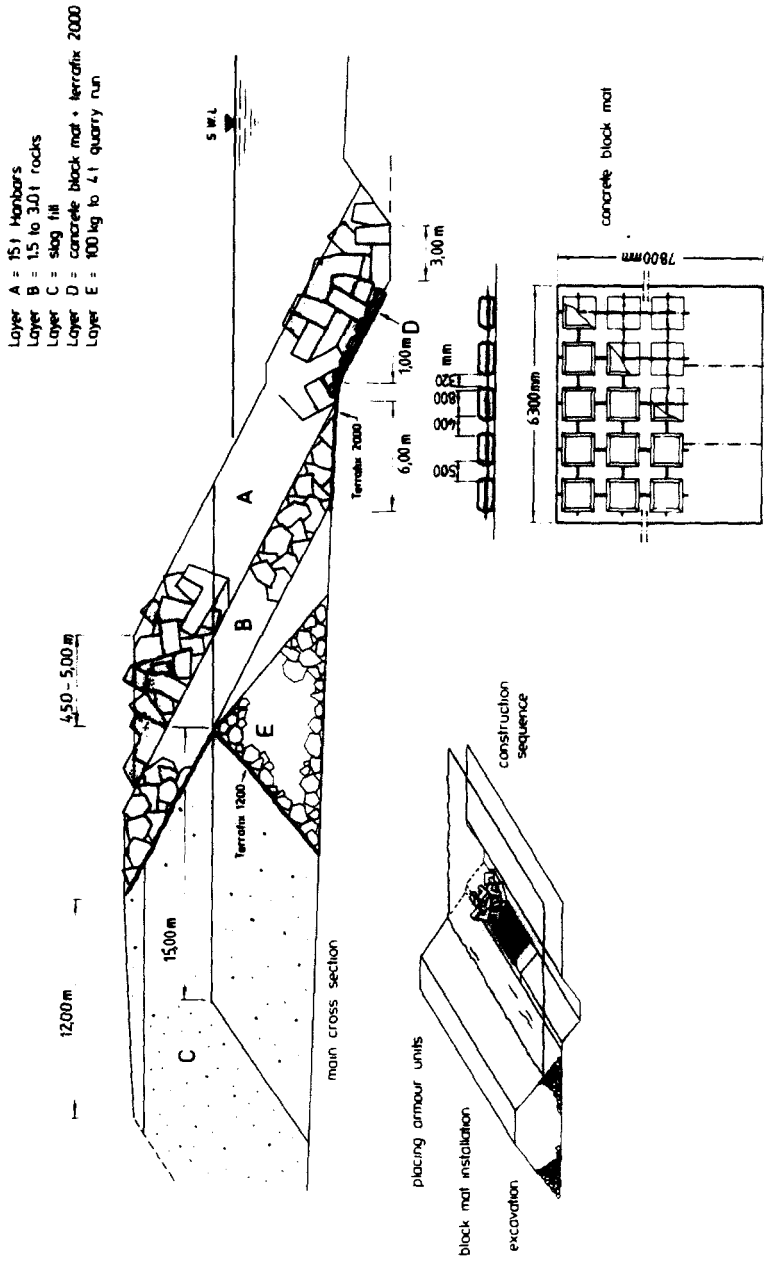

Fig. 12. Port Kembla Seawall, Australia: construction details, SWL = sea water level.

Fig. 13. Port Kembla Seawall, Australia: field tests on geotextile penetration resistance.

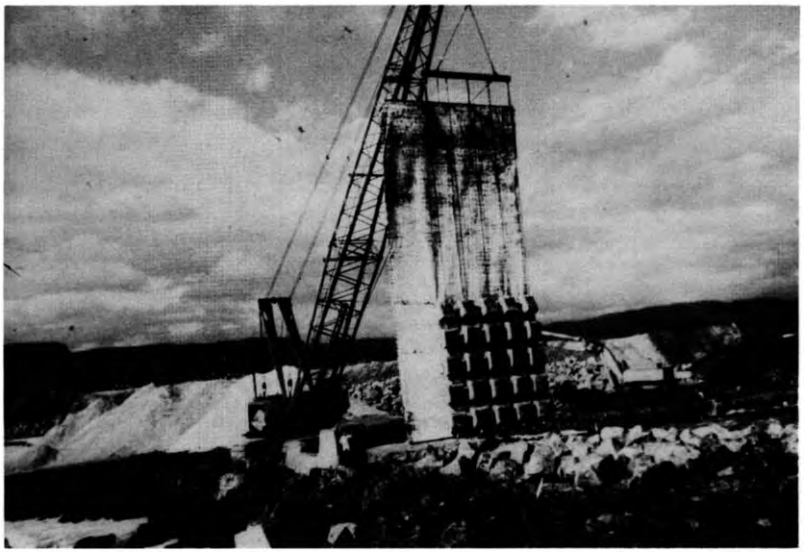

Fig. 14. Port Kembla Seawall, Australia: fabric and concrete block mat installation.

4.3. River works at the River Weser, Germany

With the increase in the size of ships many estuaries up to the important ports have been deepened. As well as the increased use of large scale dredging, river works to control flow and tidal range such as groins and training walls have been erected.

At present, the River Weser having been deepened to 12·0 m below chart datum up to Nordenham and to 9·0 m below chart datum up to Bremen, several groins are under construction. The groins will serve to stabilize the shipping channel and to minimize the increase of the tidal range, which has been expressed mainly as a sinking of the tidal low water.

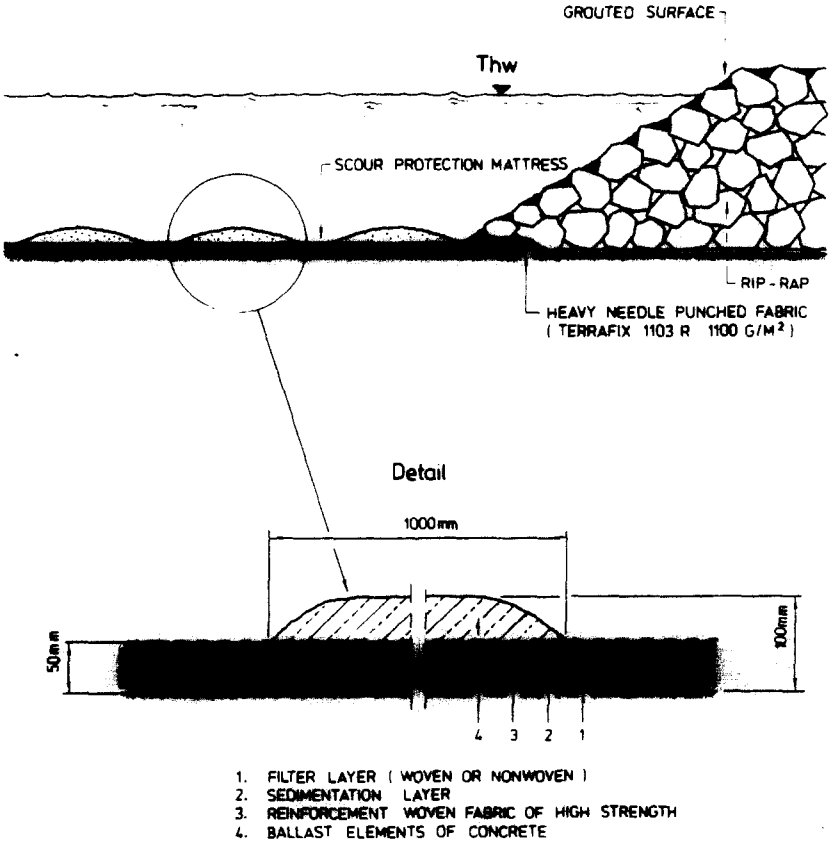

Fig. 15. Groins at the River Weser: construction details.

In a large river work programme 100 groins will be built using a new construction method, with geotextiles in the groin section down to tidal low water. In the underwater section the conventional construction method using a willow-fascine mattress for the groin foundation will be used.

Figure 15 shows the groin cross-section with the foundation base above tidal low water using the new construction method as follows. On a heavy weight needle-punched nonwoven fabric (1100 g/m^2) the rip-rap core of the groin is dumped. With an overlap of approximately 500 mm on both sides of the groin a special scour protection mat is installed. Instability problems caused by scouring at the sides in the past led to crest sinking and damage of the groins. By fixing the upper stones of the groin core by grouting with concrete mortar an additional demand for high stability is dealt with.

The filter mat in the foundation base of the groin has to fulfil the tough requirements on geotextiles for hydraulic engineering laid down by the Federal Institution of Waterways Engineering (BAW), Karlsruhe, Germany. This means, for the given local soils of silty sand, clay and mud, that the geotextile has to prove, for example, its filtering efficiency in the very tough turbulent test and its penetration resistance in a special test with a dynamic load of 600 Nm, corresponding to a 300 N stone falling from a height of 2·0 m. Standard requirements, confirmed in more than 10 years of installing millions of square metres of geotextiles in revetments and other hydraulic structures, are a minimum thickness of 6·0 mm and a strength (DIN 53858, grab-test) of 800 N for safe installation and adequate long-term behaviour.

The scour protection mat is composed of four parts (Fig. 15):

(i) woven or nonwoven filter layer: soil-tightness, permeability and acting load have to be considered;
(ii) sedimentation layer: approximately 5 cm thick, made of needle-punched and chemically bonded curled coarse fibres, it reduces the drag forces in the boundary layer of the seabed so that sedimentation takes place increasing the weight and stability of the structure;
(iii) reinforcement fabric: by means of wide meshes (approximately 20 mm) and very high tensile strength the fabric combines and reinforces the ballast elements securely, providing a high degree of flexibility and adaptability with plenty of strength in reserve;
(iv) ballast elements: approximately 0·5 m in diameter and 0·1 m in

height, with a minimum distance of approximately 0·2 m between the rims of the elements, they stabilize the scour protection mattress during the sedimentation phase.

Figure 16 shows a groin under construction. The nonwoven geotextile and the scour protection mattress are installed. The geotextile is fixed on the seabed by a first layer of stones. The special concrete vessel is still anchoring after ballasting the mat at the site.

Fig. 16. Groin at the River Weser: under construction at tidal low water.

5. CONCLUSION

In this short paper some fundamentals of geotextile applications in coastal engineering are given. The case studies of geotextile applications in coastal engineering works show the necessity of knowing the geotextile performance for successful design and construction. In many cases the geotextile, its suitable selection, its safe installation and its adequate long-term behaviour, are of decisive importance for the life-time and safety of the whole structure. In coastal engineering there is a demand for heavy fabrics of high robustness.

REFERENCES

1. Koerner, R. M. and Welsh, J. P., *Construction and Geotechnical Engineering Using Synthetic Fabrics*, John Wiley & Sons Inc., New York (1980).
2. Heerten, G., Long-term experience with the use of synthetic filter fabrics in coastal engineering. *Proc. 17th Int. Coastal Engineering Conf., Sydney* (1980) 2174–93.
3. Heerten, G., Dimensioning the filtration properties of geotextiles considering long-term conditions. *Proc. Second Int. Conf. on Geotextiles, Las Vegas*, **1** (1982) 115–20.
4. Wittmann, L., Soil filtration phenomena of geotextiles. *Proc. Second Int. Conf. on Geotextiles, Las Vegas*, **1** (1982) 79–83.
5. Teindl, H., Filterkriterien von Geotextilien, *Straßenforschung Heft 153, Bundesministerium fur Bauten und Technik*, Vienna (1980).
6. Scour protection and foundations for the storm surge barrier, *Report no. 28E, Information Dept., Ministry of Transport and Public Works*, The Hague (1981).
7. Dorr, H. G. and de Haan, D. W., The Oosterschelde filter mattress and gravel bag. *Proc. Second Int. Conf. on Geotextiles, Las Vegas*, **1** (1982) 271–6.
8. van Harten, K., Analysis and experimental testing of load distribution in the foundation mattress. *Proc. Second Int. Conf. on Geotextiles, Las Vegas*, **1** (1982) 277–82.

LONG TERM PERFORMANCE OF GEOTEXTILES

Andre L. Rollin, ing., F_{eic}, F_{csme}, Montreal, Canada

ABSTRACT
Geotextiles installed in many geotechnical and environmental works must have a short term performance in retaining sol particles, filtering liquids, be a separator between sols, protect geomembrane against puncture and to accomplish many other functions. Their short term performance, survivability, is related to the engineering design of the work, to the CQA manufacture, to their installation. and the chemical nature of the products in contact. How long is the expected service life of a geotextile when installed in a earth structure and in contact with atmospheric conditions and chemical products ?

RÉSUMÉ
Les géotextiles installés dans un ouvrage de géotechnique ou de protection de l'environnement doivent être performants à court terme pour retenir les sols en place, pour filtrer et évacuer des liquides, pour séparer des couches de sols, pour protéger des géomembranes contre le poinçonnement et pour accomplir plusieurs autres fonctions. Cependant ces matériaux doivent être performants durant une longue période de temps. Quelle est la durée de vie fonctionnelle des géotextiles que l'on peut espérer en fonction des conceptions utilisées, des programmes de contrôle de la qualité durant la construction et la mise en oeuvre, de la nature des sols et des produits en contact?

1. INTRODUCTION

When a geotextile is used in a civil engineering structure, it is intended to perform a particular function for a minimum expected time, called the design life. A geotextile is a planar, permeable, polymeric (synthetic or natural) textile material, which may be woven, knitted or non-woven, used in contact with soil and/or other materials in geotechnical and civil engineering applications. Any application may require one or more functions from the geotextile such as filtration, protection, reinforcement, separation and surface erosion control. Each function uses one or more functional properties of the geotextile, such as tensile strength or water permeability.

Assessment of the durability of an application using geotextiles requires a study of the effects of time on the functional properties. The textile and polymer structures, the manufacturing process, the physical and chemical environment, the conditions of storage and installation, and the different solicitations supported by the textile are all parameters which govern its durability. The main task is to assess the evolution of the functional properties for the entire design life of the application.

The durability is related to the change of a property of an installed geotextile with time. Figure-2 is a schematic representation of the evolution of the available property of a material as a function of time, as represented by the curves on the graph. Along the time axis is indicated the events that happen between manufacture of the product and the end of product life. Each curve represents the changes in the required property during these different and successive events. One can see that after the loading phase, the property required is considered to be constant and equal to the level defined by the design.
The design life is specified on the time axis. It is set by the designer and one of several fixed durations must be set according to whether the structure is meant for short-term use (typically a few years and not exceeding 5 years), temporary use (around 25 years) or permanent use (50 to >100 years). The nature of the structure, the environmental risk involved and the consequences of failure may influence this duration: 70 years for a wall, 100 years for an abutment and beyond 100 years for landfills.

Many geotextiles have a temporary function although the system is permanent, for example an embankment over a weak soil may require a geotextile reinforcement until the embankment has settled.

At the end of the anticipated design life, the designer has to ensure a certain safety level, such that failure is predicted to be well beyond the design life. As shown in Figure-1, the variation of a property with time under condition I is significant but the degradation is not great enough to affect the performance of the application since the long term value is greater than the acceptable limit. On the other hand, the same property did degraded faster under condition II to a value lower than the acceptable limit putting in peril the application: the geotextile cannot perform its function.

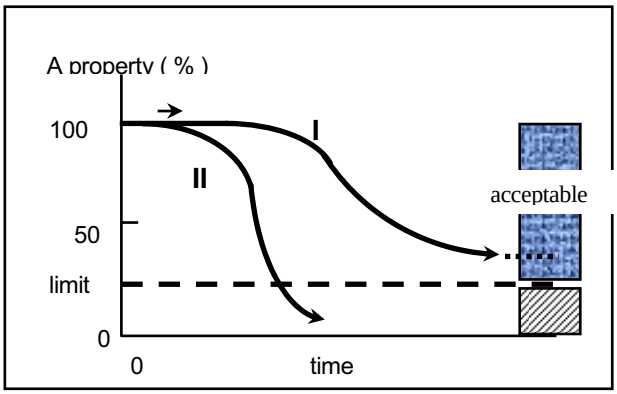

Figure-1 : Functional property variation with time

2. GEOTEXTILES

The durability of a geotextile depends upon it polymeric formulation and polymer microstructure, on any additives and fillers compounded with it, the fibre geometry and fabric layout. The geotextile should be chemically and biologically resistant if it is to be suitable for long term applications.

The polymers used to manufacture geotextiles are generally thermoplastic materials which may be amorphous or semi-crystalline. The orientation of polymers by mechanical drawing to form fibers and filaments results in higher tensile properties and improved durability. As the molecules become more oriented, the fibers become stronger. Durability of a textile may also be influenced by fiber diameter, and the volume to surface ratio: some means of degradation (oxidation and UV-exposure) are dependent on surface area and others (diffusion and absorption) are inversely related to thickness.

Any polymer consists of long chain molecules each containing many identical chemical units. Each unit may be composed of one or more monomers, the number of which determines the length of the polymeric chain and resulting molecular weight. Molecular weight can affect physical properties such as the tensile strength and modulus, impact strength, flexibility and heat resistance as well as the durability properties. The mechanical and physical properties of the plastics are also influenced by the bonds within and between chains, chain branching, and the degree of crystallinity.

Crystallinity has a strong effect on polymer properties, especially the mechanical properties, because the tightly packed molecules within the crystallites results in dense regions with high intermolecular cohesion and resistance to penetration by chemicals. An increase in the degree of crystallinity leads directly to an increase in rigidity, tensile strength, hardness and softening point, and to a decrease in permeability and gas diffusion. Neighbouring crystallites may be connected by single molecules running through the amorphous regions, which under tension make a significant contribution to the mechanical behaviour. These 'tie' molecules are, however, susceptible to chemical attack.

Geotextiles are available in a wide range of compositions appropriate to different applications and environments and the synthetic polymers used consist mainly of polyester (PET), polypropylene (PP), polyethylene (PE) and polyamide (PA).

Polypropylene (PP) is a thermoplastic long chain polymer normally used in the isotactic stereoregular form in which propylene monomers are attached in head-to-tail fashion and the methyl groups are aligned on the same side of the polymer backbone. PP has a semi-crystalline structure which gives to it high stiffness, good tensile properties and resistance to acids, alkalis and most solvents. It is possible for the tertiary carbon to react with free radicals, so that stabilizers are added to prevent oxidation during manufacture and generally to improve long term durability, including weathering.

Polyesters (PET) are a group of polymers and the type used most frequently in geotextiles is polyethylene terephthalate (PET) which is a condensation polymer of a dibasic acid and a di-alcohol. PET offers good mechanical properties, including a low creep strain rate, and good chemical resistance to most acids and many solvents. The ester group, the important polymeric link, can be hydrolysed very slowly in presence of water, and more rapid attack occurs under highly alkaline conditions. As with other polymers PET is sensitive to weathering.

Polyethylene (PE) is one of the simplest organic polymers and it is used in its low density form (LLDPE), which is known for its excellent pliability, ease of processing and good physical properties, or as high density polyethylene (HDPE) which is more rigid and chemically resistant. PE can be stabilized to increase its resistance to weathering.

Polyamides (PA) or nylons are melt processable thermoplastics that contain an amide group as a recurring part of the chain. PA offers a combination of properties including high strength at elevated temperatures, ductility, wear and abrasion resistance, low frictional properties, low permeability by gases and hydrocarbons, and good chemical resistance. Its limitations include a tendency to absorb moisture, with resulting changes in dimensional and mechanical properties, and limited resistance to acids and weathering. The PA fibres used in geotextiles have a T_g of 40-60 °C which reduces with moisture content. Nylons are sensitive to biochemical attack.

Recycled and reworked Materials: In the industry, three expressions are used to identify recycle of processed materials: *rework resin (RR) (or regrind), post-consumer resin (PCR) and post-industrial resin (PIR).* It is common practice within the plastics industry to recycle the processed material (in-house scrap polymer or rework resin), since it can be considered as comparable to virgin material as long as it is used in small percentages (less than 10%). Post-industrial resin (PIR) is the recycling of industrial resin originating from another process. The level of control over the quality of the material, and thus its durability, decreases with the number of stages and processes it has gone through after leaving the original manufacturer's plant. For severe environments and for long-term applications it is advisable not to use post consumer recycled polymer without proof of its long term durability. The composition of the polymer should be assured.

3. SOLLICITATIONS ON GEOTEXTILES

3.1. The environment below ground

Below ground the main factors affecting the durability of geosynthetics are as follows: particle size distribution of the soils and granular angularity (Figure-2); acidity/alkalinity (pH) - humates, sodium or lime soils, lime hydration, concrete; metal ions present; presence of oxygen; moisture content; organic content; temperature; and microorganisms. Chemical degradation of polymers occurs by a variety of processes including oxidation and hydrolysis, depending on the type of polymer and on the acidity or alkalinity of the soil. At higher loads, creep leads ultimately to creep-rupture, also known as stress-rupture or static fatigue: the higher the applied load, the shorter the lifetime.

hydrolysis : Polyester and polyamide fibers are susceptible to hydrolysis, which in polyester fibers takes two forms: the first, alkaline or external hydrolysis, occurs in alkaline soils above pH 10, particularly in the presence of calcium, and takes the form of surface attack and caution should be applied in the use of polyesters for long periods above pH 9; the second, internal hydrolysis, occurs in aqueous solutions or humid soil at all values of pH and it takes place throughout the cross-section of the fiber and the rate of hydrolysis is very slow, such that the process has little

effect at mean soil temperatures of 15 ºC or below, although it can be accelerated in acids. Sensitivity to hydrolysis can be reduced by selecting a PE of sufficiently high molecular weight and with limited branching, characterized by a low carboxyl end group count. Cowland et al (1998) performed tests on 14 year old PET woven textile and a woven PP slit film textile samples from a wall located in Hong Kong: the PET lost 15% of its tear resistance while the PP maintains its original resistance.

Figure-2 : Photograph of attacked geotextile by aggressive cover soil

chemical attack: Chemical attack is most serious when the polymer chain backbone is broken. Acidity and alkalinity are expressed as pH, a scale with neutral soil having a pH of 7. Topsoil generally has a pH of 5.5 – 7 (acid soils) , but anaerobic peats or soils which have been affected by acid rain may have a pH of approximately 4. Atmospheric carbon dioxide leads to generally increased acidity at the surface. Limestone or chalk soils may have a pH of 8 - 8.5. Geological deposits have a wide range of pH with values between 2 and 10 having been recorded.

micro-biological attack: In the past 25 years there have been no reports of microbial attack on synthetic geotextiles either in testing or in the ground (Ionescu et al, 1982 – Leflaive et al, 1988 - Giroud, 1996). The long chain molecules of thermoplastics used in geotextiles are generally resistant to microbial attack. Also, low molecular components and certain additives could be susceptible to biodegradation, but this can be countered by bio-stabilizers. Only geotextiles containing vegetable fibers and containing fiber-glass scrims, are likely to be affected.

3.2. The environment above ground

Ageing of exposed geosynthetics is mainly initiated by the ultraviolet (UV) component of solar radiation, heat and oxygen, with contributions from other climatic factors such as humidity, rain, oxides of nitrogen and sulphur, ozone, deposits from polluted air and pollens, and contained liquids. In most applications geotextiles are exposed to UV light for only a limited time during storage, transport and installation and are subsequently protected by a layer of soil. On the other hand, exposed geotextiles, mainly installed at top of slopes of reservoirs, ponds and channels, must resist for a longer time. The need for either short or long term resistance to weathering therefore depends on the application. In addition, atmospheric pollution and acid rain may enhance UV degradation, particularly of PA, for longer exposures above ground.

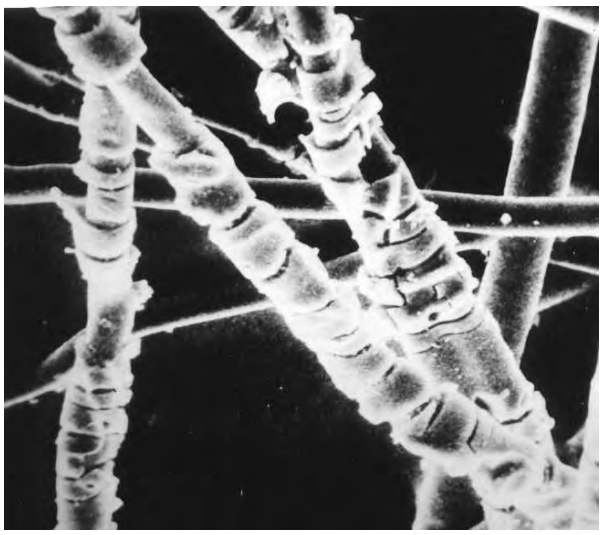

Figure-3 : Photograph of attacked geotextile by UV

ultraviolet radiation: The energy of ultraviolet radiation is sufficient to initiate rupture of the bonds within the polymer leading to subsequent recombination with, for example, oxygen in the air, or initiating more complex chain reactions. Additives increase resistance to ultraviolet radiation in a variety of ways, the most used being the carbon black. Geotextiles protected with an anti-oxidant can resist longer to the attack: few weeks for the PET and more for the PP and PE. Artieres et al (1998) showed that a PP non-woven geotextile installed on landfill cover in four sites did function well after 12 months even though it has loss 55% of its strenght. The resistance to ultraviolet radiation is affected both by the surface temperature of the sample and by precipitation, for which reason accelerated weathering tests include control of temperature and an intermittent spray cycle. UV radiation in the 400 to 280 nm range is responsible for degradation of geotextile fibers as shown in Figure-3. The photo-oxidation reaction can break chemical links (C-C or C-H) of the polymer chains and for each type of polymer a wavelength ca initiated the reaction: PE 300 nm, PET 325 nm and PP 370 nm.

oxidation : Polypropylene and polyethylene are susceptible to oxidation. This is accelerated by the catalytic effects of transition metal ions in a chemically activated state. Of these the ferric (Fe^{3+}) ion is the most common but copper and manganese have also been shown to be important. However, the sensitivity to oxidation is dramatically reduced by the inclusion of antioxidant stabilizers or additives and is retarded by the high level of orientation in polymer fibers as are found in most geotextiles. All

chemical reactions occur more rapidly at higher temperatures, as described by Arrhenius' Law.

rodents and roots: Geotextiles in soil also come in contact with animals such as rodents and with the roots of plants. Rodents can locally destroy a geotextile while roots can penetrate and clog it. No specific tests have been proposed to simulate attack by rodents, while tests the susceptibility to penetration by roots have been developped.

mineral and bacterial clogging: mineral and bacterial clogging of geotextiles can drastically shorten the serfice life of a drainage system. The filling up of the textile void by soil particles (Rollin et al, 1988 et Giroud, 1996) or by biomass formation (Rollin et al, 1996 ; Rowe, 1998 and Giroud et, 1996) have been reported by many authors.

3.3. Tensile Load

A major difference between polymers and metals is that at normal operating temperatures and tensile loads, polymers extend with time, that is they creep. This was recognized early in the development of geotextiles and led to an increasing number of testing programs to provide the information necessary for the design of reinforced soil structures. Creep and creep-rupture should only be regarded as a relevant design criterion in slopes and walls when the geotextile is expected to perform a reinforcing function in the long-term, or in reinforcement over a soft foundation. Of equal importance is definition of the creep strain, which even at low loads may cause a reinforced soil structure to reach a serviceability limit by movement or sagging without leading to total collapse. At higher loads creep leads ultimately to creep-rupture, also known as stress-rupture: the higher the applied load, the shorter the lifetime. The load which, if applied continuously over the lifetime of the product, is predicted to lead to creep-rupture on the last day of the design life, is defined as the unfactored design load.

At the microscopic level, when a load is applied to a polymer, it will cause the long chain molecules to stretch or rearrange themselves. While the crystalline areas remain relatively stable under load, rearrangement takes place in the amorphous regions, and it is noticeable that in polymers such as PE and PP used above T_g , where the amorphous regions are in a rubbery rather than a glassy state, creep takes place more rapidly and is more sensitive to temperature than those such as PET used below T_g In oriented polymers an important part is played by the "tie" molecules which link one crystallite with another across the amorphous regions. For example, in PET molecules the load can cause these highly stressed molecules to change the arrangement of their side branches, resulting in a temporary reduction in secant modulus and in the characteristic S-shaped stress-strain curve. These processes of rearrangement continue under the combined effects of load and thermal activation.

4. EMPIRICAL EVIDENCE FROM RETRIEVED GEOTEXTILES

Will geotextiles last for 5, 50, 100 years or longer? To answer this question we should start by investigating empirically what has been established over the past 35 years. Some examples giving clear evidence of durability are given below (Sotton et al (1982), Delmas (1988), Leflaive (1988), Wisse et al (1992), Mlynarek (1994), Troots et al (1994), Rollin (1996) et Rowe (1998)).

During the period 1965-1980, Sotton et al reported on PET and PP non-woven samples retrieved from 25 sites in France, ten to fifteen years after installation. These fabrics were still functioning as filters, separators and drainage layers. Losses in tensile strength of up to 30% were observed, but with laboratory analysis no chemical or biological attack could be identified.

In the following decade 1980-1990, Leflaive reported on a 5 m high vertical wall in France, which had been constructed in 1970. In this case 5 m long PET straps had been embedded in the concrete facing elements and anchored in the backfill, which had a pH of 8.5. Testing of the straps after 17 years showed a 2% reduction in tensile strength in the backfill but up to 40% reduction at the point where the straps enter the concrete facing units. Here the pH value has believed to have reached 13 to 14 at a temperature of 30ºC for some time. Subsequent analysis showed that this degradation could be explained by alkaline surface attack (25%), internal hydrolysis (5-10%) and mechanical damage.

In 1990, Wisse et al reported on samples of 1000 g/m² woven PP, part of 4 Mm^2 that had been laid as the backing of block mattresses on the sea bed of the Oosterschelde in 1978 to prevent scouring. The fabric had been in sea water at 10ºC for 9 years with a local partial pressure of 3% oxygen. The permanent load was only 10% of the tensile strength. Retrieved samples were subjected to accelerated oven ageing and compared with unexposed samples from the original source of material: the estimated time to embrittlement in sea water at 10ºC was calculated to be 80-120 years.

In 1994, Troost et al reported on the condition of large quantities of woven PET fabric retrieved from a soil retaining structure. A multi-layered geotextile reinforced wall, 4 m high, with slopes of 2:1 and 4:1, was constructed in the Netherlands. Thirteen years later the wall was carefully dismantled and the mechanical and chemical properties of the yarns investigated. The 50 m long embankment had slopes partially covered with bitumen and vegetation to prevent ultraviolet attack. After the retrieved fabric had been tested no hydrolysis could be detected on material either from the interior of the embankment or from the protected slopes, i.e. the mechanical properties, molecular weight (M_W = 33000), and carboxyl end group count had not changed. On the unprotected slopes, a reduction of between 15% and 50% in tensile strength was observed, which was concluded to be due mainly to UV radiation.

5. CONCLUSION

Flow chart of the process of evaluation of durability of geotextiles is under development at the European Standard Committee (DIN EN 13249 Annexe E). A modified version is presented as a conclusion.

Note: For service life greater than 100 years, in the accompanying document the retained strength should be clearly identified: hydrolysis for PET and PA, oxidation for PP, PE and PA, stabilizer content for PE and PP

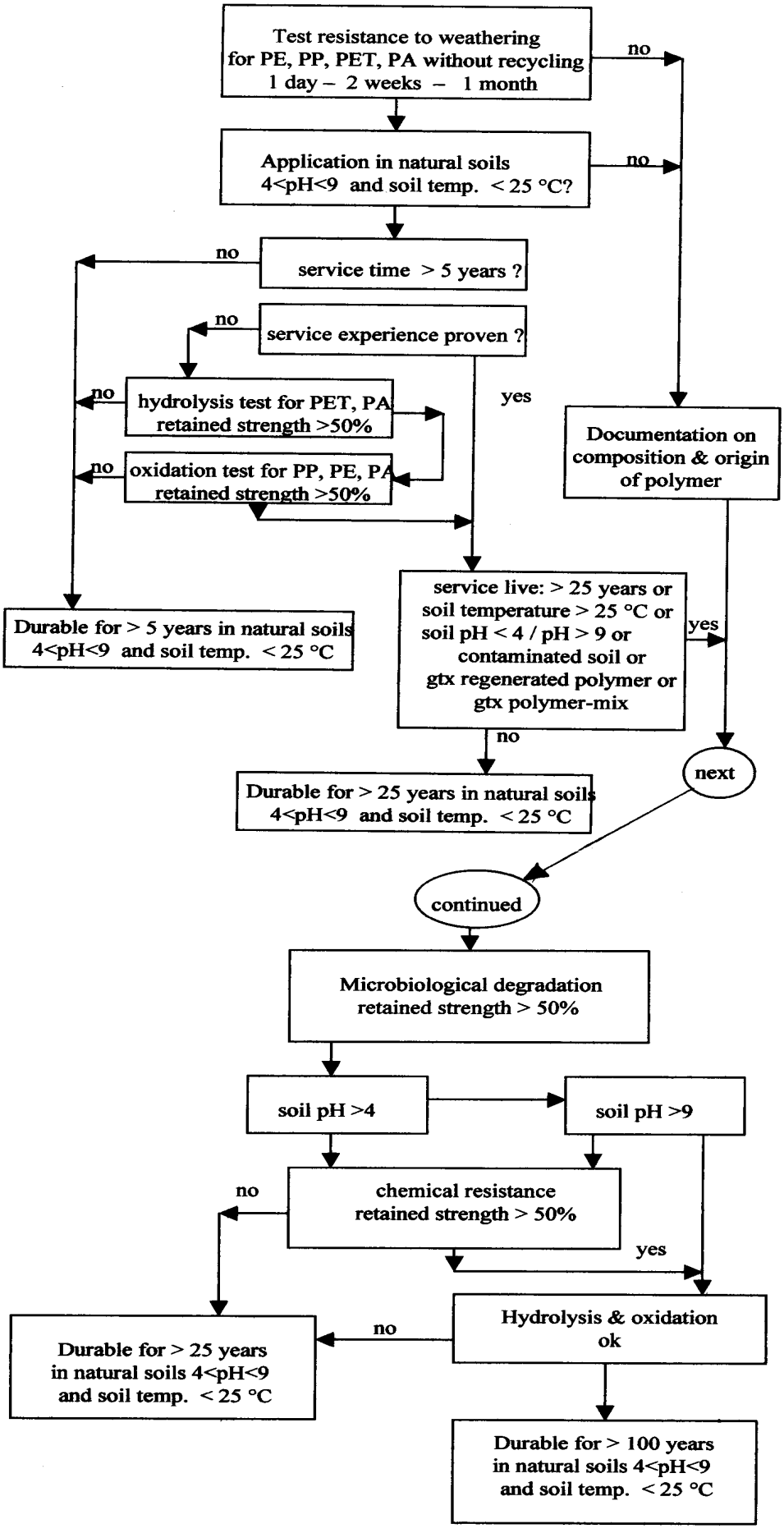
Test resistance to weathering for PE, PP, PET, PA without recycling 1 day – 2 weeks – 1 month
no
Application in natural soils 4<pH<9 and soil temp. < 25 °C?
no
no
service time > 5 years ?
no
service experience proven ?
yes
no
hydrolysis test for PET, PA retained strength >50%
no
oxidation test for PP, PE, PA retained strength >50%
Documentation on composition & origin of polymer
Durable for > 5 years in natural soils 4<pH<9 and soil temp. < 25 °C
service live: > 25 years or soil temperature > 25 °C or soil pH < 4 / pH > 9 or contaminated soil or gtx regenerated polymer or gtx polymer-mix
yes
no
next
Durable for > 25 years in natural soils 4<pH<9 and soil temp. < 25 °C
continued
Microbiological degradation retained strength > 50%
soil pH >4
soil pH >9
no
chemical resistance retained strength > 50%
yes
Hydrolysis & oxidation ok
no
Durable for > 25 years in natural soils 4<pH<9 and soil temp. < 25 °C
Durable for > 100 years in natural soils 4<pH<9 and soil temp. < 25 °C

6. REFERENCES

Artières O., Gaumet S. and Bloquet C. 1998. Prediction of the UV Ageing of Polypropylene Geotextiles – Landfills case, proceedings 6th Conf. Geosynthetics, IGS, vol 1, pp 393-398

ASTM D 5819, 1998, Standard Guide for Selecting Test Methods for Experimental Evaluation of Geosynthetic Durability

Cowland J.W., Yeo K.C. and Greenwood J.H. 1998. Durability of Polyester and Polypropylene Geotextiles Buried in a Tropical Environment for 14 Years , proceedings 6th Conf. Geosynthetics, IGS, March, vol 2, pp 669-674

Delmas Ph., Faure Y., Farkouh B. and Nancy A. 1994. Long Term Behavior of a Geotextile as a Filter in a 24 year Old Earth Dam : Valcros, proceedings 5th Conf. Geosynthetics, IGS, Singapore, pp 1199-1202

Giroud J.P. 1996. Granular Filters and Geotextile Filters, proceedings Geofilters'96, Montreal, pp 565-680

Koerner R.M., Lord A.E. and Hsuan Y.G. 1988. Long-Term Durability and Ageing of Geotextiles», Geotextiles and Geomembranes, vol 7, pp 147-158

Koerner R.M., Lord A.E. and Hsuan Y.G. 1992. Arrhenius Modeling to Predict Geosynthetic Degradation, Geotextiles and Geomembranes, vol 11, pp 151-183

Ionescu A. et al 1982. Methods Used for Testing the Bio-Colmatation and Degradation of Geotextiles Manufactured in Romania, proceedings 2nd Conf. Geotextiles, IFAI, pp 547-552

ISO 13434 (1997), "Guide to durability of geosynthetics", under revision

Leflaive E. 1988. Durability of Geotextiles : the French Experience , Geotextiles and Geomembranes, vol 7, pp 23-31

Mlynarek J., Bonnell R.B., Broughton R. and Rollin A.L. 1994. Long Term Effectiveness of Geotextiles on Subsurface Agricultural Drainage Systems, proceedings 5e Conf. Int'l Geotextiles, IGS, Singapore, pp 949-952

Rollin A.L. and Lombard G. 1988. Mechanisms Affecting Long-Term Filtation Behaviour of Geotextiles, Geotextiles and Geomembranes, vol 7, pp 119-145

Rollin A.L. 1996. Bacterial Clogging of Geotextiles, proceedings Geofilters'96, Montréal, pp 125-134

Rowe, R.K. 1998. Geosynthetics and the Minimization of Contaminant Migration through Barrier Systems Beneath Solid Waste, proceedings 6th Conf. on Geosynthetics, IGS, pp 27-102

Sotton M, Leclercq B, Paute J L and Fayoux D. 1982. Some answer's components on durability problem of geotextiles, Proceedings 2nd Conf. Geotextiles, Vol 2, Las Vegas, pp553-558

Troost G H , den Hoedt G, Risseeuw P, Voskamp W. and Schmidt H M 1994. Durability of a 13 year old embankment reinforced with polyester woven fabric, 5th International Conference on Geotextiles, Geomembranes and Related Products, Singapore, IGS, pp1185-1190

Wisse J.D.M., Broos C.J.M. and Boels W.H. 1990. Evaluation of the life expectancy of polypropylene geotextiles used in bottom protection structures around the Ooster Schelde Storm Sturge Barrier - A Case Study, 4th Conf. Geosynthetics, The Hagen, Netherlands, pp 697-702

LONG-TERM WEATHERING BEHAVIOUR OF GEOTEXTILES

by

Heike Vogt [1]

ABSTRACT

Geotextiles have been used for many years in hydraulic and coastal engineering, e.g., for revetments geotextile filter layers are considered as standard construction elements. Nowadays, geotextile constructions are designed whose main function is the packing (wrapping) and separation of the material (KOHLHASE, 1999). However, despite technical and financial advantages compared to conventional constructions such geotextile constructions are still rare.

In the practical experience of coastal engineering reservations have been expressed concerning the long-term weathering behaviour of geotextiles, which are directly exposed to the extreme loads of the coastal environments. Therefore, it is important to examine these characteristics and with it to assess the reliability of geotextile constructions in coastal engineering.

The following report is limited to conceptual questions for the determination of abrasion resistance against scour stresses caused by hydrodynamic loads in connection with transport of sediments in the littoral system.

1. INTRODUCTION

Constructions for the protection of sandy coasts have the task to protect locally eroding coastal sectors against progressive erosion. Protection can be achieved by constructions parallel to the coastline (revetment or seawall), by constructions normal to the coastline (groynes) or by offshore-constructions arranged parallel to the coastline (offshore breakwater) in order to reduce wave-induced energy-input. Basically, all of these constructions can provide local protection only (Figure 1): Neighbouring coastal areas are often subject to down drift erosion due to a local fixation of the coastline, which reduces the longshore sediment transport (KOHLHASE, 1992).

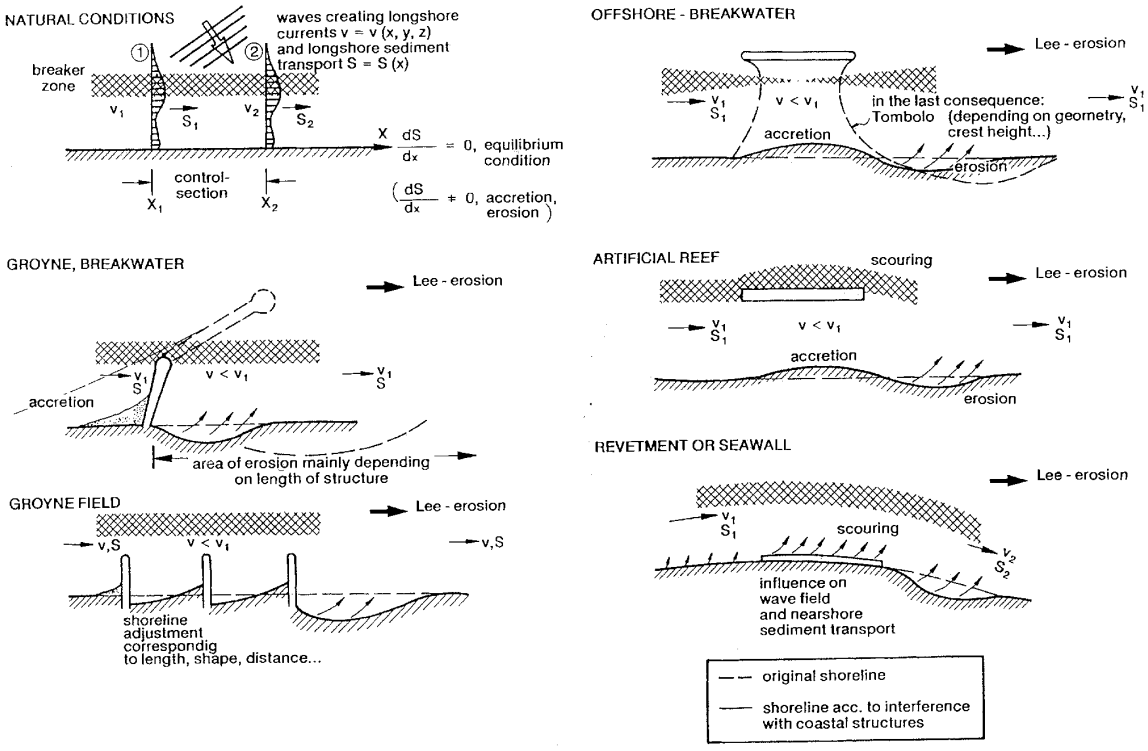

Figure 1: Coastal chances caused by constructions of the coastal protection (CERC, 1984)

[1] Dipl.-Ing., Scientific Assistant, Institut for Hydraulic and Coastal Engineering, University of Rostock, Heike.Vogt@bau.uni-rostock.de

An effective protection of a coastline with a deficit of sand can only be achieved by compensating the sand deficits by beach nourishment such as beach fills. This measure intervenes with the material budget and thus change the flow of morpho-dynamic processes. The transport energy of the currents can be used to its full capacity by the artificial supply of sediments in the coastal and pre-coastal areas and abrasion by the coastal current can thus be reduced.

Nevertheless, coastal protection constructions are of importance: The effect of beach nourishment is temporarily restricted and its stability cannot be calculated. In order to prolong the retention time of the artificially supplied sediments and to possibly reduce the costs for preservation and protection of the coast-line it is useful to carry out beach nourishment in combinations with structural measures.

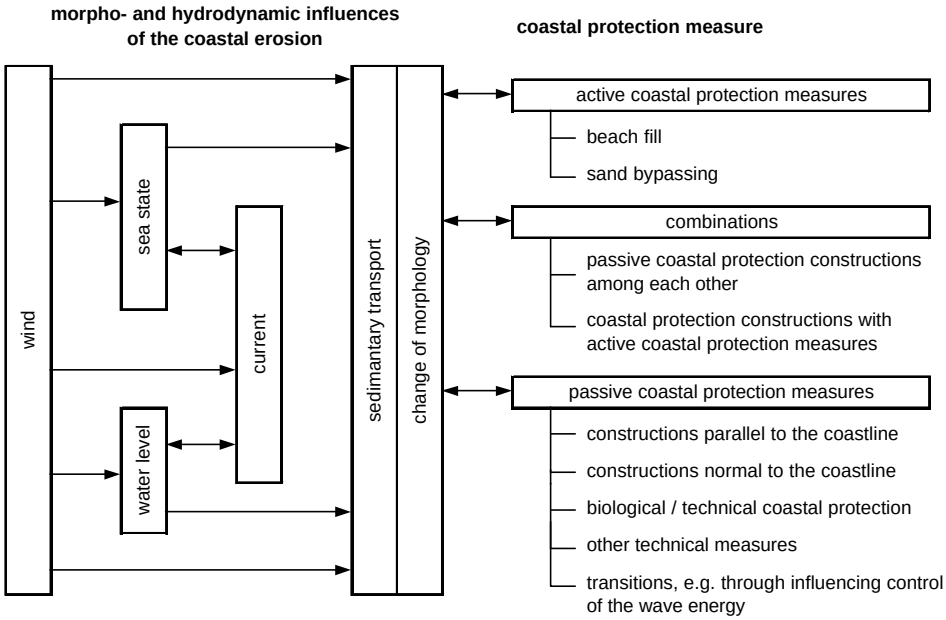

Figure 2: Passive and Active coastal protection measures (following Witte, 2002)

This is where the advantage of geotextiles becomes apparent: Hydrodynamic loads caused by waves and currents and morphological changes induced by coastal constructions cannot be calculated with satisfying accuracy. Despite a remarkable progress in the field of numerical models, any prognosis remains uncertain. As a consequence, the effect of neighbouring coastal areas cannot be assessed. Geotextile constructions can be removed with comparatively small expenditures if the desired effect cannot be achieved or if negative side effects become apparent. On the other hand, if the geotextile construction has a positive effect, it can be integrated into a more conventional construction, as e.g. by later covering it in order to protect it from vandalism or abrasion (KOHLHASE, 1992).

Furthermore, geosynthetics provide flexible solutions. Especially in the transition area between the construction and the erosive bottom of the sea considerable advantages can be seen. With stiff constructions, scours due to sea conditions and currents and with considerable maintenance costs are unavoidable. Geotextile construction can easily adjust to the altered conditions at the ground, due to its high flexibility.

The idea to pack construction materials into a geotextile, i.e. to use the geotextile mainly as a packing material, often shows essential advantages compared to conventional solutions in the field of coastal and hydraulic engineering (KOHLHASE,1998):

- The possibility of using local materials causes a considerable reduction of cost.
- The prefabrication of the geotextile constructions causes short installation times and guarantees a constant quality.
- Geotextile constructions can be simply extended (for example by integration into a conventional construction, if the planed effect has been achieved).

Despite of technical and financial advantages the use of packed constructions in Gemany is not very common. Examples for their use are, for example, the artificial reef near Kampen (Island of Sylt, Germany) with geotextile containers (KOHLHASE, 1999) and the dune protection by a light geotextile revetment (NICKELS AND HEERTEN, 2000) as well as the embankment and bottom protection of the harbour of List (Island of Sylt, Germany) by using geotextile containers (SCHMIDT, 2002).

Figure 3: Protection of an artificial dune near Kampen (Island of Sylt, Germany) by a light geotextile revetment

In the practice of coastal defence there are concerns about the long-term behaviour of geotextile constructions, especially if they are not protected by stone or sediment layers against extreme environmental and mechanical stress.

Concerns are due to a lack of design criteria, which reliably describe the requirements that geotextile construction should fulfill in order to avoid failure within the designed lifetime. Research for these criteria is of great importance for the development of recommendations for the design of geotextile constructions. In this context there is a special interest in the research for:

- Reliable structural design methods, which include all environmental and mechanical stresses effective in the tasks of coastal defence.
- Reliable specifications about the long-term weathering behaviour of geotextiles during unprotected use in the environment of coastal and hydraulic engineering.

The following considerations are restricted to the long-term weathering behaviour of geotextiles.

2. LONG-TERM WEATHERING BEHAVIOUR OF GEOTEXTILES

During the last years many investigations about the long-term weathering behaviour of geotextiles have been carried out, producing valuable knowledge about the fundamental mechanisms of the weathering of geotextiles. Nevertheless, until now reliable specifications about the long-term weathering behaviour of geotextiles are still not available. Previous investigations only looked at single effects, as the number of coexisting stresses was relatively small in the hitherto fields of application of geotextiles as layer for separation and filtering. Often those stresses consisted of tensile loading.

The number of stresses has increased with the development of packed constructions, in which geotextiles are exposed in the environment of the coastal and hydraulic engineering. A summary of the possible stresses is given in figure 3.

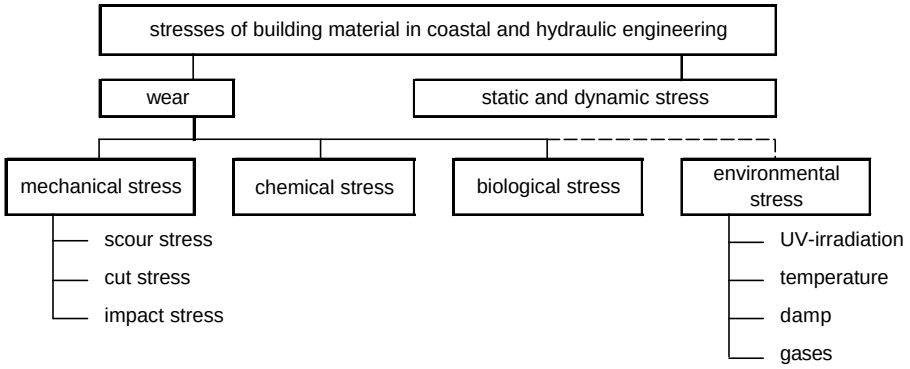

Figure 3: Stresses on building material in hydraulic engineering (following HAROSKE, 1998)

Under certain circumstances these stresses can show dangerous synergy effects regarding the weathering behaviour of geotextiles. The weathering speed of the materials used can possibly be higher than to be expected by the assessment of single weathering mechanisms only.

The general suitability of geotextiles for a long-term use in the unprotected environment of coastal and hydraulic engineering has been proven in the beginning of the 1980's by an extensive research program of the Franzius-Institute for hydraulic, waterways and coastal engineering at the University of Hannover (HEERTEN, 1979).

The results are summarised as follows (SAATHOFF AND ZITSCHER, 1997):

- No biological and chemical influence on the stability of the geotextiles in seawater.
- A unprotected weathering of the geotextiles was connected with a loss of strength caused by UV-irradiation. As the geotextiles were dimensioned to stand high installation stresses, and thus had high reserves concerning stresses during use, the investigated samples were intact and serviceable.
- Damages of the geotextiles could be led back to mechanical influences during installation or scour, impact and cut stresses.

Based on these investigations the durability of geotextile constructions is determinated by scour, impact and cut stresses.

Cut stresses are usually caused by vandalism. A protection of geotextile constructions against vandalism is possible by inaccessibilty, by a protective layer of sand or by integrating the geotextile into a conventional construction.

Scour and impact stresses often lead to a continuous loss of material from the surface of the geotextile, mainly caused by wave and currents and the related transport of sediments in the littoral system. According to DIN 50320, this mechanism is called abrasion wear and can lead to a considerable reduction of the tensile strength and thickness of the filter layer resulting in a decreas of the effectiveness of filtration.

To exclude damages caused by scour and impact stresses during the lifetime of a geotextile construction, the assessment of the abrasion resistance of geotextiles is of great importance. A geotextile is considered abrasion-proof if:

- during the lifetime of the construction the filtration effectiveness is guaranteed with respect to the ability to detain the soil and a high water permeability and
- the tensile strength of the geotextile guarantees a long-term capability to stand tensile loads, as for example from soil deformations.

Standardised national testing procedures for the assessment of abrasion resistance of geotextiles are missing. In the following paragraph the fundamental mechanisms of abrasion wear of geotextiles by scour and impact stress are analysed and conceptional considerations for the development of a testing procedure with realistic simulation of the erosive stress are carried out.

3. FUNDAMENTAL MECHANISMS OF WEAR OF GEOTEXTILES AND CONCEPTIONAL CONSIDERATIONS FOR THE DEVELOPMENT OF A TESTING PROCEDURE

In general abrasion wear, which becomes apparent in the appearance of wear debris as well as in the change of material and form, can be seen as a loss of size of the tribological system (DIN 50320,1979). The tribological system for the abrasion wear of a geotextile is due to a combination of gliding, rolling and impact stress by bed load transport and is given schematically in figure 4.

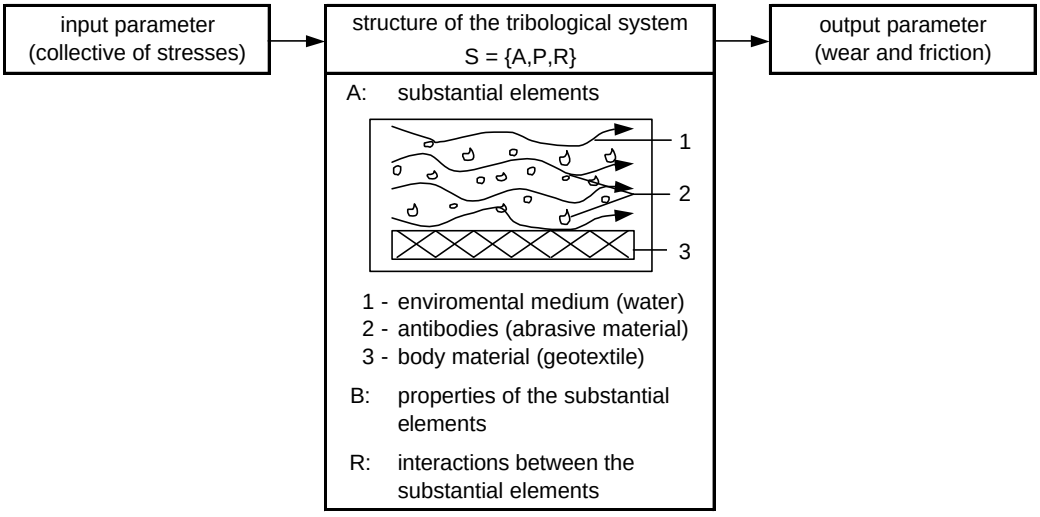

Figure 4: Tribological system of the erosive wear of geotextiles (following HABIG, 1980)

As shown in figure 4, the elements which are involved in the abrasion wear, together with their properties and interactions (as decisively the abrasion mechanisms), build the structure of the tribological system. Stresses acting from the outside are converted by the structure into a loss of stability by friction and wear. Abrasion wear of a geotextile does not only depend on the material properties of the geotextile and the abrasive material but it also depends on their interactions and the number of stresses:

Wear is not a material property but a system property.

This means that for the exact quantification of abrasion resistance it is necessary to create an exact model of the tribological system, as given in figure 4 (UETZ AND WIEDEMEYER, 1985). The first steps to such a model consist of:

- a description of the collective of stressors with respect to:

  a) the movement of the abrasive material in time and

  b) the physical, chemical and thermal stress parameters in size and duration

- a characterisation of the structure of the tribological system with respect to:

  a) material and form properties of the geotextile and the abrasive material

  b) the interaction of the elements.

wear mechanisms	character	characteristic features
abrasive wear	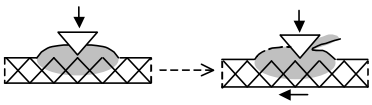	scratch, hollow and ripple
disruption of the surface	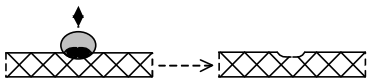	cracks and pitting

Figure 7: Wear Mechanisms in conjunction with abrasion wear (UETZ AND WIEDEMEYER, 1985)

It can be concluded that the assessment of the abrasion resistance of geotextiles against scour and impact stress depends on field experiments. Only there the real collective of stresses is effective and external and usually unknown influence sizes are additionally integrated.

	laboratory tests	field tests
I. collective of stresses		
a) measurment of the size of stress	++	–
b) realistic size of stress	– –	++
II. structure of the tribological system		
a) registration of the influence of the substantial properties	+	+
b) registration of the influence of the form properties of the construction	– –	+
c) registration of the wear mechanisms	+	–
III. measurment of the sizes of loss	++	–
IV. inclusion of external, partly unknown influences	–	++
V. costs	++	– –

Figure 5: Assessment of different testing procedures for wear (HABIG, 1980)

Asessment of the natural tribological system in a model is only partially possible, due to the following reasons (HAROSKE, 1998):

- The material, which acts abrasive on the geotextile, is built from natural detrital rocks of different size and origen, which leads to different degrees of hardness and degree of rounding.

- Water levels, waves and currents are varying. Consequently transport rate and angle of attack of the abrasion material are constantly changing.
- Currents are influenced by the design of the geotextile construction.
- The properties of the elements, which are involved in the abrasion wear, are not constant. By abrasion wear the micro- and macro-dimensions of the geotextile and the abrasive material are changing.
- The properties of the geotextile surface involved in the wear process is continuously influenced by the storage of sediment particles, growth of natural cover and UV-irradiation.

The suitability of a model experiment for the assessment of the abrasion resistance of geotextiles is measurable by a transfer of the results to natural conditions. Comparisons are possible, if the constellation of the abrasion wear mechanisms in model and nature are similar. For this purpose, the tribological system of nature and model may only differ in 4 parameters at most (HABIG,1979):

- stress
- speed
- time
- form properties of the elements

	system parameter	paramter to be identical in the testing procedure and the natural tribological system	parameter, that can be different in the testing procedure and the natural tribological system
collective of stresses	form of movement	×	–
	motion	×	–
	stress	–	×
	speed	–	×
	temperature	×	–
	time	–	×
structure of the tribological system	number of substantial elements	×	–
	substantial properties of elements	×	–
	form properties of elements	–	×
	interactions between elements	–	–
	a) friction	×	–
	b) constellation of the wear mechanisms	×	–
output parameter	rate of wear	×	–
	fricion coefficient	×	–
	increase in temperature	×	–

Figure 6: Parameters to be considered for the simulation of wear (HABIG, 1980)

Information about the compatibility of the model results can be given by microscopy of the wear areas of a naturally stressed geotextile and a model tested geotextile. Similarities of the abrasion wear areas lead to the same constellation in the abrasion wear mechanisms of model and nature.

A testing procedure for investigation of the abrasion resistance of geotextiles should have the following properties:

- For a realistic simulation of the abrasion wear mechanisms caused by a combinations of scour and impact stresses by abrasive materials on geotextile constructions, a movement of the abrasive material should be enforced.
- For a simulation of the natural abrasion wear mechanisms for a special application, relevant test parameters such as speed, and kind and quantity of the abrasive material should be variable.

4. STATE OF TESTING PROCEDURES IN GERMANY

A standardised testing procedure, which might deliver reliable quantitative statements about the suitability of geotextiles for their use in unprotected environment in coastal zones does not yet exist. The determination of required material properties is based on experience and is summarised as follows:

- Sufficient thickness and weight of geotextile can achieve a high degree of robustness against scour and impact stresses.
- Mechanically bonded non-woven geotextiles are showing best resistance against scour and impact stresses because of their high degree of flexibility.
- The resistance of geotextiles increases with the increase of fibre thickness.
- Geotextiles made of polyamide (PA)-fibres are showing a high degree of abrasion resistance but are much more expensive than polyester (PES) and polypropylene (PP)-fibres. Therefore, the use of compound geotextiles made of different types of fibre is recommended.

According to the recommendations of the German Society of Geotechnical Engineering (DGGT) for the use of geotextiles in hydraulic and coastal engineering the abrasion resistance of geotextiles can be tested on the basis of the guidelines provided by the Federal Agency of Hydraulic Engineering (BAW) for the use of geotextile filters for the embankment and bottom protection.

The testing procedure of the BAW simulates the scour stress of geotextiles which can be caused e.g. by movement of stones in the revetment. Figure 8 shows the BAW setup. Inside of a rotating drum a mixture of crushed stones and water slips over geotextile samples in two test series of 40,000 rotations each. Every 5,000 rotations the direction of the rotation is changed. The abrasive material will be renewed after the first 40,000 rotations if the samples are not yet destroyed.

According to the guidelines of the BAW geotextiles are considered as abrasion-proof if the following conditions are met after testing (BAW, 1987):

- The average thickness of the samples has to be greater than or the same as the demanded minimum thickness of the filter layer.
- The average tensile load has to be 900 N / 10 cm.
- The deviation of the average k-value after testing needs to be 50 % of the average k-value before testing, otherwise a proof of the filter effectiveness is necessary.

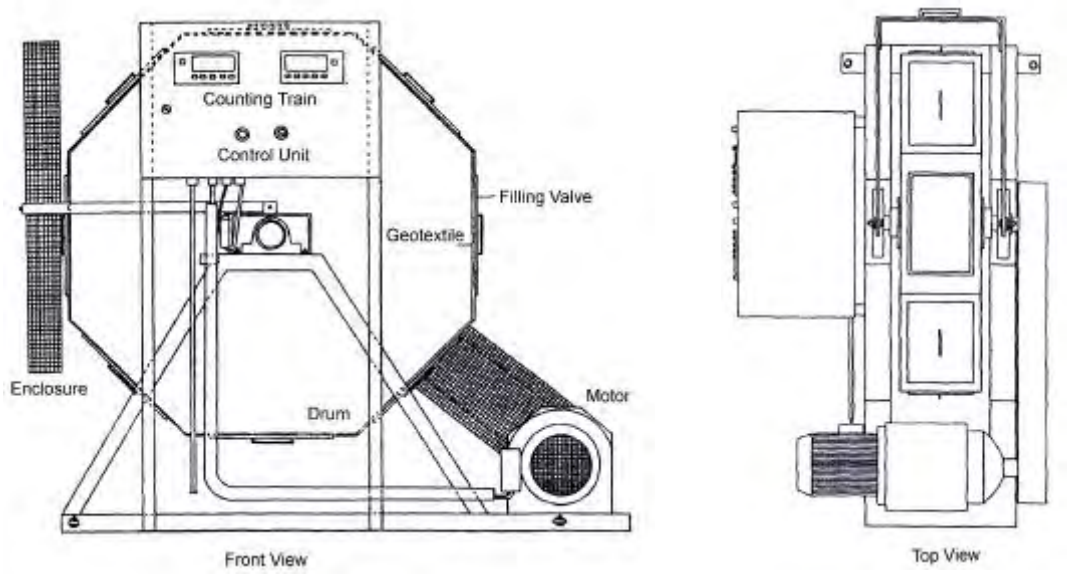

Figure 8: Testing facility for the determination of the abrasion resistance according to BAW (BAW, 1987)

The application of the described testing setup of the BAW for the use of geotextiles in the unprotected environment of hydraulic and coastal engineering has not yet been proven scientifically. Thus, there is a need for the following:

- Proof of suitability of the testing procedure for the simulation of abrasion wear mechanisms for geotextile constructions.

- Formulation of specific demands on long-term mechanical and hydraulic properties of geotextiles for their use in the unprotected environment of hydraulic and coastal engineering.

For the proof of suitability of the testing procedure the relevant testing parameters like velocity as well as sort and amount of abrasive material has to be varied in preliminary tests. The transferability of the test results to natural conditions has to be shown by microscopy of the abrasion wear surfaces of naturally stressed and model tested geotextile samples. For this purpose, field tests are indispensable.

The results of field tests are sensitive to even small deviations in the tribological system. Therefore, the geotextile test construction must be installed on different locations on the North and Baltic Sea coast to cover a great variety of natural conditions. The installation of test constructions has the disadvantage of high costs. Therefore, it would be useful to combine the testing with on-going construction works. Geotextile samples fixed on construction elements can be taken out of the system at different time intervals for laboratory testing. Up to now, only the operativeness of geotextile constructions is being examined from time to time.

5. CONCLUSIONS

With the application of geotextile constructions, new strategies for the extension of effective period of beach nourishments were designed. They contribute to the stabilisation of the coast line as light revetment, as an artificial reef by decreasing energetic force onto the coastal line or as groyne to control morphological processes. These constructions have a higher flexibility than conventional coastal engineering constructions: they can be removed at comparatively low costs if the desired success is not achieved or if negative side effects appear.

Up to now, unprotected geotextile constructions are only rarely used in the coastal environment because the long-term behaviour of geotextiles has not yet been sufficiently examined. In particular, reliable quantitative statements of abrasion resistance of geotextiles are still missing.

The following basic questions regarding the abrasion resistance of unprotected geotextiles in coastal environment can be summarised:

(1) Which synergetic effects can be expected due to the simultaneous appearance of different weathering mechanisms (figure 4)?

(2) Which are the influences on the wear process of changes of the geotextile surface like the storage of sediment particles or a natural cover?

(3) What is the influence of the design of the geotextile construction on the wear process?

(4) Can a realistic simulation of the abrasion wear mechanisms of geotextile constructions be achieved by an adaptation of the testing procedure as supplied by the BAW?

To answer these questions, it is necessary to develop a laboratory testing procedure for the determination of the abrasion resistance of geotextiles. For verification of the testing procedure field tests have to be carried out. To minimise costs these field tests should be carried out in combination with on-going coastal construction works.

6. REFERENCES

BAW (1987): Anwendung von geotextilen Filtern an Wasserstraßen (MAG), Hrsg. Bundesanstalt für Wasserbau (BAW), Karlsruhe, 1987

CERC (1984): Shore Protection Manual, U.S. Corps of Engineers, Department of Army, Vicksburg, Mississippi, 1984

DIN 50 320 (1979): Verschleiß - Begriffe, Systemanalyse von Verschleißvorgängen, Gliederung des Verschleißgebietes, Hrsg. Deutsches Institut für Normung e.V., Beuth Verlag, Berlin, 1979

DVWK (1992): Anwendung von Geotextilien im Wasserbau, Hrsg. Deutscher Verband für Wasserwirtschaft und Kulturbau e.V. (DVWK), DVWK-Merkblatt 221, Verlag Paul Parey, Berlin, 1992

HABIG, K.-H. (1980): Verschleiß und Härte von Werkstoffen, Carl Hanser Verlag, München, 1980

HAROSKE, G. (1998): Beitrag zum Hydorabrasionsverschleiß von Betonoberflächen, Fachbereich Bauingenieurwesen, Fachgebiet Baustoffe, Universität Rostock, 1998, unpublished

HEERTEN, G. (1979): Langzeitbeständigkeit von Geotextilien im Küstenschutz, Franzius-Institut für Wasserbau und Küsteningenieurwesen der Universität Hannover,1979

KOHLHASE, S. (1992): Verpackte Baustoffe im Küstenwasserbau - Neue Entwicklungen bei der Verwendung von Geotextilien im Küstenschutz, Technische Akademie Wuppertal, Seminar „Geotextilien für den Einsatz im Wasserbau“, 1992

KOHLHASE, S. (1999): Geokunststoff-Baukörper im Küstenschutz, Geokunststoff-Kolloquium „Geokunststoffe in der Geotechnik“, Hrsg. Naue Fasertechnik GmbH & Co. KG, Lübbecke, 1999

KOHLHASE, S. ET AL. (2000): Projektskizze zum Aufbau eines Kompetenzzentrums „Geotextilien im Küstenwasserbau“, Institut für Wasserbau, Universität Rostock, 2000, unpublished

NICKELS, H. AND HEERTEN, G. (2000): Objektschutz Haus Kliffende, HANSA , Heft 3, 2000

SAATHOFF, F. AND ZITSCHER, F.-F. (1996), Geokunststoffe in der Geotechnik und im Wasserbau, Grundbau-Taschenbuch, 5.Auflage, Teil 2, Verlag Ernst & Sohn, Berlin, 1996

SCHMIDT, O. (2002): Böschungs- und Kolksicherungen im Wasserbau - Erfahrungen mit neuen Bauweisen, Institut für Wasserbau, Universität Rostock, 2002, unpublished

UETZ, H. AND WIEDEMEYER, J. (1985): Tribologie der Polymere - Grundlagen und Anwendungen in der Technik, Carl Hanser Verlag, München/Wien, 1985

WITTE, J.-O. (2002): Strategien und Optionen der Küstenplanung Sylt, in: Klimafolgen für Mensch und Küste - Am Beispiel der Nordseeinsel Sylt, Hrsg. Daschkeit, A. und Schottes, P., Spinger - Verlag, Berlin, 2002

ELCO**MAX®** **TECHNOTE 1**

Abrasion

Geotextiles in an exposed coastal interface application are subject to three predominant methods of deterioration throughout their usable life; these are,sediment abrasion due to water borne sand, shell and coral fragments; Ultra-violet (UV) light attack as well as abrasion due to trafficking of the geotextile. The degree of influence of the above varies on the application and location of the geotextile. Sediment abrasion can be a significant factor for containers located in the near-shore surf zone where the movement of water and coarse material is continually occurring, and is particularly noticeable in containers located at sea bed level. Trafficking abrasion becomes more influential with the degree of pedestrian and vehicle accessibility while UV degradation is dependent on sunlight exposure (Note damaging UV wave lengths are filtered out in 300mm of water depth).

A number of textile abrasion test methods are available; however, these are based on a modified Stoll abrasion test which is used to determine the abrasion resistance of women's woven and knitted stockings. The test method which best mimics actual field abrasion is the German Rotating Drum test method BAW Federal Waterways Engineering & Research Institute (1994), which was developed specifically for geotextiles used in coastal and waterway applications. This test subjects the geotextile to 80,000 abrasion cycles with a mixture of water and gravel and measures the strength retained on completion of the test.

Recently an exhumation of ElcoMax material has been taken from a seven year old job site which had a high degree of sediment abrasion, UV exposure and pedestrian (but no vehicle) trafficking; this material was then tested to ascertain the total damage to the product. In reviewing these results it is important to remember that the geotextile is damaged in two manners and as such we have taken the various forms of abrasion and the damage caused by sunlight exposure to be approximately equal in magnitude (that is any damage is attributed equally to UV and abrasion damage). The results from the various tests are shown below;

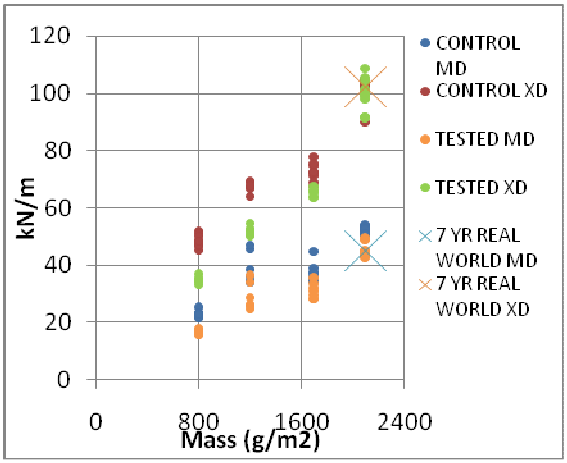

The results (above) show that the geotextile is damaged approximately equally in terms of strength loss when comparing a 7 year exposed product and the rotating drum test. There is however a larger degree of elongation loss which is largely attributed to the way ultraviolet light damages the polymers of the geotextile. The conditions of the 'real world' test are some of the most extreme a geotextile is likely to be placed and would it would be realistic to say that at least half of the damage was UV related. As a consequence it is reasonable to suggest that a geotextile subject to high levels of abrasion exclusively should be able match the rotating drum results after fifteen years and remain serviceable well after that.

Chemical Resistance Guide at 73°F

LEGEND	
Blue	No/Slim Absorption. No/Slim Mechanical Property Effects.
Green	Slight Absorption. Mild Degradation In Mechanical Properties.
Yellow	Moderate Absorption. Mechanical properties break down.
Red	Complete Decomposition Of Material
-	No Comprehensive Data Available
CW%	Concentration Weight %

ABS	**Ace**	**Acr**	**CAB**	**ECTFE**	**Flu**	**HDPE**	**Nyl**	**PEEK**	**PET**	**Poc**
ABS	*Acetal*	*Acrylic*	*CAB*	*ECTFE (Halar)*	*Flurosint*	*HD-PE*	*Nylon*	*PEEK*	*PET*	*Polycarbonate*

Pop	**Pos**	**PPS**	**PVC1**	**PVC2**	**PVDF**	**TFE**	**Tor**	**UHMW**		
Polypropylene	*Polysulfone*	*PPS*	*PVC, Type I*	*PVC, Type II*	*PVDF*	*TFE Fluorocarbon*	*Torlon*	*UHMW*		

Name		ABS	Ace	Acr	CAB	CPVC	ECTFE	Flu	HDPE	Nyl	PEEK	PET	Poc	Pop	Pos	PPS	PVC1	PVC2	PVDF	TFE	Tor	UHMW
Acetaldehyde Aq.	40				-		-						-		-				-			
Acetal Acid Aq.	10	-							-					-								
Acetone					-																-	-
Alcohols, Aliphatic		-			-	-			-				-	-	-		-	-	-			
Aluminum Chloride Aq.	10	-	-	-			-			-					-				-			
Aluminum Sulphate Aq.	10	-	-	-						-		-			-				-			
Ammonia Gas		-	-	-	-								-		-	-			-		-	-
Ammonium Carbonate Aq.	10	-	-	-	-										-				-		-	-
Ammonium Chloride Aq.	10	-	-	-											-				-			
Amyl Acetate			-		-	-	-					-	-		-				-			
Aniline		-			-								-		-							
Antimony Trichoride Aq.	10	-	-		-							-	-		-	-			-		-	-
Barium Chloride Aq.	10	-	-		-							-	-		-				-			
Barium Sulphate Aq.	10	-	-	-	-					-		-	-		-	-			-		-	-
Benzene																					-	-
Benzene Sulphonic Acid	10	-	-	-	-	-						-	-	-	-		-	-				
Bleaching Lye	10		-	-	-							-	-		-	-			-			
Boric Acid Aq.	10	-	-	-	-								-		-				-		-	-
Boron Trifluoride		-	-	-	-		-				-	-	-		-	-			-	-	-	-
Bromine Aq.	30	-	-	-	-			-				-	-		-				-			

Name		ABS	Ace	Acr	CAB	CPVC	ECTFE	Flu	HDPE	Nyl	PEEK	PET	Poc	Pop	Pos	PPS	PVC1	PVC2	PVDF	TFE	Tor	UHMW
Butanol		-	-	-	-		-						-	-					-			
Butyric Acid Aq.	20	-	-		-	-	-					-	-		-		-	-	-		-	-
Butyric Acid	coinc		-		-	-	-					-	-		-				-		-	-
Calcium Hypochlorite		-	-	-		-									-				-		-	-
Camphor		-	-	-	-	-	-		-			-	-	-	-		-	-	-		-	-
Carbon Tetrachloride				-									-									-
Chloral Hydrate		-	-	-	-		-					-	-		-	-			-		-	-
Chloride Aq.	10	-	-	-	-		-					-	-			-					-	-
Chloroform			-	-																		
Chlorosulphonic Acid Aq.	10	-	-		-	-						-	-		-							
Chrome Alum Aq.	10	-	-	-	-	-	-		-			-	-	-	-	-			-			
Chromic Acid Aq.	10	-	-																			
Citric Acid Aq.	10		-																			
Creosote		-	-	-	-	-	-		-			-	-	-	-	-	-	-	-			
Cresylic Acid		-	-	-	-							-	-		-	-			-			
Cyclohexanol		-	-	-	-								-		-				-			
Cyclohexanone		-	-	-									-			-			-			
Detergents, Organic		-	-	-	-				-				-	-	-				-		-	
Dibutylphthalate		-	-	-	-	-	-		-			-	-	-	-	-	-	-	-			
Diesel Oil		-	-		-	-			-				-	-	-		-	-	-			
Dioxan		-		-	-	-			-				-	-	-	-	-	-	-			

Name		ABS	Ace	Acr	CAB	CPVC	ECTFE	Flu	HDPE	Nyl	PEEK	PET	Poc	Pop	Pos	PPS	PVC1	PVC2	PVDF	TFE	Tor	UHMW
Edible Oils		-		-	-	-	-		-				-	-	-		-	-	-			
Ether, Diethyl		-		-	-	-	-		-				-	-	-		-	-	-			
Ethyl Acetate					-	-						-			-				-			
Ethylene Dichloride			-	-	-								-		-				-			-
Ethylene Glycol Aq.	96	-	-									-										
Ferrous Chloride Aq.	10	-	-		-				-			-	-	-	-						-	-
Fluorine		-	-	-	-							-	-		-	-			-			
Fluosilicic Acid Aq.	10	-	-	-		-		-			-	-	-		-		-	-	-	-	-	
Freon 12 (Arcton 12)		-	-	-											-				-		-	-
Formaldehyde Aq.	40	-																	-			
Formic Acid Aq.	3	-			-				-					-	-							
Fruit Juices	coinc		-	-	-										-				-			
Glycerine			-																-			
Heptane		-		-	-	-			-					-					-			
Hydrobromic Acid Aq.	10		-	-	-	-			-			-	-								-	
Hydrochloric Acid Aq.	0.4	-	-							-											-	
Hydrofluoric Acid Aq.	4	-				-														-		
Hydrogenated Vegetable Oils		-	-	-	-	-	-		-				-	-	-		-	-	-			
Hydrogen Peroxide Aq.	0.5	-	-	-		-															-	

Name		ABS	Ace	Acr	CAB	CPVC	ECTFE	Flu	HDPE	Nyl	PEEK	PET	Poc	Pop	Pos	PPS	PVC1	PVC2	PVDF	TFE	Tor	UHMW
Hydrogen Peroxide Aq.	1	-	-	-	-	-			-	-				-			-	-			-	
Hydrogen Peroxide Aq.	3	-		-	-	-			-					-			-	-			-	
Hydrogen Sulphide Aq.	sat	-											-		-						-	
Hydroquinone		-	-	-		-						-	-		-	-			-		-	-
Iodine (in Alcohol)		-	-	-	-	-						-	-		-	-	-	-	-		-	
Iodine (in Pot. Iodine) Aq.	3	-	-	-	-	-						-	-		-	-	-	-	-		-	
Isopropyl Alcohol				-		-							-		-		-	-			-	
Lactic Acid Aq.	10	-		-		-									-				-		-	
Lactic Acid Aq.	90	-	-	-	-	-			-	-		-	-	-	-		-	-	-			
Lead Acetate Aq.	10	-	-	-	-							-	-		-				-			
Linseed Oil		-		-	-							-		-					-	-	-	
Lubrication Oils (Petroleum)		-		-	-		-								-				-			
Magnesium Chloride Aq.	10	-		-	-										-				-			
Maleics Acid	coinc	-	-	-	-					-		-	-		-	-			-		-	
Malonic Acid Aq.	coinc	-	-	-	-	-	-		-	-		-	-	-			-	-	-		-	-
Mercuric Chloride Aq.	6	-			-							-	-		-	-			-		-	
Methyl Acetate		-		-		-	-		-				-	-	-		-	-	-		-	-
Methyl Ethyl Ketone																			-			
Methyl Chloride		-		-															-			
Milk				-	-										-				-		-	
Mineral Oils		-		-	-							-			-							
Naphthalene			-	-	-								-		-						-	
Nickel Sulphate Aq.	10	-	-		-							-			-				-		-	
Nitric Acid Aq.	0.1											-				-					-	
Nitric Acid Aq.	10	-		-	-				-				-	-							-	
Name		**ABS**	**Ace**	**Acr**	**CAB**	**CPVC**	**ECTFE**	**Flu**	**HDPE**	**Nyl**	**PEEK**	**PET**	**Poc**	**Pop**	**Pos**	**PPS**	**PVC1**	**PVC2**	**PVDF**	**TFE**	**Tor**	**UHMW**
Oleic Acid		-		-		-						-							-		-	
Oxalic Acid	10	-			-							-	-								-	
Ozone		-		-												-					-	
Paraffin		-		-	-	-			-				-	-	-			-	-			
Perchloric Acid Aq.	10	-		-	-								-		-	-			-		-	
Petrol		-		-	-	-							-	-	-		-	-	-			
Phenol Aq.	75	-		-	-	-			-				-	-	-	-	-	-	-		-	
Phosphoric Acid Aq.	0.3	-	-							-												
Phosphoric Acid Aq.	3	-		-	-				-	-			-	-								
Phosphoric Acid Aq.	10	-		-	-				-				-	-								
Phthalic Acid Aq.	sat	-	-	-	-	-	-		-			-	-	-	-	-	-	-			-	
Potassium Bicarbonate Aq.	60	-	-	-	-		-					-	-		-	-			-		-	-
Potassium Choride Aq.	10	-	-	-	-		-						-		-				-		-	

Name		ABS	Ace	Acr	CAB	CPVC	ECTFE	Flu	HDPE	Nyl	PEEK	PET	Poc	Pop	Pos	PPS	PVC1	PVC2	PVDF	TFE	Tor	UHMW
Potassium Ferrocyanide Aq.	90		-												-				-		-	
Propane gas	30	-	-		-				-			-	-	-	-	-			-		-	-
Salicylic Acid		-	-	-									-		-				-		-	
Silicone Fluids		-	-	-	-	-			-				-	-	-	-	-	-	-		-	-
Silver Nitrate			-	-	-	-			-				-	-	-		-	-	-			
Soap Solutions		-		-									-		-				-		-	
Sodium Acetate Aq.				-	-								-		-				-		-	
Sodium Bicarbonate Aq.	50	-													-				-			
Sodium Hypochlorite 15% (Chlorine Bleach)		-			-	-													-			
Sodium Nitrate Aq.	50	-			-								-		-				-		-	
Stannic Chloride Aq.	10	-	-	-	-	-	-					-	-		-		-	-	-		-	-
Stearic Acid		-	-	-	-							-	-		-	-			-		-	
Styrene (Monomer)		-	-	-		-			-				-	-	-		-	-	-		-	-
Sulphur Dioxide (Dry Gas)	100												-		-							
Sulphuric Acid Aq.	2				-																	
Sulphuric Acid Aq.	5	-		-	-	-			-				-	-								
Sulphurous Acid Aq.	10	-			-								-		-	-			-		-	
Tallow		-	-	-	-	-	-					-	-	-	-		-	-	-			
Tar		-	-	-	-	-			-			-	-	-	-		-	-	-			-
Toluene				-			-															
Transformer Oil		-	-		-	-			-			-	-	-	-		-	-	-			
Trichlorethylene		-		-									-						-			
Triethanolamine		-	-	-	-	-							-		-				-			
Turpentine				-	-							-							-			
Trisodium Phosphate Aq.	95	-	-		-					-			-		-				-		-	-
Urea		-		-	-								-		-				-		-	
Vaseline				-	-									-	-				-			
Vegetable Oil				-	-	-			-				-	-	-		-	-	-			
Vinegar				-	-								-		-				-			
Vinyl Chloride		-	-	-	-	-	-		-			-	-	-	-		-	-	-		-	-
Water				-	-														-			
Wax (Molten)				-	-	-			-				-	-			-	-	-			
White Spirit		-		-	-				-			-	-	-	-		-	-	-		-	
Wines and Spirits			-	-	-				-					-	-				-			
Xylene			-										-						-			
Xylenol		-	-	-	-	-			-			-	-	-	-	-	-	-	-			-
Zinc Chloride Aq.	10	-	-			-						-							-		-	

back to top

PlasticsEurope
Association of Plastics Manufacturers

General Chemical Resistance of PET - Products

The below data reflect the information available to the PET producers members of Plastics*Europe* . They should not be construed as implying a legal guarantee for specific properties of the products or for their suitability for a particular application.

Chemical resistance data are for storage at room temperature of the substance in the physical state that is specified in the relevant column. When a percentage is indicates, it refers to the concentration of a solution in water, unless otherwise indicated.
The meaning of the symbols for chemical resistance is:
1 = PET exhibits good resistance to attack; chances of successful testing are very good.
2 = PET has marginal resistance to attack; significant chance of container failure.
3 = PET exhibits poor resistance to attack; should not be considered for this application.

Substance	Physical state or concentration	Plastics*Europe*
Beer	liquid	1
Brake fluid	liquid	1
Camphorated Oil	liquid	1
Carbonated Soft Drinks	liquid	1
Castor Oil	liquid	1
Cottonseed oil	liquid	1
Detergents	1%	1
Diesel Oil	liquid	1

Plastics*Europe*
Avenue E. Van Nieuwenhuyse 4/3 - B -1160 Brussels - Belgium
Tel (32-2) 675 32 97 - Fax (32-2) 675 39 35
VAT BE 416 155 338 – www.plasticseurope.org

Fruit Juices and Nectars	liquid	1
Gasoline	liquid	2
Grease	See Lubricating grease	
Kerosene	liquid	1
Linseed Oil	liquid	1
Lubricating Grease	solid	1
Medical Syrups	liquid	1
Milk and milk products	liquid	1
Mineral Oils	liquid	1
Mineral Spirits	liquid	2
Mineral water	liquid	1
Mouthwashes	liquid	1
Motor Oils	liquid	1

Naphtha Solvent	liquid	2
Olive oil	liquid	1
Paraffin (medicinal)	solid	1
Petrol	liquid	1
Petroleum Ether	liquid	1
Silicone Fluids	liquid	1
Soap Solution	1%	1
Transformer oil	liquid	1
Turpentine	liquid	1
Vaseline	solid	1
Vegetable oils	liquid	1
Vinegar	liquid	1
Water	pure (liquid)	1

White Spirit	liquid	1
Wine and Spirits	liquid	1

General Chemical Resistance of PET - Chemicals

The below data reflect the information available to the PET producers members of Plastics*Europe* . They should not be construed as implying a legal guarantee for specific properties of the products or for their suitability for a particular application.

Chemical resistance data are for storage at room temperature of the substance in the physical state that is specified in the relevant column. When a percentage is indicates, it refers to the concentration of a solution in water, unless otherwise indicated.
The meaning of the symbols for chemical resistance is:
1 = PET exhibits good resistance to attack; chances of successful testing are very good.
2 = PET has marginal resistance to attack; significant chance of container failure.
3 = PET exhibits poor resistance to attack; should not be considered for this application.

Substance	Physical state or concentration	Plastics*Europe*
Acetic Acid	1-10% 10-40% > 40%	1 2 3
Acetic Anhydride	pure (liquid)	3
Acetone	pure (liquid)	3
Aliphatic Hydrocarbons	liquid	1
Allyl Alcohol	pure (liquid)	1
Aluminium Sulphate	pure (solid)	1

Ammonia	pure (gas)	3
Ammonium Chloride	pure (solid)	1
Ammonium Hydroxide	>10%	3
Ammonium Persulphate	pure (solid)	1
Ammonium Sulphate	pure (solid)	1
Amyl Acetate	pure (liquid)	2
Amyl Alcohol	pure (liquid)	2
Amyl Methyl Ketone	pure (liquid)	2
Aniline	pure (liquid)	3
Anthraquinone	pure (solid)	1
Aqua Regia	liquid	3
Barium Chloride	pure (solid)	1
Benzene	pure (liquid)	3

Benzoic Acid	pure (solid)	1
Benzyl Acetate	pure (liquid)	3
Benzyl Alcohol	pure (liquid)	3
Benzyl Benzoate	pure (liquid)	2
Bromine	pure (liquid)	3
Butane	pure (liquid)	1
Butyl Acetate	pure (liquid)	3
Butyl Alcohol	pure (liquid)	2
Butyl Lactate	pure (liquid)	1
Butyl Stearate	pure (liquid)	1
Calcium Chloride	10%	1
Calcium Hypochlorite	pure (solid)	1
Camphor	pure (solid)	1

Carbon Disulphide	pure (liquid)	1
Carbon Tetrachloride	pure (liquid)	1
Cetyl Alcohol	pure (solid)	1
Chloral Hydrate	pure (solid)	3
Chlorobenzene	pure (liquid)	3
Chloroform	pure (liquid)	3
Chromic Acid	1-10% 10-40% > 40%	1 2 3
Citric Acid	10% pure (solid)	1 1
Citronellol	pure (liquid)	1
Copper (II) sulphate	pure (solid)	1
Copper (III) sulphate	pure (solid)	1
Cyclohexane	pure (liquid)	1

Cyclohexanol	pure (liquid)	1
Cyclohexanone	pure (liquid)	3
Di (1-Phenyl) Ethanol	pure (solid)	2
Di (2 -Ethylhexyl) Phthalate	pure (liquid)	1
Diacetone Alcohol	pure (liquid)	1
1,2-Dibromoethane	pure (liquid)	3
Dibutyl Phthalate	pure (liquid)	1
Dibutyl Sebacate	pure (liquid)	1
o-Dichlorobenzene	pure (liquid)	3
1,2-Dichloroethane	pure (liquid)	3
Diethyl Ether	pure (liquid)	1
Diethylene Glycol	pure (liquid)	1
Diethylketone	pure (liquid)	3

Dimethyl Formamide	pure (liquid)	3
Dinonyl Phthalate	pure (liquid)	1
Dioctyl Phthalate	pure (liquid)	1
Dioxane	pure (liquid)	3
Dipentene	pure (liquid)	1
Ethanol	See Ethyl Alcohol	
2-Ethoxy Ethanol	pure (liquid)	1
Ethoxylated Alcohols	pure (liquid)	3
Ethyl Acetate	pure (liquid)	3
Ethyl Alcohol	1 - 100%	1
Ethyl Benzene	pure (liquid)	2
Ethylene Chlorohydrin	pure (solid)	3
Ethylene Glycol	pure (liquid)	1

Ethylene Oxide	pure (liquid)	2
Eugenol	pure (liquid)	3
Ferric Nitrate	pure (solid)	1
Formaldehyde	40%	1
Formic Acid	5 - 30% 90%	1 3
Freon 11 (fluorotrichloromethane)	pure (gas)	1
Freon TF (1,1,2-trichloro-1,2,2-trifluoroethane)	pure (gas)	1
Furfuryl Alcohol	pure (liquid)	3
Geraniol	pure (liquid)	1
Glycerol (Glycerine)	pure (liquid)	1
Heptane	pure (liquid)	1
Hexane	pure (liquid)	1

Hydrobromic Acid	50%	1
Hydrochloric Acid	10% concentrated	1 3
Hydrofluoric Acid	5% 50%	1 3
Hydrogen Peroxide	3% 30%	1 1
Hydroquinone	pure (solid)	1
Iron(III) Nitrate	pure (solid)	1
Isooctane	pure (liquid)	1
Isopropyl Alcohol	pure (liquid)	1
Lanolin	solid	1
Linalol	liquid	1
Magnesium Chloride	aqueous	1
Maleic Acid	50%	1

Mercury	pure (liquid)	1
Mercury (II) chloride	pure (solid)	1
Mercury (III) chloride	pure (solid)	1
2-Methoxy Ethanol	pure (liquid)	2
Methyl Alcohol	pure (liquid)	1
Methyl Cyclohexanol	pure (liquid)	1
Methyl Ethyl Ketone	pure (liquid)	3
Methyl Isobutyl Ketone	pure (liquid)	3
Methyl Methacrylate	pure (liquid)	2
Methyl Propyl Ketone	pure (liquid)	3
Methyl Salicylate	pure (liquid)	3
Methylene Chloride	pure (liquid)	3
Nitric Acid	1-10% 10-20% > 20%	1 2 3

Nitrobenzene	pure (liquid)	3
n-Octane	pure (liquid)	1
Oleic Acid	pure (liquid)	1
Oxalic Acid	aqueous pure (solid)	1 1
Oxygen	pure (gas)	1
Perchlorethylene	pure (liquid)	3
Phenol	5%	3
Phosphoric acid	1-10% 10-30% > 30%	1 2 3
Pinene	pure (liquid)	1
Potassium Bromide	pure (solid)	1
Potassium Chloride	10%	1
Potassium Chromate	pure (solid)	1

Potassium Cyanide	pure (solid)	1
Potassium Dichromate	10% pure (solid)	1 1
Potassium Hydroxide	1 - 10%	3
Potassium Permanganate	10% pure (solid)	1 2
Propionic Acid	pure (liquid)	3
Propyl Alcohol	pure (liquid)	1
Propylene Glycol	pure (liquid)	1
Salicylic Acid	pure (solid)	1
Sodium Acetate	40%	1
Sodium Bicarbonate	10% pure (solid)	1 1
Sodium Bisulfide	40%	1
Sodium Bisulphite	10%	1

Sodium Borate	pure (solid)	1
Sodium Bromide	pure (solid)	1
Sodium Carbonate	1-20% pure (solid)	1 1
Sodium Chloride	10%	1
Sodium Cyanide	pure (solid)	1
Sodium Hydroxide	1-30%	3
Sodium Hypochlorite	1-10%	1
Sodium Nitrate	pure (solid)	1
Sodium NitrIte	pure (solid)	1
Sodium Phosphate	pure (solid)	1
Sodium Sulphate	pure (solid)	1
Sodium Sulphite	pure (solid)	1

Sodium Thiosulphate	pure (solid)	1
Stearic Acid	pure (solid)	1
Sucrose	pure (solid)	1
Sulphur	pure (solid)	1
Sulphuric Acid	1-30% > 30%	1 3
Tartaric Acid	pure (solid)	1
Tetrachloroethylene	pure (liquid)	1
Tetrahydrofuran	pure (liquid)	3
Tetralin	pure (liquid)	1
Toluene	pure (liquid)	1
Trichloroacetic Acid	pure (solid)	3
1,1,1,-Trichloroethane	pure (liquid)	3
Trichloroethyl Phosphate	pure (liquid)	1

Trichloroethylene	pure (liquid)	3
Triethanolamine	pure (liquid)	3
Triisopropanolamine	pure (liquid)	3
Urea	urea/water/glycerol dispersion (1:1:1)	1
Xylene	pure (liquid)	1
Zinc Chloride	pure (solid)	1

ELSEVIER

Geotextiles and Geomembranes 13 (1994) 591–626
1994 Elsevier Science Limited
Printed in Ireland.
0266-1144/94/$7.00

Chemical Aging Effects on the Physio-Mechanical Properties of Polyester and Polypropylene Geotextiles

A. Mathur[a], A. N. Netravali[a]* & T. D. O'Rourke[b]

[a]Fiber Science Program, Department of Textiles and Apparel, [b]Civil and Environmental Engineering, Cornell University, Ithaca, New York 14853-4401, USA

(Received 9 April 1993; revised version received 16 December 1993; accepted 16 January 1994)

ABSTRACT

The influence of groundwater chemistry on the durability of geotextiles is important for the design of municipal and hazardous waste landfills, geotextile reinforcement of slopes and subgrades, and earth retention systems. A series of tests are described in this paper, which explore the effects of various pH and saline environments on geotextiles, thus contributing to an improved understanding of durability as a basis for design. Accelerated aging was performed on polyester and polypropylene geotextiles at room temperature and temperatures elevated to 95°C for six months in saline (pH ~8), strong alkaline (pH 10) and acidic (pH 3) media. Property changes as a result of aging were studied using tensile testing, differential scanning calorimetry (DSC), thermogravimetric analysis (TGA) and intrinsic-viscosity (I.V.) measurements. Scanning electron microscopy (SEM) was employed to study changes in the surface topography of the fibers upon aging. An Arrhenius model was used to extrapolate results of this short term study to the actual lifetime of the geotextiles.

Results indicate that polyester undergoes hydrolytic degradation under both acidic and alkaline conditions at and above the glass transition temperature, with the degradation being more severe under alkaline conditions. The polypropylene geotextile, on the other hand, was relatively inert to the pH conditions and showed no changes in strength. An increase in crystallinity in the initial period of aging was observed for both polyester

*To whom correspondence should be addressed.

and polypropylene. In polyester, this was due to preferential attack on the amorphous regions whereas in polypropylene this may be due to nucleation growth and lamellar thickening.

1 INTRODUCTION

Geotextiles have played an increasingly important role in the past decade in promoting secure landfills, stabilizing roadbeds and embankment foundations, and reinforcing slopes and earth retention systems (Ingold *et al.*, 1988; Giroud, 1984; Koerner, 1986; IFAI, 1990). In landfills, for example, geotextiles are used to filter and separate drainage layers from adjacent waste and soil, thus contributing to the unimpeded collection of leachates and restricting the build-up of internal fluid pressure. Depending on the facility into which they are incorporated, geotextiles may need to perform for relatively few years (as in the case of temporary retaining structures) or for 100 years or more (as in the case of landfills).

To survive aggressive underground environments, geotextiles must be resistant to various forms of attack, such as mechanical, chemical and biological. Chemical attack may be initiated directly by acidic or alkaline soils or indirectly by the active wastes present in the landfills. Depending on the type of chemical compound, changes in the polymer structure can be brought about by oxidation, chain scission, crosslinking, swelling or dissolution of the polymers, volatilization or extraction of ingredients of the polymeric compound, or an increase in the crystallinity of the polymer. In addition, the effects of chemical degradation may be accelerated by the service temperature.

A great deal of information has been compiled on the chemical resistance of polymers from a number of geotextile manufacturers (Horz, 1986). Cassidy *et al.* (1992) have summarized the resistances of various geosynthetic materials to different exposure media and the mechanical and chemical test methods which could be used to evaluate the ensuing property changes. More specifically, the effects of high levels of alkalinity on the flow and strength behavior for several geotextiles have been investigated by some researchers (Halse *et al.*, 1987; Montalvo, 1989). Accelerated aging in a chemical environment has also been studied to predict the long term properties of PET (polyester) and PP (polypropylene) geotextiles (Cassidy *et al.*, 1990). Koerner *et al.*, (1992) have suggested the use of the Arrhenius model to predict the lifetime of geosynthetics by studying the changes in the physical and mechanical properties after accelerated aging tests. In general, polypropylene fibers and geotextiles are relatively inert to chemical attack, whereas polyester geotextiles show limited resis-

tance to strong acids and alkalis. Results obtained for polyester geotextiles aged for 120 days at 22°C and 50°C in de-ionized water, sodium hydroxide (pH 12) and calcium hydroxide (pH 12·4) in the laboratory indicate the strong susceptibility of polyester to alkaline hydrolysis at elevated temperatures (Sprague, 1990).

Differences in physical and chemical properties of various geotextiles depend closely on the constituent fiber-forming polymers. The chemical and the supermolecular structure of the fiber as well as the method of manufacture of both the fiber and geotextile have a strong bearing on the geotextile properties.

Polypropylene (PP) generally assumes a linear structure, but due to the methyl group (CH_3), it can exist in three forms of different tacticity (i.e. the (CH_3) group may be present in three different spatial arrangements: isotactic, atactic and syndiotactic). Most commercial polymers and fibers of PP are approximately 90 per cent isotactic and crystallize in a helix form (Cooke & Rebenfeld, 1988). The methyl (CH_3) side group on the repeat unit of PP creates some reactive sites along the polymer backbone by the formation of a tertiary carbon which makes it susceptible to chemical attack.

Polyester (PET) is synthesized from terephthalic acid and ethylene glycol. The phenyl ring structure and the adjacent ester linkage supply rigidity and molecular flexibility, respectively, to the polymer through resonance stabilization. However, under strong acidic and alkaline conditions, PET undergoes hydrolysis, wherein a long chain linear molecule is split by a water molecule resulting in a scission of an ester linkage (Risseeuw & Schmidt, 1990). In addition, hydrolysis in alkaline media has been found to be more severe as compared to hydrolysis in an acidic environment (Risseeuw & Schmidt, 1990; Reich & Stivala, 1971).

The chemical properties of fibers, such as solubility and chemical resistance, are largely dependent on their chemical structure. These properties can be further influenced by the supermolecular structure of the fibers. Fibers are generally modeled as semi-crystalline, oriented polymers that take on a two-phase structure. This two-phase structure consists of crystalline regions, where the polymer chains are well oriented and closely packed into a three-dimensional ordered lattice structure, and non-crystalline (amorphous) regions, where the polymer chains are present in a random coil configuration with little or no packing regularity. Many of the important properties such as chemical absorption, extensibility and resilience of fibers are directly associated with these amorphous regions (Cooke & Rebenfeld, 1988).

The observation and examination, at a macrostructural as well as at a microstructural level, of geotextiles installed for several years under highly

diverse conditions, can reveal important information about their physical and mechanical properties. While long-term *in situ* tests are indispensable, they have the disadvantages of long durations, poor reproducibility and high cost. Under such circumstances, it is important to simulate the aging processes in a shorter time. While, in practical applications, changes occur slowly and are due to relatively weak influences, accelerated tests are based on more intensive action over a short period.

In this study, accelerated chemical aging was carried out at different temperatures and time periods under controlled conditions. The effects of aging on the physical and mechanical properties were determined using several analytical techniques such as tensile testing, thermal analysis by differential scanning calorimetry (DSC) and thermogravimetric analysis (TGA), intrinsic viscosity (I.V.) and scanning electron microscopy (SEM). Using these techniques, changes occurring at the microstructure level were analyzed. Finally, an attempt has been made to fit the data to a standard Arrhenius aging model to predict the long term performance of the geotextiles.

2 EXPERIMENTAL PROCEDURES

Two geotextiles were selected for this study, namely: (i) PET/GT, a continuous filament, nonwoven, lightly needle-punched polyester geotextile; and (ii) PP/GT, a continuous filament, nonwoven, heavily needle-punched polypropylene geotextile. The continuous filament geotextiles were produced by the spun bonded process wherein the fibers were continually extruded, drawn, cooled, sprayed to form a uniform web and needle-punched in one continuous operation. Typical values of some geotextile properties supplied by the manufacturers, are presented in Table 1.

2.1 Exposure conditions

Standard buffer solutions of pH 3 and pH 10 were used for the acidic and alkaline environments, respectively. The saline environment was simulated using a synthetic sea salt (Instant Ocean) which is commonly used for salt water fish aquariums (Mandaikar, 1985). Sea water normally contains a number of cations (weak acids), and although there are a lesser number of anions (bases or alkalies), some of these, such as chlorine, are quite strong. As a result, sea water is slightly alkaline, with pH ranging from 7·5 to 8·3. Since this was not a standard buffer, the solution was replaced every ten days in this study.

Specimens of dimensions suitable for tensile testing were randomly cut

Table 1
Physical Properties of the Geotextiles

Property	*PET/GT*	*PP/GT*
Mass/area	252 g/m^2 (7·4 oz/yd^2)	218 g/m^2 (6·4 oz/yd^2)
Thickness	2·54–2·80 mm	1·9–2·0 mm
Grab strength	1·08 kN	0·54 kN
Grab elongation	80%	50%
Average pore size	0·21 mm	0·21–0·15 mm

from the rolls supplied by the manufacturers and aged at 21°C (room temperature), 45°C, 70°C and 95°C for a period of 2 weeks, 6 weeks, 12 weeks and 24 weeks (6 months) in 32 oz (811·2 g) wide mouth glass bottles. Three air circulation ovens were used for this purpose. The temperatures were maintained within ±2°C of the required temperature. Although temperatures as high as 70°C and 95°C may not be commonly observed in practice, they were used for two reasons. Firstly, at elevated temperatures, the reaction rates are higher. Secondly, these temperatures enabled us to study the degradation kinetics of polyester both below and above its glass transition temperature (T_g), of about 70°C. At the end of each exposure, the specimens were removed from the ovens, washed thoroughly in reverse osmosis water and dried for at least 24 h prior to testing.

2.2 Tensile testing

The tensile tests were performed on the Instron Universal Testing Machine (Model #1122) interfaced with a Hewlett Packard 86B computer. To observe the effects of the accelerated aging treatment, the Cut Strip test was used in accordance with ASTM D 1682, which gave easily reproducible results. A gauge length of 76 mm (3 in) was used for a strip width of 25·4 mm (1 in). A crosshead speed of 200 mm/min was used which gave a strain rate of 2·63 min^{-1}. All specimens were conditioned at 21°C and 65% RH for at least 24 h before testing. Peak tensile strength (N/m) and elongation at peak strength (peak strain) in both machine and cross directions (since material is anisotropic) were obtained from the load vs elongation plots from an average of 10 readings.

2.3 Fiber tests

The deterioration of the fibers comprising the geotextile due to chemical aging has a strong bearing on the strength of the geotextile. The strength

of the geotextile is attributed to the network of fibers comprising the geotextile, with each fiber having its own contribution to the overall strength. The fiber strength, in turn, is directly related to the fiber morphology, the molecular weight and chemistry of the inherent polymer. Therefore, the tensile properties of the fibers before and after aging were also determined. To account for the variability in fiber diameters, fiber strengths are generally reported in terms of stress, for which the peak strength and area of cross section of the fiber were measured.

About 25–30 fibers each were carefully extracted from the polyester geotextiles for the untreated as well as for the extreme conditions. The peak fiber strength was measured on the Instron in accordance with ASTM D 3379. A gauge length of 20 mm and a crosshead speed of 20 mm/min (a strain rate of 1 min^{-1}) was used for the test. Exact details of the procedure are discussed elsewhere (Netravali *et al.*, 1989). Fibers from the polypropylene geotextile, however, could not be tested for tensile strength, since the lengths of the extracted fibers were too short to be tested.

2.4 Thermal analysis

The temperature dependence of the property changes occurring in the polymer due to aging was evaluated by DSC and TGA. A Perkin–Elmer DSC-4 with a System 4 microprocessor controller and a Model 3700 data station were used in this study. Specimens weighing 5–8 mg were scanned from 50°C to 300°C at a rate of 10°C/min in a nitrogen atmosphere and their melting characteristics (the melting point and the enthalpy of fusion) recorded. It was difficult to detect the glass transition temperature (T_g) for the polyester specimens in the first run due to the plasticization effect of the diffused water. The specimens were therefore quenched at 60°C/min and reheated at 10°C/min to eliminate the volatiles and other plasticizers, mainly water. The T_g, the onset of melting (T_m) and heat (enthalpy) of fusion (ΔH) were determined for the specimens treated under extreme conditions and compared to the values obtained for the untreated specimens.

Thermogravimetric studies were performed using a Perkin–Elmer TGS-2 with a System 4 microprocessor controller and a Model 3700 data station. Typically, a small piece of the geotextile (2–5 mg) was placed in a platinum pan enclosed in the furnace, and heated at 40°C/min in a nitrogen atmosphere. The degradation onset temperatures (T_d) and the weight losses for specimens exposed to extreme conditions were determined and compared with those for the untreated specimens.

2.5 Intrinsic viscosity

The degradation of polymers due to chain scission is reflected in changes in the molecular weight and molecular weight distribution. The molecular weight of a polymer is directly related to its intrinsic viscosity, $[\eta]$, by the following relationship:

$$[\eta] = KM^{\alpha} \tag{1}$$

where M is the molecular weight of the polymer, and K and α are material constants.

Since polyester is susceptible to chain scission resulting from hydrolysis, the $[\eta]$ values for polyester geotextiles were expected to decrease after aging. Representative specimens obtained under extreme treatment conditions were sent to Firestone Fibers and Textile Company for $[\eta]$ determination. Intrinsic viscosity was measured in 25/75, para-chlorophenol and tetrachloroethane mixture at 25°C using a standard viscometer.

2.6 Electron microscopy

Photomicrographs of fiber surfaces obtained using a Scanning Electron Microscope (Jeolco JSM 35) were inspected for evidence of pitting, etching or scratching of the individual geotextile filaments and for changes in the geotextile structure.

3 RESULTS AND DISCUSSION

A discussion of the test results for polyester geotextile (PET/GT) and polypropylene geotextile (PP/GT) are now given.

3.1 PET/GT (polyester)

3.1.1 Tensile test results

Changes in the tensile properties in the case of PET/GT were ascertained by observing the changes in their load elongation behavior before and after aging for both fabric as well as fiber specimens of the geotextile.

3.1.1.1 Geotextile strength. PET/GT is a lightly needled nonwoven geotextile. Due to the loose assemblage of fibers, the application of stress initially aligns the fibers along the direction of stress prior to failure. This behavior is evident in the stress–strain plot shown in Fig. 1, where three

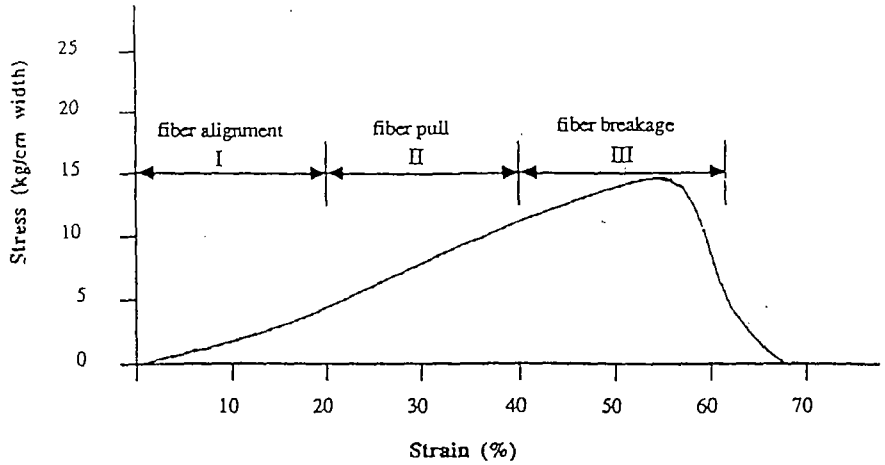

Fig. 1. Typical stress–strain plot for PET/GT.

distinct regions can be identified. The first region has a low modulus where the fibers align themselves in the direction of the stress. The second region exhibits a higher modulus. In this region, the fiber alignment is complete or further alignment becomes more difficult. This region also exhibits linear stress–strain behavior. Finally, in the third region, the modulus falls again as the fibers begin to break. While the fracture strength is influenced by the strength and orientation of the fibers in the geotextile, the fracture strain depends mostly upon the amorphous content in the fiber and the fiber orientation.

The average peak (breaking) stress for the untreated PET/GT geotextile was 15·37 kN/m with a corresponding peak strain of 65·36% in the machine direction and 12·65 kN/m with a peak strain of 64·60% in the cross direction. The higher strength in the machine direction reflects the anisotropy in the geotextile wherein a larger number of fibers are aligned in the machine direction than in the cross direction.

The plots of strength values obtained in the machine direction after each exposure condition are shown in Figs 2, 3 and 4. As shown in Fig. 2, no apparent change in the stress values is seen at either 21°C or 50°C in pH 10, even after 24 weeks of exposure. In contrast, a steady decrease in strength is observed as a function of aging at 70°C. At 95°C, an approximate 80% drop in strength occurs within the first 4 weeks of exposure, and the specimens dissolve completely within the next 2 weeks. A similar trend is observed for the specimens tested in the cross direction, which indicates that the effects of aging are not so much dependent on the structure of the geotextile as they are on the constituent fiber or the polymer type.

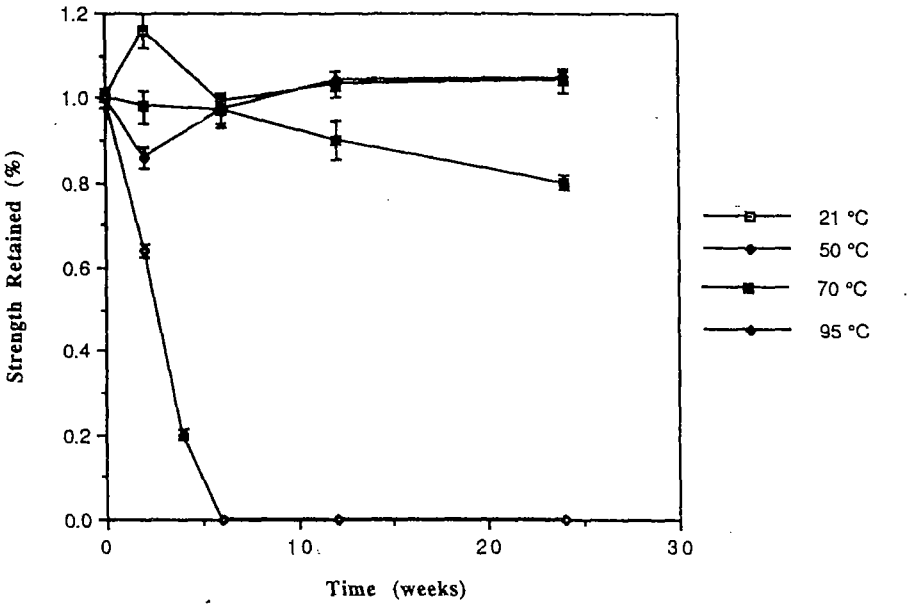

Fig. 2. Effect of pH 10 on PET/GT tensile strength.

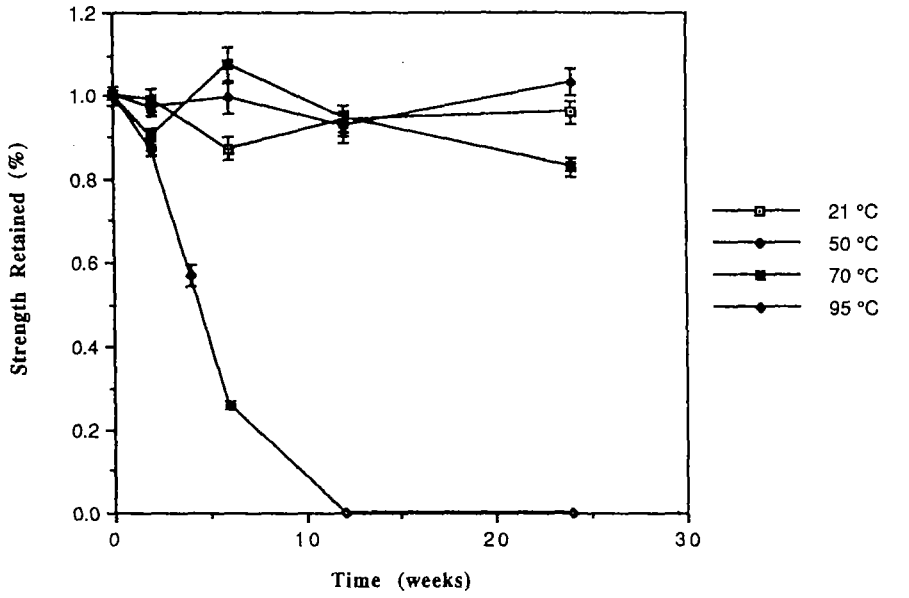

Fig. 3. Effect of pH 3 on PET/GT tensile strength.

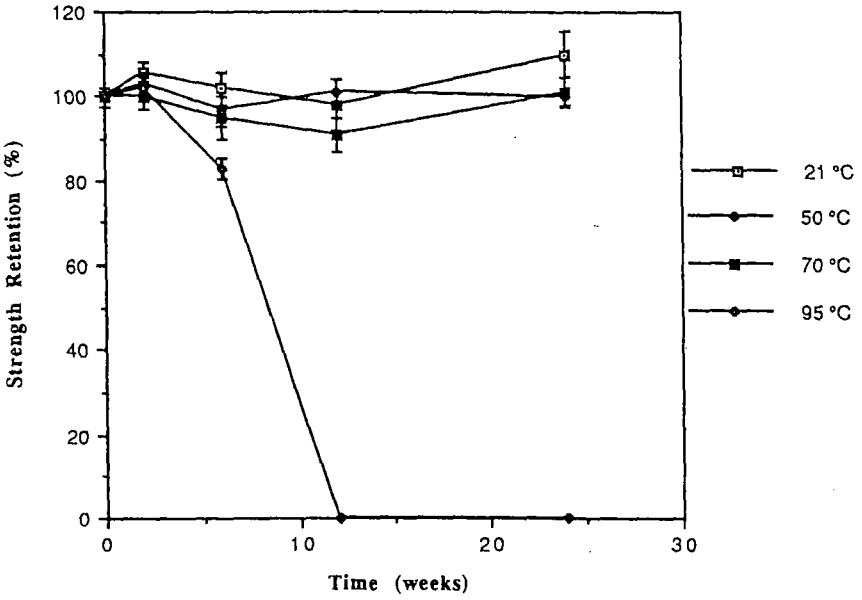

Fig. 4. Effect of sea water on PET/GT tensile strength.

The effect of pH 3 on the tensile strength of the PET/GT under various exposure conditions is shown in Fig. 3. As in the case with pH 10, for pH 3, there was no change in the strength values at 21°C and 50°C, while at 70°C, a slight strength reduction was observed after 24 weeks of aging. At 95°C, the effect of pH 3 was less severe than that obtained for pH 10, although the trend is similar. A 43% reduction in peak strength was observed after 4 weeks of aging and the specimens dissolved completely between the 6 week and 12 weeks aging period. Again, the results obtained in the cross direction followed a similar trend.

The action of sea water on PET/GT, as shown in Fig. 4, was milder than both pH 3 and pH 10. No significant change in strength was observed at 70°C, even after 24 weeks of exposure. At 95°C, however, a strength reduction of 18% was observed after 6 weeks of aging with complete dissolution occurring after 12 weeks.

Another noticeable observation was that the strains to failure for PET/GT decreased with increasing aging time for all pH conditions. Percentage retention of the failure strains after increasing periods of aging are shown in Figs 5, 6 and 7. For pH 10, the strain value for PET/GT decreased by around 15% after 24 weeks of exposure at 70°C and by 60% within 6 weeks at 95°C. Similar changes were obtained for pH 3, while for sea water conditions, the maximum reduction in strain was 15% after 6 weeks of aging at 95°C.

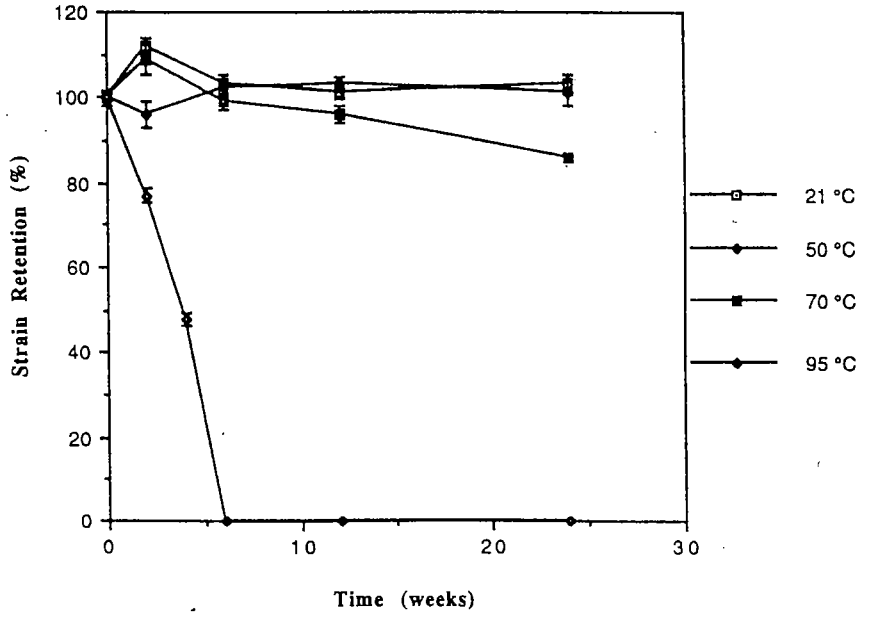

Fig. 5. Effect of pH 10 on PET/GT strain.

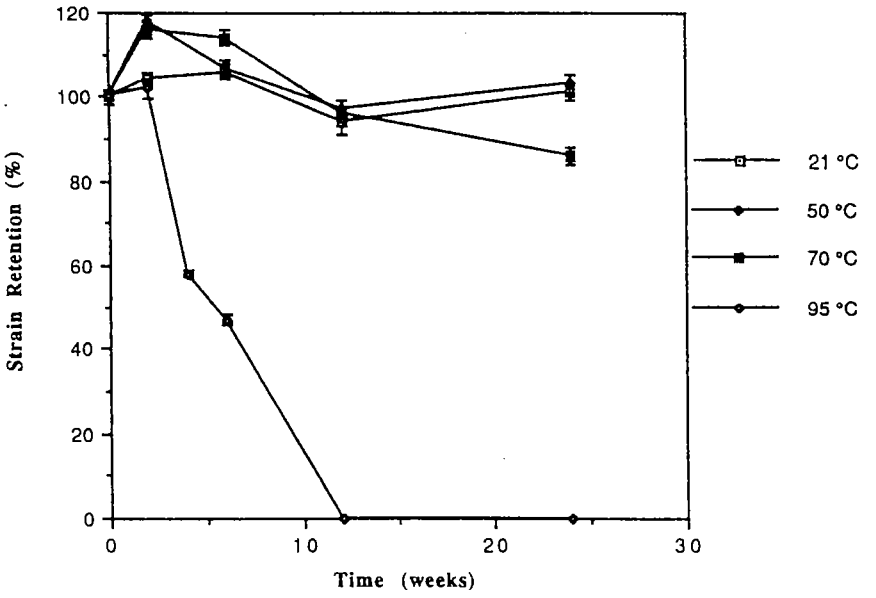

Fig. 6. Effect of pH 3 on PET/GT strain.

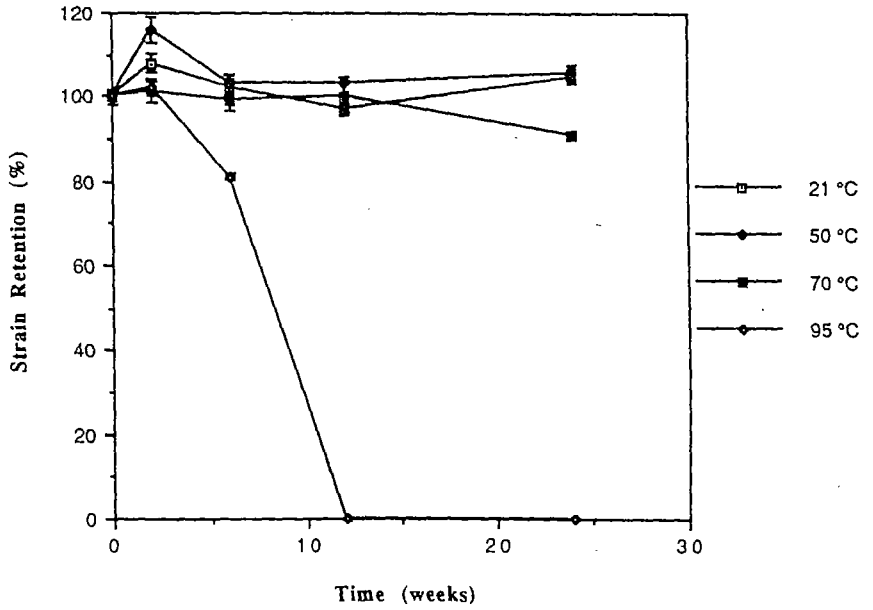

Fig. 7. Effect of sea water on PET/GT strain.

3.1.1.2 Fiber strength. Plots of the PET/GT fiber strength tests performed for the extreme conditions for aging temperatures of 70°C and 95°C are shown in Figs 8, 9 and 10. As evident from the results, the fiber strength loss shows a similar trend as that obtained for the geotextiles. The severity of fiber degradation is greater in alkaline media as compared to acid and sea water. The reduction in fiber strength after 4 weeks of aging at 95°C was around 63% for pH 10, 47% for pH 3 and 21% for sea water. The tensile results for both the geotextile and fiber indicate that PET/GT is relatively inert to chemical attack at temperatures below 70°C. However, at temperatures above the glass transition temperature of polyester (~73°C), such as 95°C in the present study, some severe hydrolytic degradation occurs. These results agree with those obtained by other researchers (Cassidy *et al.*, 1990; Sprague, 1990; Risseeuw & Schmidt, 1990; Schneider & Groh, 1987). Hydrolysis in neutral water and acidic media is catalyzed by the free hydrogen (H^+) ions, while alkaline hydrolysis is due to the more reactive hydroxyl (OH^-) radicals (Risseeuw & Schmidt, 1990).

3.1.2 Intrinsic viscosity measurements

The splitting or scission of the ester linkages due to hydrolysis, results in the reduction of the molecular weight. The molecular weight of a polymer

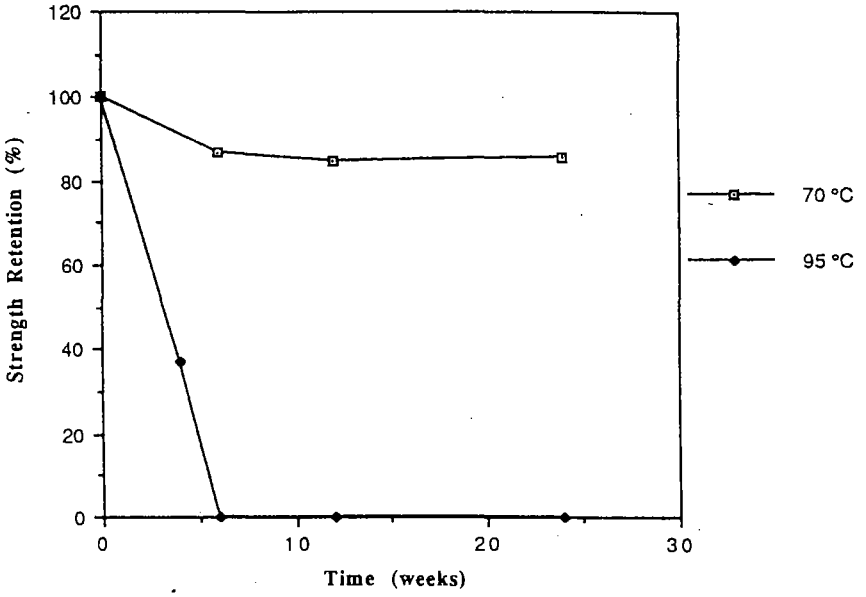

Fig. 8. Effect of pH 10 on PET/GT fiber strength.

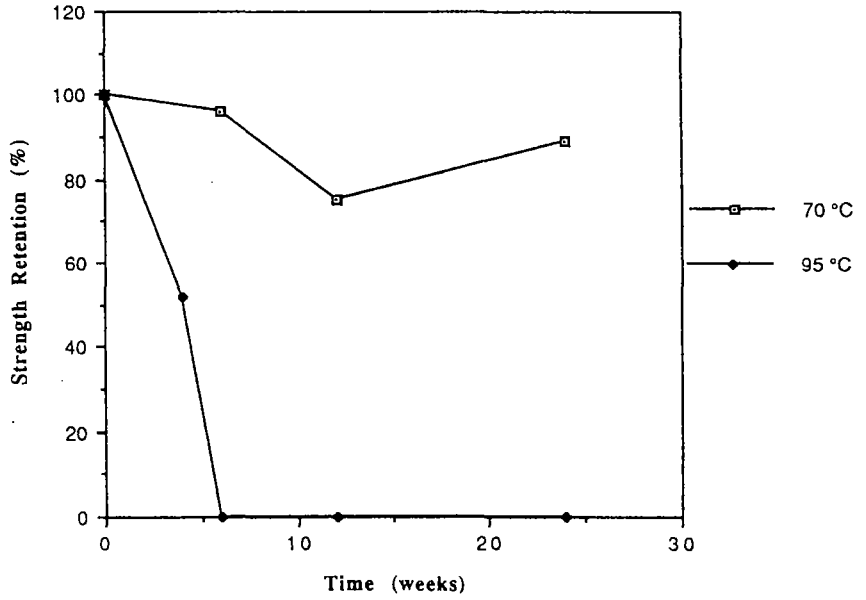

Fig. 9. Effect of pH 3 on PET/GT fiber strength.

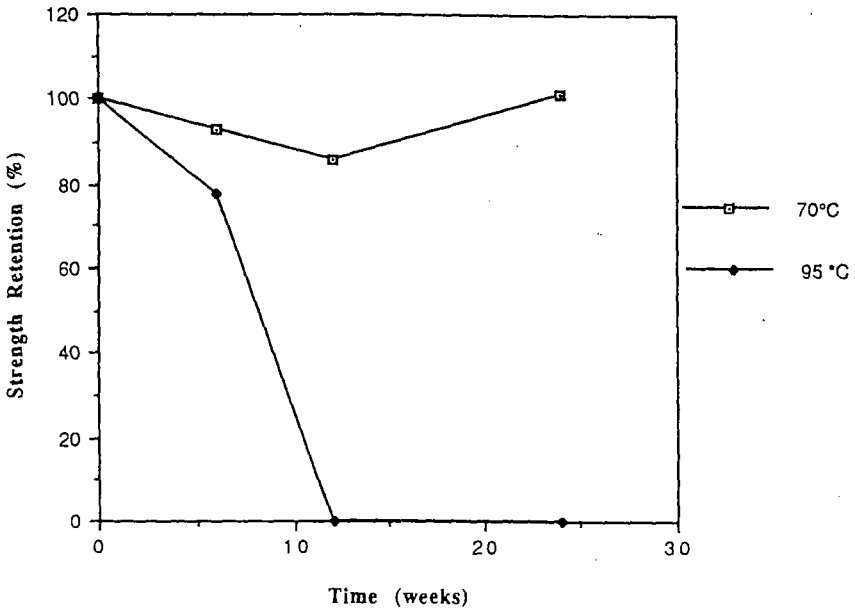

Fig. 10. Effect of sea water on PET/GT fiber strength.

is related to its intrinsic viscosity [η] as explained earlier. Intrinsic viscosity data for PET/GT treated under some extreme conditions are presented in Table 2 below.

The [η] results for 95°C indicate a significant reduction (greater than 50%) in the molecular weight of the polyester specimens confirming the molecular chain scission after hydrolysis. The [η] results for 50°C, on the other hand show only a weak trend of reduced values with time implying that hydrolysis is at an incipient stage below the glass transition temperature.

Table 2
Intrinsic Viscosity (dl/g): PET/GT

Temp		50°C		95°C		
Time	Untreated	12 weeks	24 weeks	4 weeks	6 weeks	12 weeks
pH 3	0·612	0·596	0·602	0·233	0·220	—
pH 10	0·612	0·598	0·605	0·288	0·253	—
Sea water	0·612	0·604	0·600	—	0·373	0·214

3.1.3 DSC results: PET/GT

Figure 11 shows a typical DSC thermogram obtained for untreated PET/GT, showing the melting point (T_m) between 250°C and 255°C with an enthalpy of fusion of around 50·21 kJ/kg.

Table 3 compares the onset of melting point (T_m) and the enthalpy of fusion (ΔH) for the untreated specimens and those treated under extreme conditions.

The T_m and ΔH data for all pH conditions at 70°C show a slight increase indicating an increase in crystallinity. However, the specimens treated in pH 10 at 95°C, where the hydrolytic degradation is more severe, behave differently. In contrast to degradation at 70°C, a decrease in both T_m and ΔH values was observed. While the melting point onset was lowered from 254·5°C to 248·6°C, the enthalpy of fusion decreased from 50·21 kJ/kg to 36·40 kJ/kg within six weeks of aging.

During the initial period at 70°C, the ΔH values seem to increase for the fibers treated with pH 10 and pH 3. We attribute this to the decrease in the amorphous content rather than the increase in the crystallinity. Degradation proceeds initially in the amorphous region which is considered 'open', with sufficient free volume or voids, compared to the crystal-

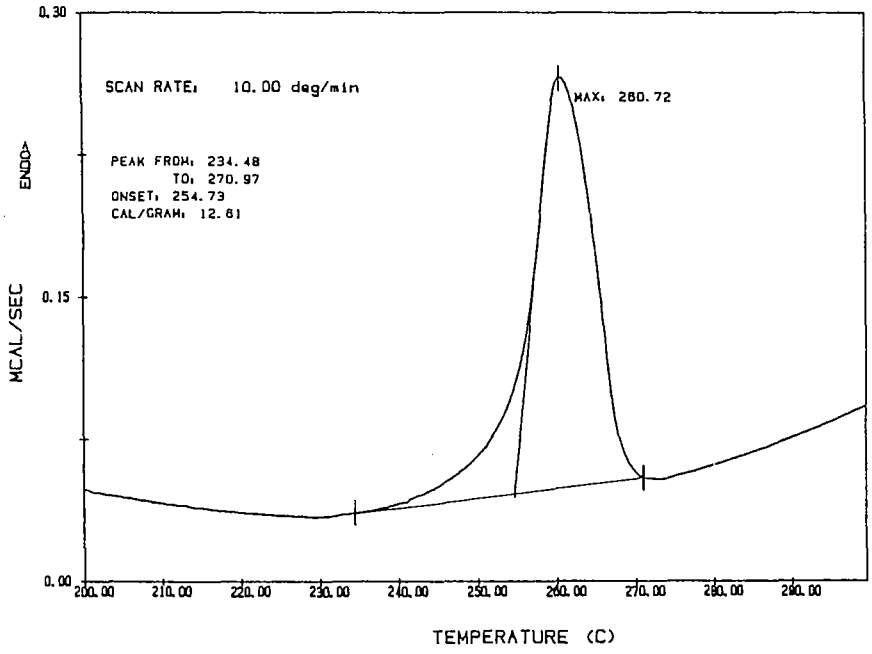

Fig. 11. Typical DSC thermogram for PET/GT.

Table 3
DSC Results for PET/GT

Temp		70°C			95°C	
Time	Untreated	6 wks	12 wks	24 wks	2 wks	6 wks
*pH 10**						
T_m (°C)	253·4	254·2	255·0	254·6	254·5	248·6
	(0·96)	(0·45)	(0·28)	(0·70)	(0·62)	(1·19)
ΔH	50·21	58·16	53·56	54·81	48·95	36·40
(kJ/kg)	(2·05)	(1·76)	(1·38)	(3·10)	(3·26)	(4·94)
*pH 3**						
T_m (°C)	253·4	254·2	255·5	253·2	254·3	252·3
	(0·96)	(0·64)	(0·84)	(0·78)	(0·47)	(1·65)
ΔH	50·21	51·04	55·22	50·21	47·70	61·09
(kJ/kg)	(2·05)	(3·68)	(1·42)	(2·18)	(4·31)	(3·47)
*Sea water**						
T_m (°C)	253·4	253·0	255·2	253·7	255·0	251·7
	(0·96)	(0·69)	(0·67)	(1·1)	(0·76)	(1·74)
ΔH	50·21	50·63	52·30	49·79	48·12	49·79
(kJ/kg)	(2·05)	(1·59)	(3·56)	(3·51)	(2·43)	(7·41)

*Each reading is an average of three specimens with the standard deviations shown in parentheses.

line region, which is tightly packed and dense. This relatively high accessibility of the amorphous regions to water molecules causes the chains to hydrolyze into fragments during the initial period. As hydrolytic degradation progresses with time, the molecular fragments decrease in size until they are small enough to leach away into the surrounding medium, thus increasing the 'apparent' crystallinity. The molecular weight reduction due to the loss in material is reflected in the reduced strengths of the geotextile and fiber as well as the reduced intrinsic viscosity values for these conditions. This phenomenon occurs for the PET/GT geotextile treated in all the pH conditions during 12 weeks of aging at 70°C and continues for six months for specimens treated with pH 10.

An increase in crystallinity may also occur when undegraded chain segments remaining in the amorphous regions acquire more chain mobility, thus enabling them to get incorporated into the existing crystals (Jailloux & Verdu, 1990). This process, involving an increase in the density during aging, is called chemicrystallization (Ballara & Verdu, 1989; Jailloux & Verdu, 1990; Sprague, 1990). An increase in the melting temperature, T_m, and the enthalpy of fusion, ΔH, indicates possible lamella thickening linked to the chemicrystallization process.

With continuing chemicrystallization and leaching of the amorphous material, the crystallinity reaches a maximum, until a stage comes when the crystals start getting attacked. As a result, the crystal size decreases, which is manifested in a decrease in T_m, with an overall decrease in crystallinity in the polymer, as indicated by the lower ΔH values. Degradation of the crystalline regions, however, occurs much more slowly than the amorphous regions. This explains the drop in the melting point and enthalpy of fusion after prolonged exposure of six months at 70°C for pH 3 and sea water. In the pH 10 environment, where hydrolytic degradation is more severe due to the reactive hydroxyl groups, the crystals get attacked much earlier, i.e. within three months of aging.

At 95°C, the effects of aging differ slightly for the three pH conditions. In pH 10, this phenomenon is reflected both in the decrease in T_m and the large drop in the enthalpy of fusion from 48·95 kJ/kg to 36·40 kJ/kg within 6 weeks of aging. The increasing brittleness can also be attributed to the increase in the crystallinity of the polymer, since it is the amorphous regions which give the fiber its extensibility. For pH 3, where the hydrolytic degradation is not as severe as in pH 10, degradation seems to occur simultaneously in both amorphous and crystalline regions. While the 'apparent' crystallinity (ΔH) increases, the crystal size decreases which can be inferred from the lower T_m values. In sea water, the hydrolytic attack is the least severe and degradation in the two regions compete with each other. As a result, there is no significant change in the overall crystallinity of the fibers. However, the degradation of the crystalline region is reflected in the lower value of T_m after 6 weeks of aging at 95°C.

3.1.4 TGA results: PET/GT

Thermogravimetric analysis yields similar results for all the pH conditions. Figure 12 shows a typical thermogram obtained for the untreated PET/GT geotextile. The degradation onset for polyester was around 425°C and the weight loss around 86%. The 14% residual carbon, probably in the form of graphite, is contributed mainly by the decomposed benzene functional group (Hsuan, 1991). Table 4 compares the results obtained for PET/GT before and after aging for the adverse conditions. All the degradation onset temperatures (T_d) fall within the narrow range of 425–430°C, indicating no fundamental change in chemistry.

3.1.5 Microstructure: PET/GT

SEM photomicrographs of the untreated PET/GT and that treated for 6 weeks in pH 3 and pH 10 solutions at 95°C are shown in Figs 13, 14 and

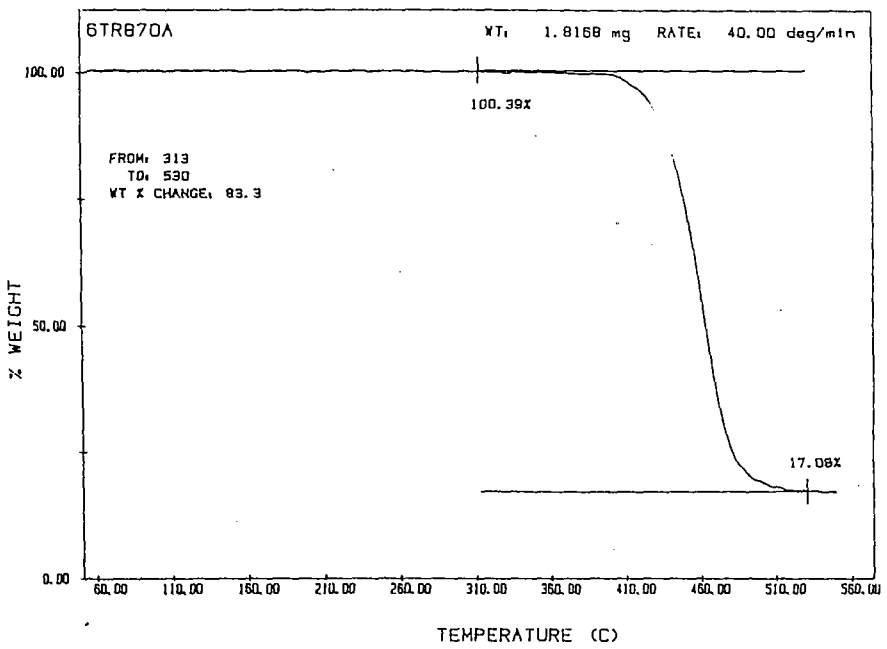

Fig. 12. Typical TGA plot for PET/GT.

15, respectively. They confirm the results of Halse *et al.*, (1987), Solbrig & Obendorf (1986), and Collins *et al.*, (1988) who showed that alkaline hydrolysis occurs primarily on the surface of the fiber. A loss of material is evidenced by etching marks on the surface of the fibers. Acid and sea

Table 4
TGA Results: PET/GT

Temp		70°C				95°C	
Time	Untreated	2 wks	6 wks	12 wks	24 wks	2 wks	6 wks
*pH 10**							
T_d *(°C)*	425·3	428·0	430·3	433·5	436·9	428·9	430·7
Wt. Loss (%)	87·2	85·3	85·4	84·4	82·2	86·5	83·2
*pH 3**							
T_d *(°C)*	425·3	426·6	430·0	430·4	431·0	424·9	431·8
Wt. Loss (%)	87·2	86·1	86·4	88·0	87·3	85·7	86·1
*Sea water**							
T_d *(°C)*	425·3	429·2	434·9	434·7	434·6	428·6	432·0
Wt. Loss (%)	87·2	84·5	83·9	85·5	82·9	86·5	84·8

*Each reading is an average of 3 specimens.

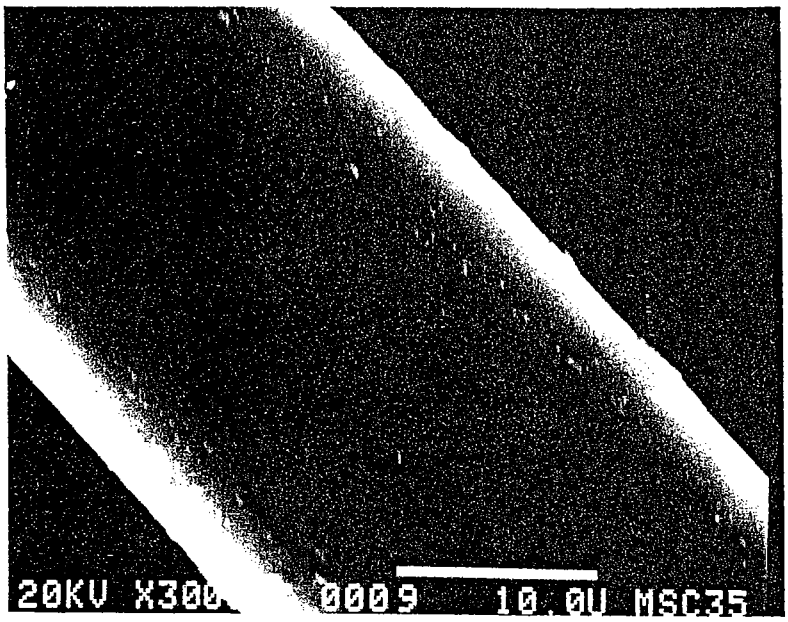

Fig. 13. SEM micrograph of untreated PET/GT.

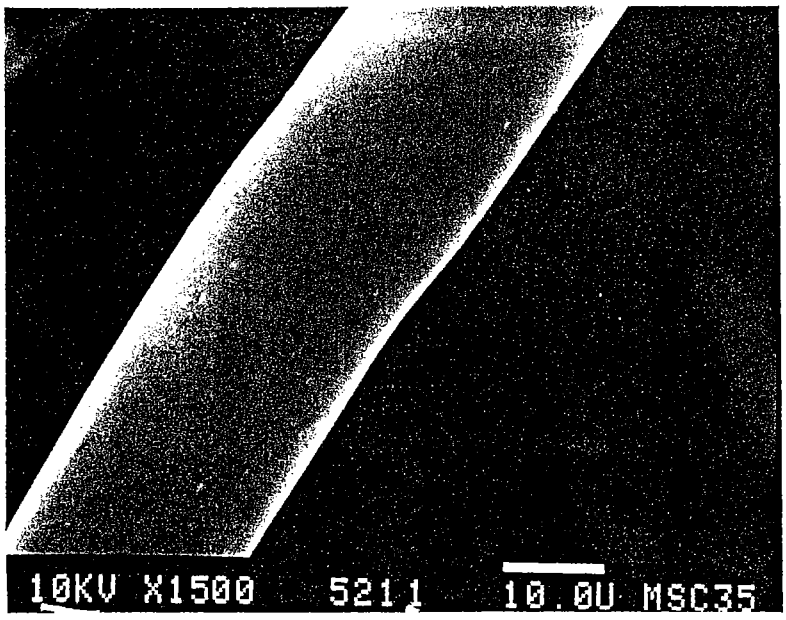

Fig. 14. SEM micrograph of PET/GT treated at pH 3 for 6 wks at 95°C.

Fig. 15. SEM micrograph of PET/GT treated at pH 10 for 6 wks at 95°C.

water hydrolysis, however, occurs within the fiber and no evidence of aging is visible on the surface. Figures 13 and 14 show the unchanged fiber surface before and after aging in pH 3 solution. However, severe etching marks can be seen in Fig. 15 on the PET fibers treated under extreme alkaline conditions, causing some cracks to develop on the fiber surface.

3.2 PP/GT (Polypropylene)

3.2.1 Tensile test results

Cut strip tests were performed on the Instron for the polypropylene geotextile, PP/GT, under the same conditions explained earlier for PET/GT in Section 2.2. A typical load-elongation plot for untreated PP/GT is shown in Fig. 16. The three zones with stress/strain characteristics similar to those for PET/GT (see Fig. 1) can be ascertained. PP/GT, however, exhibits a lower elongation at break than PET/GT. This is attributed to greater fiber entanglements in PP/GT as a result of heavier needle-punching, as compared to the lightly needled PET/GT. The lower strength of polypropylene fiber combined with a lower weight of the geotextile results in a lower strength (13·09 kN/m) in the machine direction for PP/GT as compared to the polyester geotextile. The anisotropic nature of construction of the PP/GT results in a lower value of geotextile strength (11·70 kN/m) in the cross direction, indicating a greater amount of fibers being aligned in the machine direction than in the cross direction. Peak stress data obtained before and after aging for PP/GT in the machine direction is plotted in Figs 17, 18 and 19.

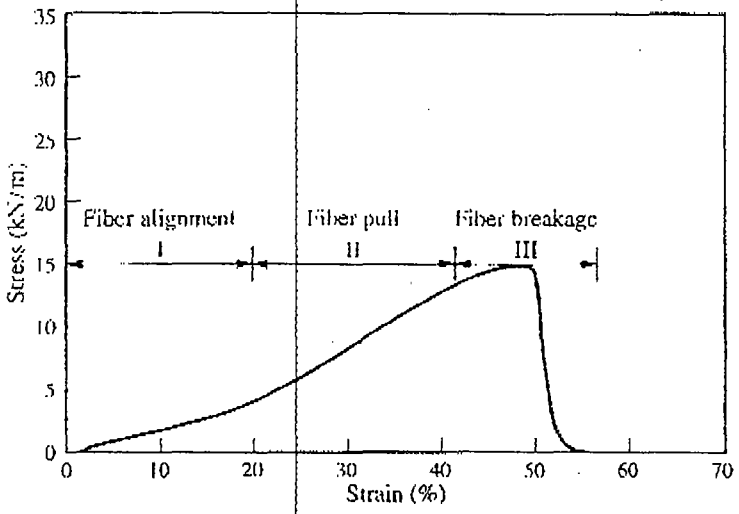

Fig. 16. Typical stress vs strain plot for PP/GT.

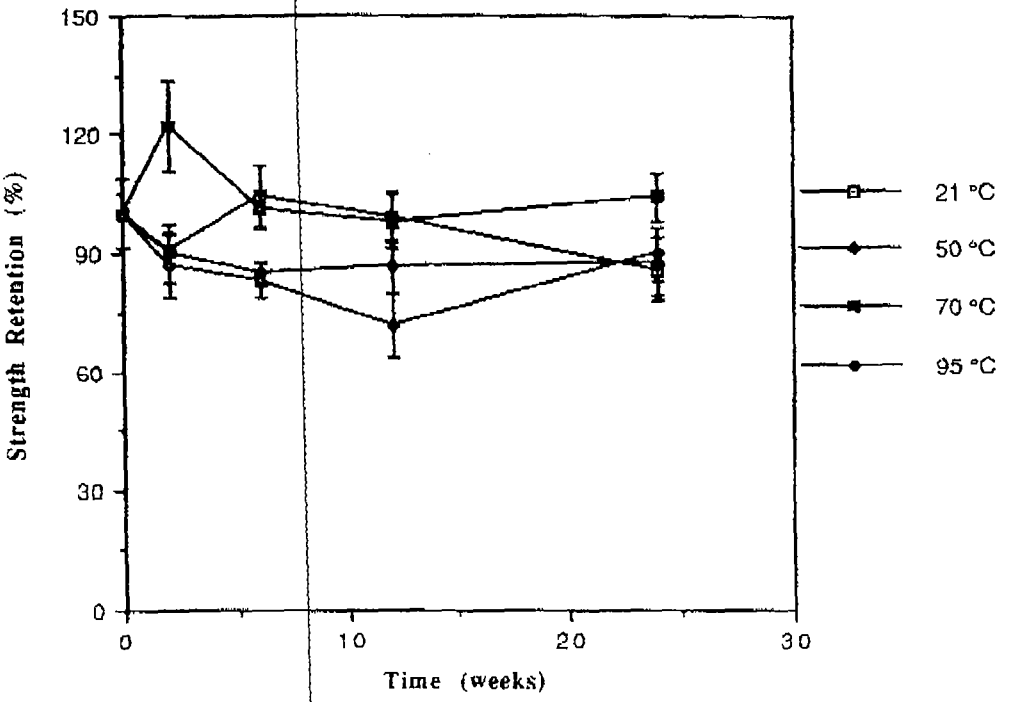

Fig. 17. Effect of pH 10 on PP/GT tensile strength.

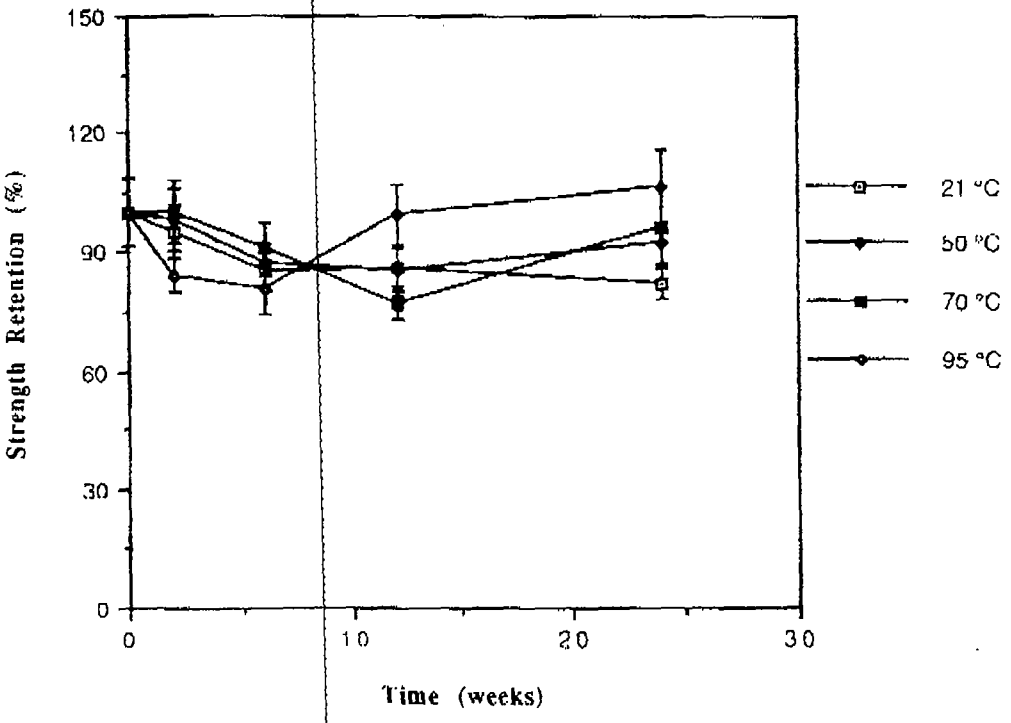

Fig. 18. Effect of pH 3 on PP/GT tensile strength.

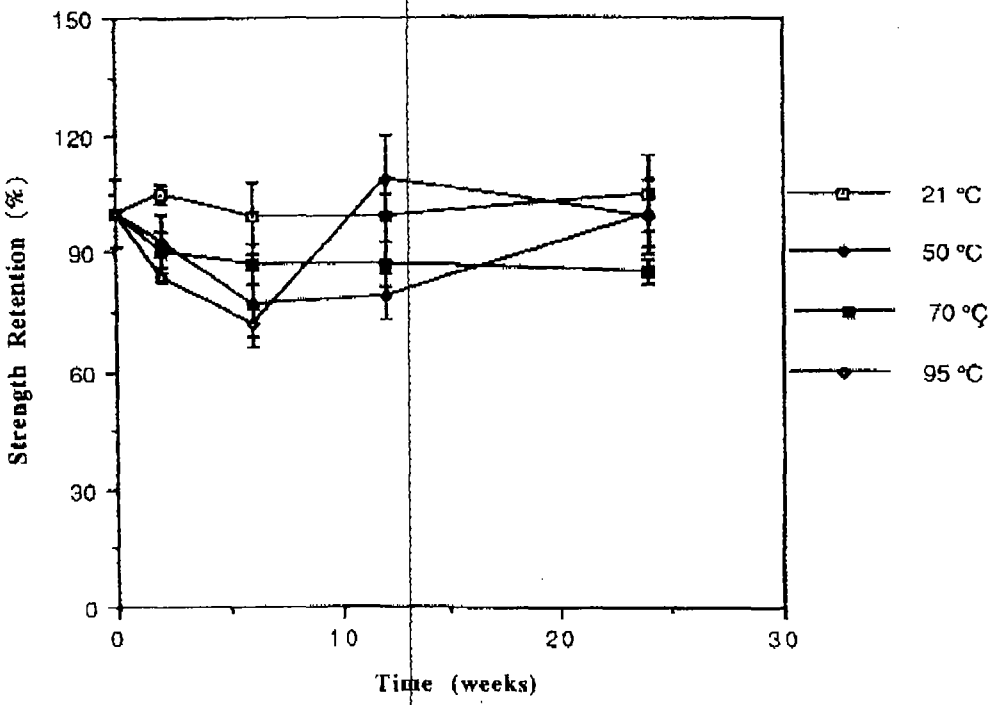

Fig. 19. Effect of sea water on PP/GT tensile strength.

In contrast to polyester, polypropylene fibers are made up of non-polar hydrocarbon chains which are relatively inert to chemical attack. No apparent strength loss occurred in PP/GT under any of the pH conditions, which agrees well with our expectations and the results obtained by earlier investigations (Halse *et al.*, 1987). All strength values were within one standard deviation of the strengths obtained with untreated PP/GT geotextiles. Even at the highest temperature of 95°C, the peak strength values in both machine and cross directions did not show any significant loss as compared to the untreated specimens. However, like polyester, the strain values of PP/GT decreased significantly in the machine and cross direction after 24 weeks of aging for all conditions. The brittleness occurred in the initial 6 weeks and then remained unchanged. Figures 20, 21 and 22 give the strain values obtained for the three pH conditions. As mentioned earlier, fiber tests could not be performed on PP/GT fibers because of difficulty in extracting fiber lengths required for testing.

3.2.2 DSC results: PP/GT

Polypropylene generally exists in its isotactic form in a fiber. The characteristic dual peak in the melting exotherm of this particular polypropylene geotextile is attributed to the slow solid phase transition from the γ (lower melting) form to the α (higher melting) form, which has time

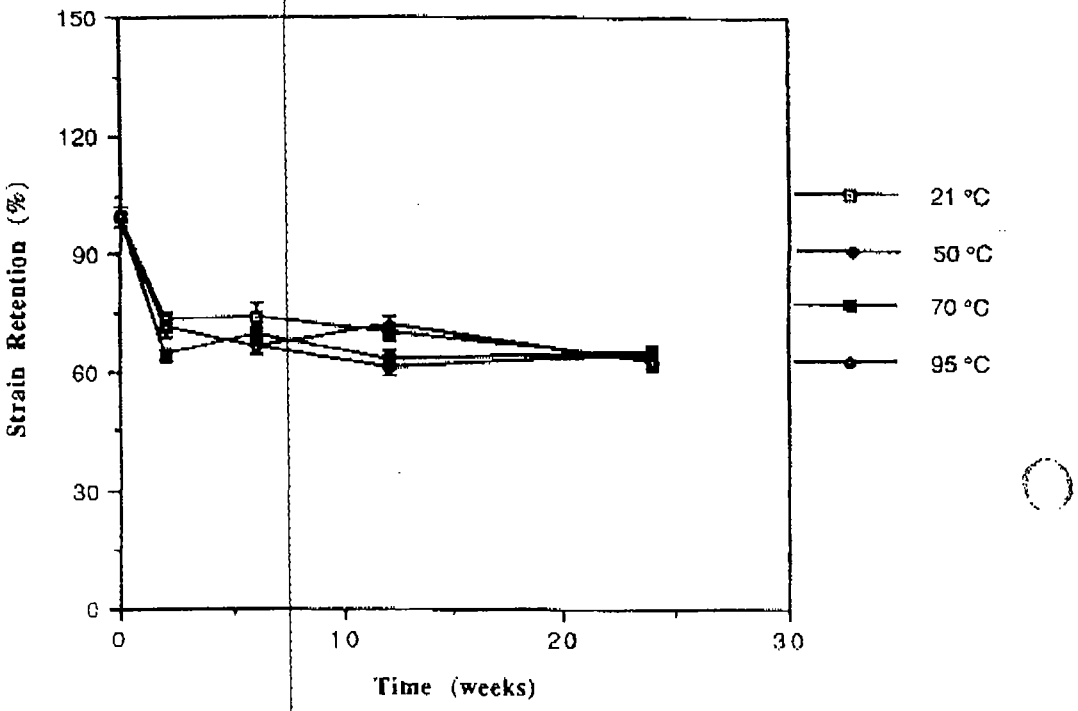

Fig. 20. Effect of pH 10 on PP/GT strain.

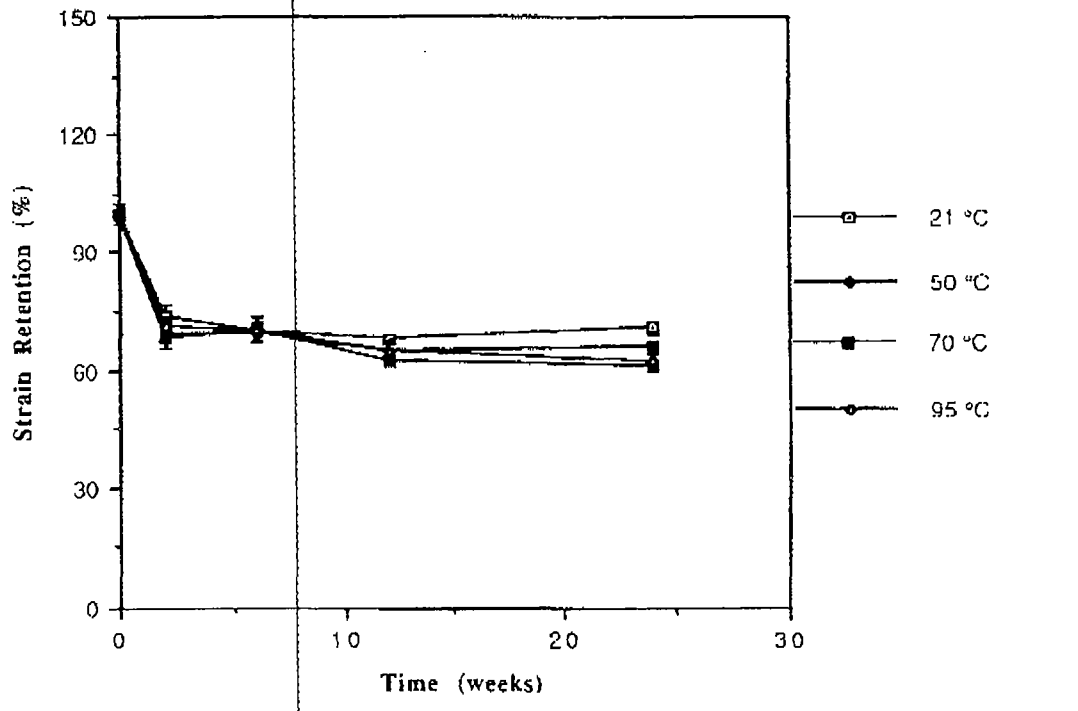

Fig. 21. Effect of pH 3 on PP/GT strain.

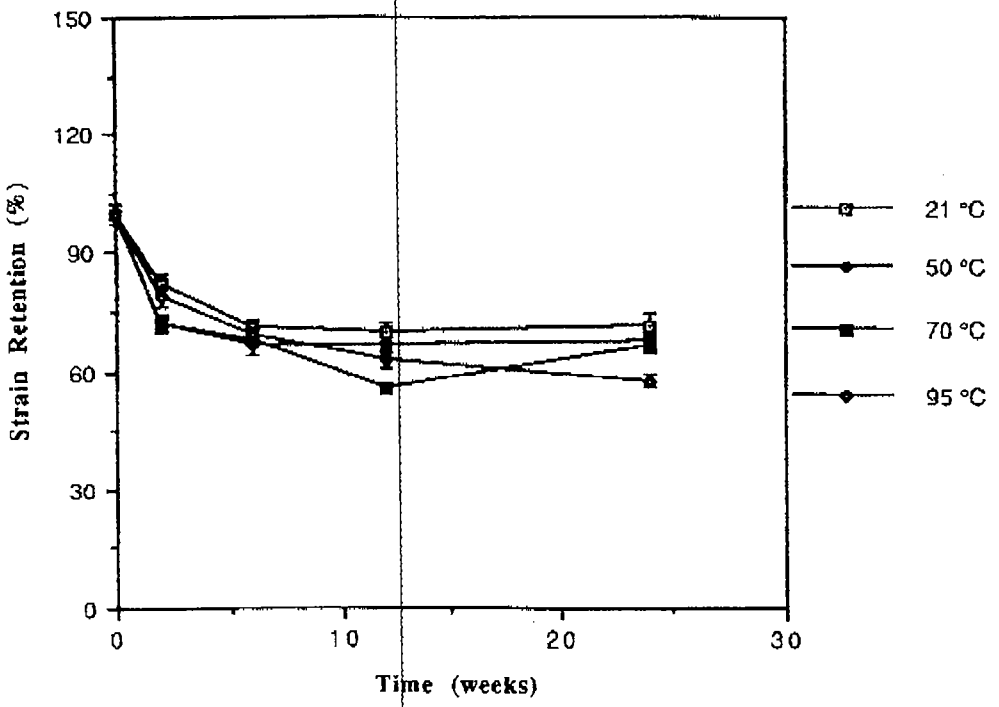

Fig. 22. Effect of sea water on PP/GT strain.

to crystallize during slow heating. Annealing the specimen just above the melting point of the γ form leads to conversion to the α form only. Figure 23 shows a typical DSC thermogram of PP/GT during the first heating run, clearly showing the two characteristic peaks. Figure 24 shows the thermogram for the second run corresponding to the annealing condition. In addition to the reasons discussed in Section 2.4, the second run was useful to maintain a constant thermal history and thus obtain the results under more controlled conditions. Also, because of the fast cooling, only one peak corresponding to the α form was observed which made it easy to compare the results of different aging conditions.

The melting point (T_m) for untreated polypropylene was found to be around 148°C, while the enthalpy of fusion (ΔH) was around 89·12 kJ/kg. Table 5 compares the values obtained for T_m and ΔH before and after aging for all pH conditions at 70°C and 95°C.

For all the three pH conditions, the DSC results follow the same trend. The T_m increases gradually from 148°C to 151°C, while ΔH gradually increases from 89 kJ/kg to 96 kJ/kg after 6 months (24 weeks) of aging, the effect being more pronounced at 95°C. The increase in both T_m as well as ΔH indicates an increase in both the crystallinity and crystal size. This may be attributed to effects of annealing at extended periods of time, wherein, molecular chains in the amorphous region get drawn out into crystalline domains. The reduction in the amorphous content is indicated

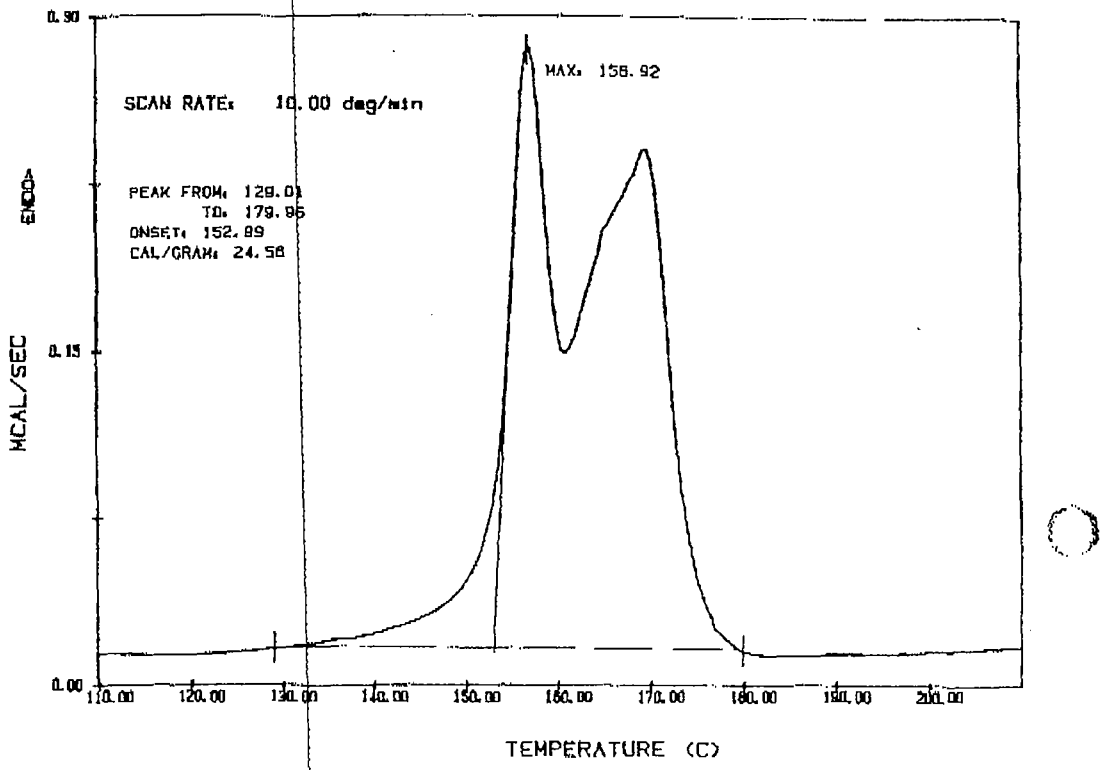

Fig. 23. Typical DSC thermogram of PP/GT (first run).

by slightly lower strains to failure after annealing. In other words, the whole system tends to equilibrate towards the lowest energy state, which is the crystalline state. This process is similar to the one for PET/GT discussed earlier in Section 3.1.3. The increased crystallinity can be explained by studying the kinetics of the crystallization process. Nucleation and growth rates, and therefore the rate of crystallization, have been found to be sensitive to temperature (Ziabicki, 1976). At certain temperatures, these nucleation and growth rates pass through a maximum. For isotactic polypropylene, crystallization starts at around 30°C, passes through a maximum at around 65°C and drops off gradually after 95°C. In this study, PP/GT was subjected to temperatures ranging from 21°C to 95°C. These temperatures spanned the range of crystallization temperatures for polypropylene, thus promoting nucleation.

3.2.3 TGA results: PP/GT

Thermogravimetric analyzer results follow the same trend as observed for the DSC results. Figure 25 gives a typical trace of the thermogram obtained for the untreated PP/GT specimen. The onset of degradation for

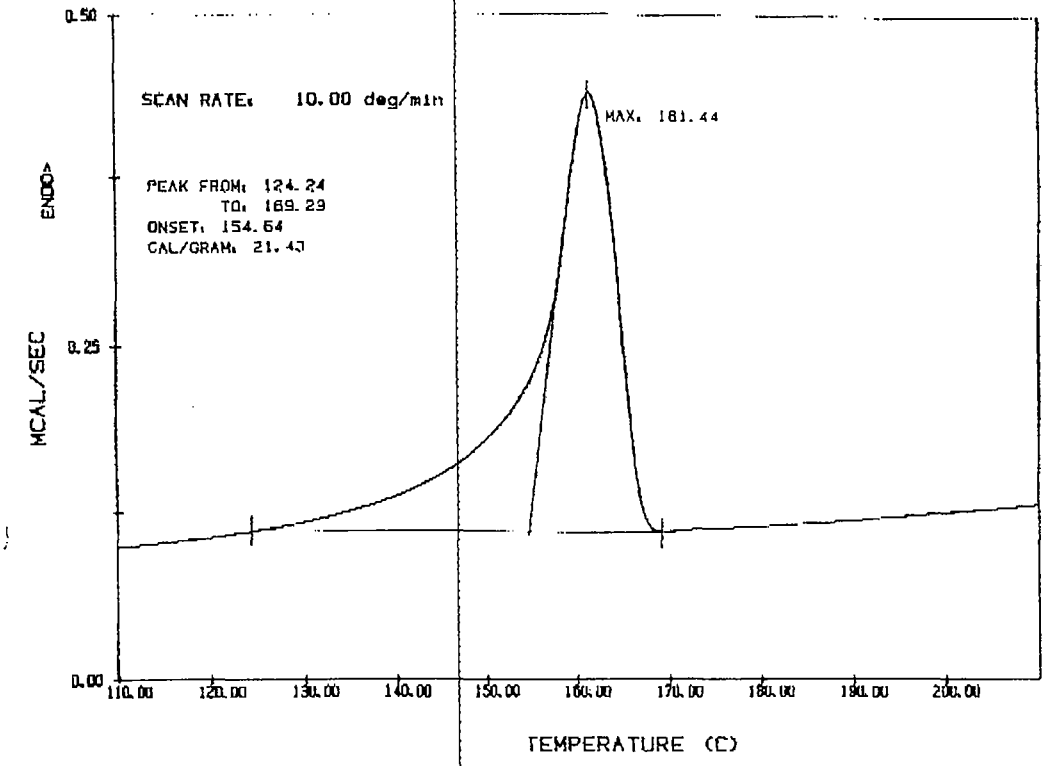

Fig. 24. Typical DSC thermogram of PP/GT (2nd run).

polypropylene at 462°C is higher than that for polyester, which agrees well with those obtained by Hsuan (1991). The absence of the oxygen in the PP structure renders it less prone to thermo-oxidative degradation as compared to PET, which has an ester group containing oxygen in its main chain.

Table 6 shows the results of the TG analysis for some extreme conditions. The degradation onset temperatures (T_d) are found to vary within a range of 459°C to 467°C for most of the cases.

3.2.4 Microstructure: PP/GT

SEM photomicrographs showing the effect of aging on the surface topology of the polypropylene fiber are shown in Figs 26 and 27. The surface of these fibers appeared relatively smooth even after the most intensive aging conditions. Unlike PET/GT, there is no evidence of etching marks or pitting of the surface. The surface features of PP/GT after 6 months of aging in pH 10, pH 3 and sea water appeared relatively smooth and similar to the untreated fiber. These observations confirm the relative inertness of polypropylene to chemical media, as determined from mechanical property testing.

Table 5
DSC Results for PP/GT

Temp		70°C		95°C			
Time	Untreated	12 wks	24 wks	2 wks	6 wks	12 wks	24 wks
*pH 10**							
T_m (°C)	148·0	150·1	150·9	150·3	150·9	151·6	151·2
	(0·78)	(0·65)	(0·88)	(0·89)	(0·15)	(0·99)	(0·71)
ΔH	89·12	94·14	102·09	89·96	96·23	106·69	103·34
(kJ/kg)	(2·26)	(4·06)	(3·31)	(3·51)	(1·13)	(7·45)	(7·24)
*pH 3**							
T_m (°C)	148·0	150·5	150·0	149·5	149·1	151·2	151·2
	(0·78)	(0·87)	(0·69)	(1·00)	(0·69)	(0·21)	(0·44)
ΔH	89·12	100·00	104·60	96·65	92·88	96·65	104·18
(kJ/kg)	(2·26)	(4·31)	(1·28)	(1·97)	(3·72)	(6·32)	(6·36)
*Sea water**							
T_m (°C)	148·0	151·9	150·7	150·3	150·4	151·6	152·6
	(0·78)	(0·78)	(0·35)	(0·47)	(0·37)	(0·47)	(0·72)
ΔH	89·12	97·91	97·06	97·49	94·56	103·76	105·86
(kJ/kg)	(2·26)	(2·34)	(4·02)	(4·35)	(4·02)	(5·40)	(0·29)

*Each reading is an average of 3 specimens with the standard deviations shown in parentheses.

4 ARRHENIUS MODEL: EXTRAPOLATION TO LONGER LIFE

Various predictive models, such as Arrhenius, Eyring and Inverse power models are currently used for extrapolating accelerated aging results to actual service conditions. The Arrhenius model, based on a time–temperature superposition principle is the most popular for polymer degradation and has the form

$$dr/dt = A \exp(-E_a/RT) \quad (2)$$

where dr/dt is the reduction of a material property with respect to time, E_a is the activation energy of the reaction, R is the universal gas constant, T is the absolute temperature and A is a material constant. The activation energy is the energy barrier which the reactants must surmount before going over into the reacted state and is characteristic of a reaction. Integration of the rate equation above, followed by taking logarithms, results in an equation of the form:

$$\ln t = (E_a/R)\,1/T + B \quad (3)$$

where t is the time to reach a specified end-point and B an experimentally

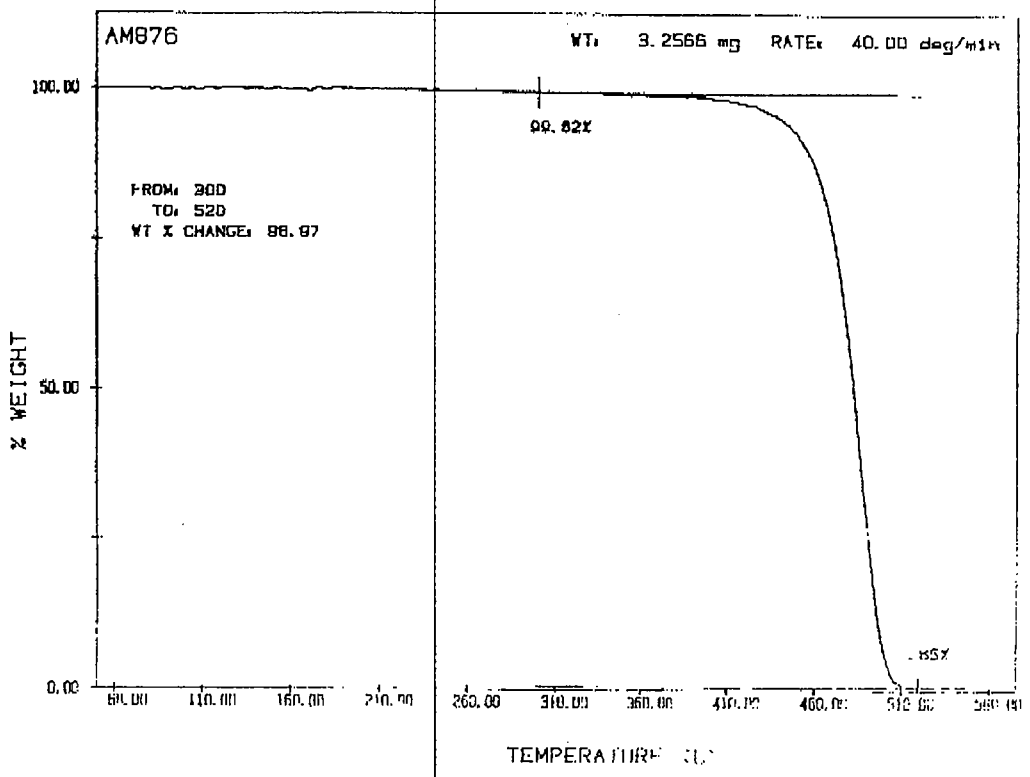

Fig. 25. Typical TGA curve for PP/GT.

Table 6
TGA Results for PP/GT

Temp		70°C			95°C		
Time	Untreated	6 wks	12 wks	24 wks	6 wks	12 wks	24 wks
T_d (°C)	462·8	461·0	458·7	463·2	464·2	463·6	464·2
Wt. Loss (%)	99·5	99·8	98·9	100	100	99·8	99·0
*pH3**							
T_d (°C)	462·8	461·8	458·2	462·1	464·3	462·5	463·1
Wt. Loss (%)	99·5	99·7	99·8	99·5	97·9	99·0	99·3
*Sea water**							
T_d (°C)	462·8	464·6	465·8	465·6	462·3	459·2	466·8
Wt. Loss (%)	99·5	99·2	99·6	99·4	99·7	98·6	96·3

*Each reading is an average of 3 specimens.

determined constant. A plot of $\ln t$ versus $1/T$ (Arrhenius plot) produces a straight line whose slope is E_a/R and has an intercept of B. This plot can then be used to extrapolate down to the service temperature of the material.

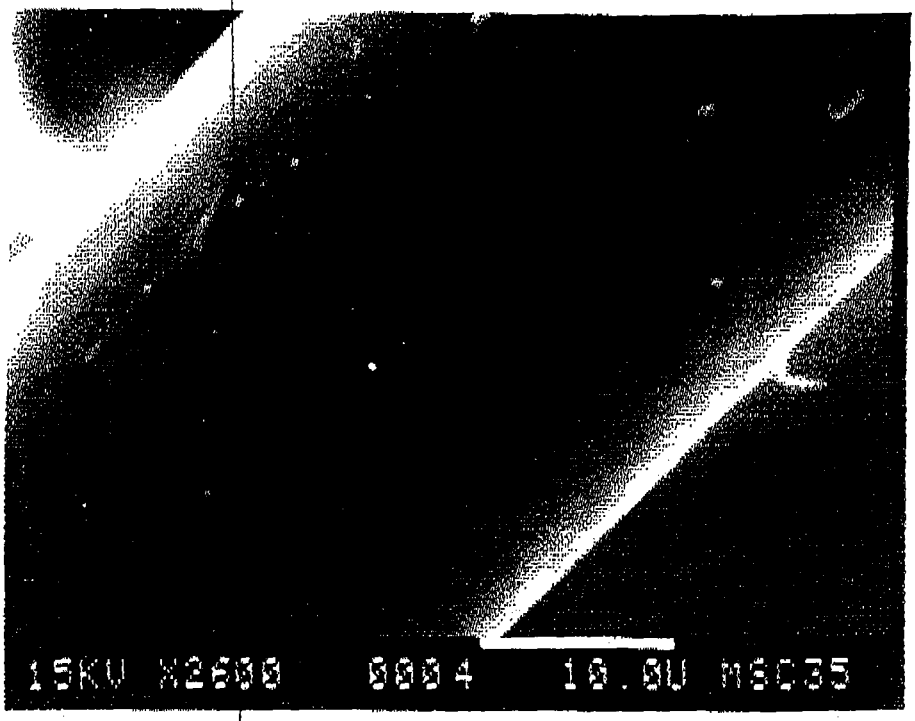

Fig. 26. SEM micrograph of untreated PP GT.

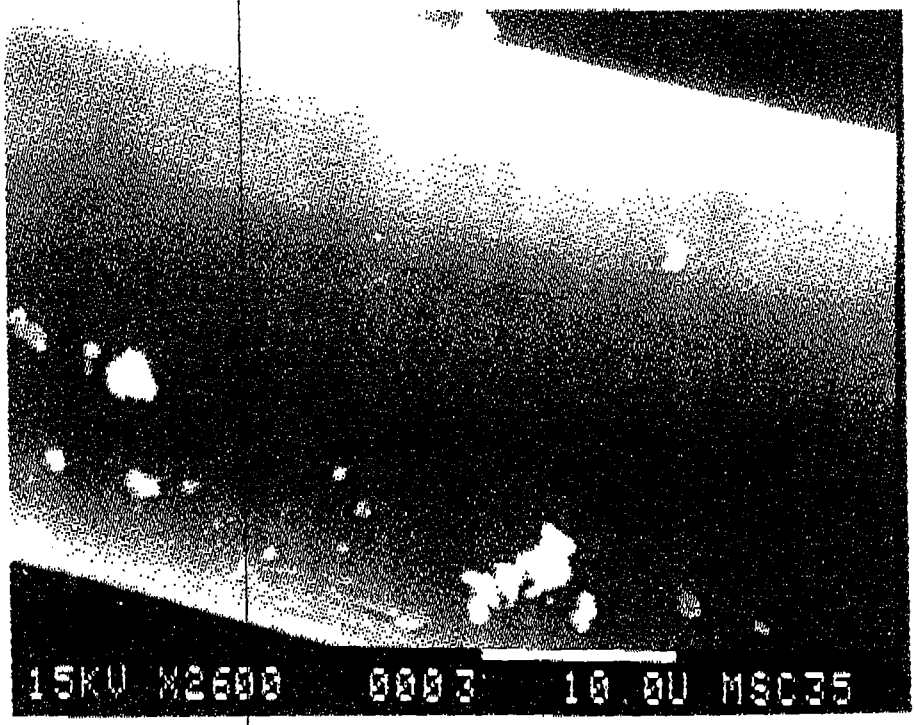

Fig. 27. SEM micrograph of PP GT treated at pH 3 for 24 wks at 95 C

It is argued that the reaction rate above the glass transition temperature may be different than below it and that a different mechanism operates at higher temperatures (Sotton & Leclercq, 1982). Results obtained by other researchers (McMahon *et al.*, 1959; Golike & Lasoski, 1960; Segrestin & Jailloux, 1988) however, do not indicate any erratic changes in the reaction rate.

McMahon *et al.* (1959) have reported activation energy values ranging between 100·4 and 121·3 kJ/mol for the hydrolysis of PET. Golike & Lasoski (1960) have reported a value of 94·6 kJ/mol, while Segrestin & Jailloux (1988) have used a value of 104·6 kJ/mol for life predictions of hydrolyzed polyester. In the degradation of polymers, it is not uncommon to observe a distribution of activation energies instead of a single activation energy. This reflects the multiplicity of 'reactions' that can lead to the final degraded products.

The selected endpoint is generally a property parameter of interest in the lifetime of the material. Koerner *et al.* (1992) have suggested the use of strength and elongation tests among 11 other candidate tests as a basis for Arrhenius modeling. The value selected as the endpoint differs from one application to another, and is generally taken to be lower than the original value. All calculations in the present study have been based on the selected endpoint of 90% of the original strength of the geotextile.

The changes in the peak strength of PET/GT with temperature and time for all the three pH values have been shown earlier in Figs 2, 3 and 4 in Section 3.1.1.1. As can be seen from these figures, the strength values at 21°C and 50°C are not significantly different from the untreated specimen values. The only significant changes (reduction) in strength are obtained at 70°C and 95°C. A similar trend was obtained for the peak strain results which are shown in Figs 5, 6 and 7.

The following assumptions are made for this model: (i) since the peak strength values obtained at 21°C and 50°C are not significantly different from the peak strength of the untreated specimen, they lie above the selected end point used for computation. Data obtained for these conditions are therefore not considered in the calculations; (ii) the reaction mechanism or the order of the reaction is the same at all the temperatures used, i.e. higher temperatures merely accelerate the rate of the degradation.

In addition, the data for all conditions have been fitted using best fit lines for ease in calculations. The activation energy (E_a) for the reaction is obtained either from the plot of $\ln(t)$ versus $1/T$ or by solving eqn (3) for the two temperature and time values. Table 7 shows the time to reach 90% of original strength at 70°C and 95°C for pH 10, 3 and sea water and the calculated activation energies.

Table 7
Activation Energy from Strength Results

pH	*Temperature (°C)*	*Time (weeks)*	*Calculated activation energy (kJ/mol)*
10	70	13·00	123·01
	95	0·67	
3	70	17·50	95·81
	95	0·75	
Sea water	70	12·88	63·76
	95	2·81	

The values for the energy of activation for pH 10 and pH 3 treatments were found to vary between 96·23 and 125·52 kJ/mol. These values are in good agreement with the values obtained by other researchers (McMahon *et al.*, 1959; Golike & Lasoski, 1960; Segrestin & Jailloux, 1988). In the case of sea water, the uneven trend in the strength data made calculations difficult, and could therefore have led to erroneous results.

Koerner *et al.* (1992) have suggested that elongation may be a more sensitive parameter to assess polymer degradation than strength. Activation energies were therefore also determined using the Arrhenius model on the breaking strain data for the same conditions as above, the results of which are presented in Table 8. For these calculations, the endpoint selected was also 90% of the original strain.

The activation energy values obtained from strain results agree with those determined using strength values for pH 10 and pH 3. Figure 28 shows the Arrhenius plot obtained from the strain data. Extrapolation to service temperatures can be performed by substituting the E_a values in eqn (3) or by extending the Arrhenius plot to that temperature. It should be noted, however, that extrapolation would be more appropriate for temperatures higher than the glass transition temperature of PET/GT. Below the glass transition temperature, the activation energy value is expected to be higher.

5 CONCLUSIONS

The changes in the physical and mechanical properties resulting from accelerated chemical aging of two geotextiles, namely PET/GT (polyester) and PP/GT (polypropylene) were studied. The PP/GT (polypropylene) geotextile was stable for all pH, saline, and temperature conditions

Table 8
Activation Energy from Strain Results

pH	*Temperature (°C)*	*Time (weeks)*	*Calculated activation energy (kJ/mol)*
10	70	19·60	130·54
	95	0·87	
3	70	21·15	108·57
	95	1·58	
Sea water	70	29·87	99·16
	95	2·79	

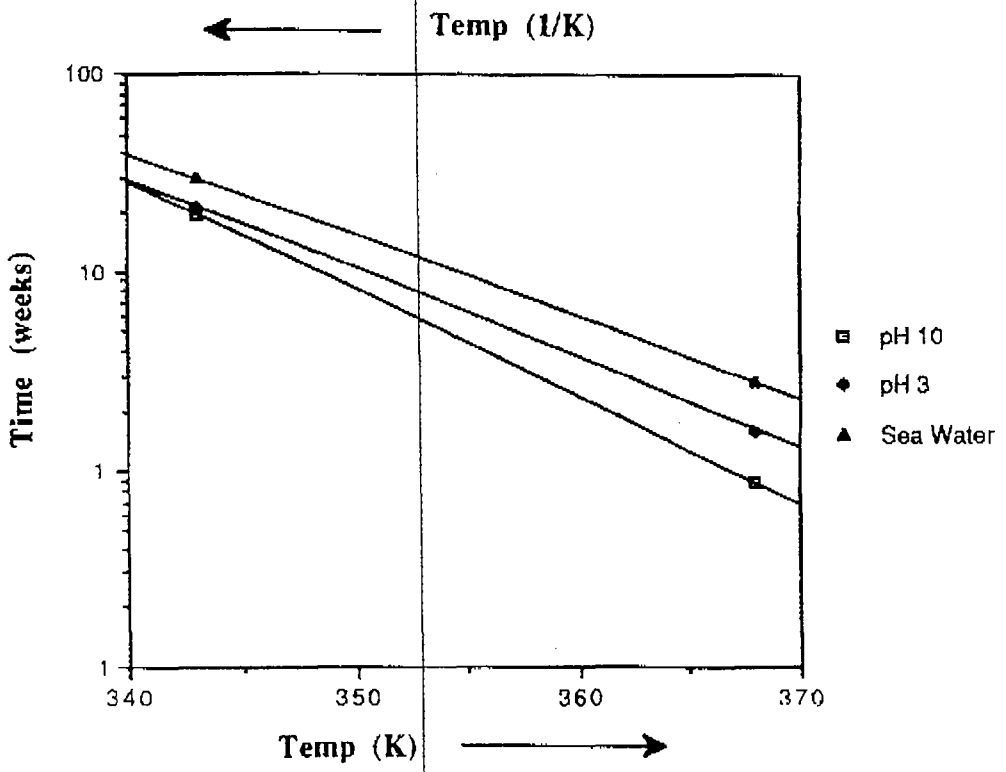

Fig. 28. Arrhenius plot for PET/GT using strain data.

studied, and showed no evidence of degradation. The polyester geotextile, on the other hand, underwent hydrolytic degradation at temperatures at and above the glass transition temperature. The extent of degradation was ascertained from the reduced tensile strengths for both the geotextile and fiber specimens, reduced elongation or increased brittleness, and the decrease in intrinsic viscosity. Importantly, for PET/GT, the decrease in breaking strength and strain was observed only at elevated temperatures

of 70°C and particularly at 95°C for relatively high and low pH. The Arrhenius model was fitted to the strength as well as the strain data to determine the activation energy of the degradation reactions, which can be used to extrapolate these results to actual service conditions. In practical terms, the energy of activation is low and implies that strength will be retained for substantial periods of time, even for rather severe pH environments.

Results from DSC analysis suggest an increase in the crystallinity for both polyester and polypropylene geotextiles during the initial period of aging. In the case of polyester, increased crystallinity was due to preferential attack on the amorphous regions and subsequent partial removal of the material. In polypropylene, this may have been the result of nucleation growth and lamellar thickening. The increased crystallinity implies that the geotextiles become stiffer with age. In a composite soil polymer structure, this stiffening may lead to a local concentration of stress in the geotextile, especially where continuing levels of deformation are imposed by the gradual accumulation of waste in a landfill or the underlying consolidation of soil along road courses and embankments. It is important to have a grasp of the variability inherent in materials and in the test methods before any predictions are made. It is hoped that the results of this study serve as a useful screening tool for geotextiles to be used in such applications.

ACKNOWLEDGEMENTS

The authors wish to thank Dr John Crouse from Firestone Fibers and Textiles Co. Inc. for conducting the intrinsic viscosity experiments. The authors also thank Teresa Emeott for assisting the authors in their tests. Acknowledgements are due to the National Science Foundation for providing the financial support for her work through NSF-REU grant No. DMR 9100873. The authors also acknowledge the financial support received from the New York State Water Research Institute, and Cornell University.

REFERENCES

Ballara, A. & Verdu, J. (1989). Physical aspects of the hydrolysis of polyethylene terephthalate. *Polymer Deg. and Stab.*, **26**, 361–374.

Cassidy, P. E., Mores, M., Kerwick, D. J., Koeck, D. F., Verschoor, K. L. & White, D. F. (1992). Chemical resistance of geosynthetic materials. Geotextiles and Geomembranes, **11**, 61–98.

Cassidy, P. E., Mores, M., Kerwick, D. J. & Koeck, D. C. (1990). Recent advances in the chemical compatibility evaluation of geosynthetic materials. In *Proc. of 4th Intl. Conf. on Geotextiles, Geomembranes and Related Products*, ed. Den Hoedt, Balkema, Rotterdam, ISBN 90 6191 1192, pp. 685–688.

Collins, M. J., Zeronian, S. H. & Semmelmeyer, M. (1988). Use of aqueous alkaline hydrolysis to reveal the fine structure of poly(ethylene terephthalate) fibers. *J. of Appl. Polym. Sci.*, **42**, 2149 2162.

Cooke, T. F. & Rebenfeld, L. (1988). Structure and properties of fibers in relation to durability of geotextiles. In *Durability and Aging of Geosynthetics*, ed. R. M. Koerner, Elsevier Applied Science, New York, NY, pp. 65–81.

Giroud, J. P. (1984). Geotextiles and geomembranes. *Geotextiles and Geomembranes*, **1**, 5 40.

Golike, R. C. & Lasoski, S. W. (1960). Kinetics of hydrolysis of polyethylene terephthalate films. *J. of Phys. Chem.*, **64**, 895 900.

Halse, Y., Koerner, R. M. & Lord, A. E. (1987). Effect of high levels of alkalinity on geotextiles. Part 1. $Ca(OH)_2$ Solutions. *Geotextiles and Geomembranes*, **5**, 261–282.

Halse, Y., Koerner, R. M. & Lord, A. E. (1987). Effect of high levels of alkalinity on geotextiles. Part 2. NaOH solution. *Geotextiles and Geomembranes*, **6**, 295–305.

Horz, R. C. (1986). Geotextiles for drainage, gas venting and erosion control at hazardous waste sites. EPA Report 600/2-86/085, Environmental Protection Agency, Cincinnati, Ohio, USA.

Hsuan, G. Y. (1991). Thermogravimetric analyses for geosynthetic materials. *Geotech. Fabric Report*, **9**(8) 18 22.

Industrial Fabrics Association International, Geotextiles Division (1990). A design primer: geotextiles and related materials. IFAI, St. Paul, MN.

Ingold, T. S. & Miller, K. S. (1988). *Geotextiles Handbook*. Thomas Telford Ltd., London, UK.

Jailloux, J. M. & Verdu, J. (1990). Kinetic models for the life prediction in PET hygrothermal aging: a critical survey. In *Proc. of 4th Intl. Conf. on Geotextiles, Geomembranes and Related Products*, ed. Den Hoedt, Balkema, Rotterdam, ISBN 90 6191 1192, p. 727.

Koerner, R. M. (1986). *Designing with Geosynthetics*. Prentice Hall Publ., Englewood Cliffs, NJ.

Koerner, R. M., Lord, A. E. & Hsuan, Y. H. (1992). Arrhenius modeling to predict geosynthetic degradation. *Geotextiles and Geomembranes*, **11**, 151–183.

Mandaikar, S. V. (1985). Mechanical behaviour of small diameter aramid braids. M.S Thesis, Cornell University, Ithaca, New York, pp. 36–39.

McMahon, W., Birdsall, H. A., Johnson, G. R. & Camilli, C. T. (1959). Degradation studies of polyethylene terephthalate. *J. of Chem. Eng. Data*, **4**(1) 57–63.

Montalvo, J. R. (1989). Evaluation of the degradation of geotextiles. In *Geosynthetics Conference Proceedings*, IFAI, St. Paul, MN, USA, pp. 501–512.

Netravali, A. N., Henstenburg, R. B., Phoenix, S. L. & Schwartz, P. (1989). Interfacial shear strength studies using the single filament composite test. *Polym. Comp*, **10**, 226–241.

Reich, L. & Stivala, S. S. (1971). *Elements of Polymer Degradation*, McGraw-Hill, USA, pp. 55–75.

Risseeuw, P. & Schmidt, H. M. (1990). Hydrolysis of HT polyester yarns in water at moderate temperatures. In *Proc. of 4th Intl. Conf. on Geotextiles, Geomembranes and Related Products*, ed. Den Hoedt, Balkema, Rotterdam, ISBN 90 6191 1192, pp. 691–696.

Schneider, H. & Groh, M. (1987). An analysis of the durability problems of geotextiles. In *Proc. of Geosynthetic '87 Conference*, Volume 2, IFAI, St. Paul, MN, USA, 433–441.

Segrestin, P. & Jailloux, J. M. (1988). Temperature in soils and its effect on ageing of synthetic materials. *Geotextiles and Geomembranes*, **1**, 51–69.

Solbrig, C. M. & Obendorf, S. K. (1986). Cell Abstract No. 10, 192nd National Meeting, American Society, Anaheim, CA.

Sotton, M. & Leclercq, B. (1982). Geotextiles and aging tests. In *Proc. of 2nd Intl. Conf. on Geotextiles*, IFAI, St. Paul, MN, USA, pp. 559–564.

Sprague, C. J. (1990). Leachate compatibility of polyester needlepunched nonwoven geotextiles. In *Geosynthetic Testing for Waste Containment Applications*, ASTM STP 1081, ed. R. M. Koerner, American Society for Testing and Materials, Philadelphia, PA, pp. 212–224.

Van Zanten, R. V. (1986). Geomembranes. Chap. 12. In *Geotextiles and Geomembranes in Civil Engineering*, ed. R. V. Van Zanten, Wiley, NY, USA.

Ziabicki, A. (1976). *Fundamentals of Fibre Formation*, Wiley Interscience, UK, pp. 110–115.

Experience with Capping of Contaminated Sediments using Armouring and Geotextile Filters

Insitu caps for contaminated sediments normally comprise clean sand, however other materials such as armour stone or geotextiles may be considered *(Palermo 1997).* If an evaluation of cap erosion indicates that the capping material will not be sufficiently resistant to erosion, an armour layer *(eg riprap)* can be incorporated into the cap design *(Palermo et al 1998).*

Filters provide an interface between the armour layer and the contaminated material. Filters prevent turbulence and groundwater from moving the material up through the cap. Filters also serve as foundations or load distributors for armour when placed over poorly consolidated material which is typical of many contaminated sediments. Filters can be either geotextile, granular, or a combination of the two. Care must be taken in the design of filter permeability and resistance to damage during construction *(Palermo et al, 1998).*

A typical armour layer cap concept including a geotextile filter is shown in Figure 1.

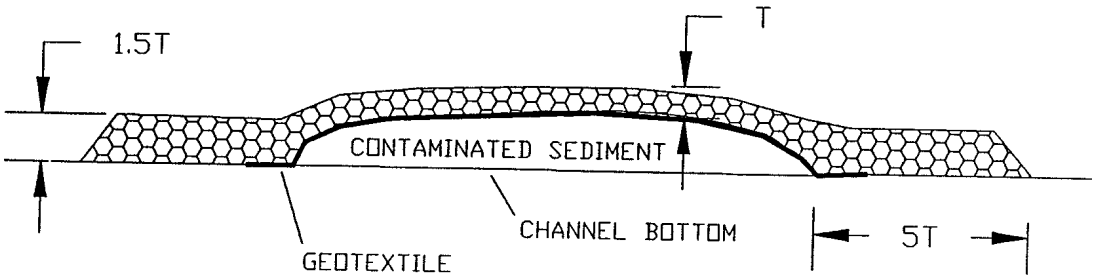

Figure 1 Source, Palermo et al (1998), Appendix A.

Examples of Insitu Capping with Armour Layers and Geotextiles

An insitu cap with armouring layer has been demonstrated at a Super-fund site in Sheboygan Falls, Wisconsin. This project involved placement of a composite cap, with layers of gravel and geotextile to cover several small areas of PCB-contaminated sediments in a shallow *(1.5 m)* river and floodway. A total area of about 4,000 m^2 of cap was placed with land-based construction equipment and manual labour *(Eleder, 1992).* At Eitrheirn Bay in Norway, a composite cap of geotextile and gabions was

constructed as a remediation project in a fjord at an area contaminated with heavy metals. A total area of 100,000 m^2 was capped, in water depths of up to 10 meters *(Instanes, 1994)*.

References

Eleder, B. (1992)
Sheboygan River Capping/Armoring Demonstration Project
Workshop on Capping Contaminated Sediments, Chicago, Illinois

Instanes D (1994)
Pollution Control of a Norwegian Fjord by use of Geotextiles
Fifth International Conference on Geotextiles, Geomembranes, and Related Products, Singapore

Palermo M, Maynord S, Miller J, Reible D (1998)
Guidance for In-Situ Subaqueous Capping of Contaminated Sediments
EPA 905-B96-004, Great Lakes National Program Office, Chicago, Illinois.

Palermo MR (1997)
In-Situ Capping of Contaminated Sediment Overview and Case Studies
EPA National Conference on Management and Treatment of Contaminated Sediments
Cincinnati, OH, May 13-14, 1997

GPB
13/10/09

GEOTEXTILES FOR FILTERING WATER AND OIL FLUIDS

J. Don Scott, Professor Emeritus
Geotechnical Centre, Department of Civil & Environmental Engineering
University of Alberta, Edmonton, Alberta, Canada, T6G 2W2

ABSTRACT

Geotextile filters protecting drainage systems at oil sand mining operations must filter mixtures of heavy oil and water during construction of the oil sand plants and during operation of the mine. The filtration properties of seven non-woven geotextiles to water and oil were determined over a range of hydraulic gradients and confining pressures.

The geotextile filter design criteria considered the grain size distribution, coefficient of uniformity, density and permeability of the sand surrounding the drainage systems and the apparent opening size, porosity and permeability of the geotextile filters. Permeability criteria, retention criteria and clogging criteria were examined for the non-woven fabrics. Geotextile filters for water and oil permeants should be made of fibers that are both hydrophobic (repelling water) and oleophobic (repelling oil) to provide a higher permeability for a given porosity.

The environment in a mixture of heavy oil and water is aggressive. To meet the chemical environmental durability criterion, the fibers must be chemically compatible with the heavy oil fluid so that there is no significant change in pore size or reduction of permeability due to fiber swelling and degregation.

All seven selected non-woven geotextiles satisfied permeability and piping criteria and serious clogging or blinding was not observed. Three of the geotextiles were chosen for detailed testing as they best satisfied the retention criteria over a range of sand densities. All three fabrics complied with the permeability requirement with the polyester fabrics being slightly more permeable to oil and the polypropylene fabric being significantly more permeable to water.

INTRODUCTION

Oil sand mines and plant sites in northern Alberta (Figure 1) require extensive drainage systems during construction and operation. The importance of this growing industry to the oil supply of Canada and the United States is now recognized. The volume of oil in the oil sands is the largest reserve in the world equaling that of Saudi Arabia. The initial in place reserves are 1,629 billion barrels (Table 1) and production has now exceeded 1,000,000 barrels a day (EUB, 2004). Construction of new mines and plants results in expenditures of several billion dollars per year. Although subsurface drainage systems are not a big expenditure, their long-term effectiveness is important to the efficient operation of the mines. This paper summarizes a laboratory research program which evaluated geotextile filters for subsurface drainage systems where a mixture of water and oil flows to the drains.

Table 1: Reserves summary 2003 (EUB, 2004)

	Crude Bitumen		Crude Oil	
	(millions m^3)	(billion barrels)	(millions m^3)	(billion barrels)
Initial in place	258,900	1,629	9,852	62
Initial established	28,392	179	2,634	16.6
Cumulative production	667	4.2	2,380	15
Remaining established	27,726	174	254	1.6
Annual production	56	0.352	37	0.23
Ultimate potential (recoverable)	50,000	315	3,130	19.7

TEST SAND AND FLUIDS

The granular material available for drain construction at the mine sites is the tailings sand from the McMurray Formation oil sands. It is a clean, fine, uniform sand (Figure 2) with a C_u = 1.8, a C_u' = 1.4 (Giroud, 1988) and a C_c = 1.0. The d_{85} and d_{50}' of the sand are 0.25 mm and 0.18 mm respectively. The heavy oil used in the testing program was a low sulphur content crude oil, (also known as sweet crude oil), from a heavy oil well. The sweet crude oil was a dark, brown-black colour with a strong tar odor. The characteristics of the heavy oil are summarized in Table 2. The density of the heavy oil varies from 956 to 958 kg/m^3 at 15.6°C. To determine the effect of laboratory temperature on the viscosity of the heavy oil during permeability tests, a Fann direct indicating viscometer was used to measure the viscosities of the heavy oil. The viscosity of the heavy oil varied from 7700 to 11700 mPa.s when the temperature varied from 22.8 to 20.8°C. The results of the viscosity measurements are presented in Figure 3. The density of the heavy oil was also measured in the laboratory by the density bottle method. Because the temperature variation in the laboratory was less that 4°C, it was assumed that the density for the heavy oil of 975 kg/m^3, measured at a laboratory temperature of about 22°C, remained constant within the temperature range of 24.0 to 20.8°C. The most significant property of the oil is the sensitivity of the viscosity to temperature as shown in Figure 3. A decrease of 4°C doubles the viscosity or cuts the flow in half. For this reason, during the tests involving oil, the temperature of the oil was carefully monitored.

Table 2: Characteristics of the Heavy Oil

Density	975 kg/m³ at 22ºC
ºAPI	14
Carbon Content	75.3%
Hydrogen Content	10.6%
Nitrogen Content	6.4%
Oxygen Content	10.2%
Sulphur Content	2.7%

The interstitial water that occurs with the oil was also used in the durability tests. The water has a high content of dissolved salts, usually higher than the salt content of seawater. An

analysis indicated that the cations present in the water were sodium (12,066.9 mg/L), calcium (609.2 mg/L), magnesium (274.8 mg/L) and dissolved iron (3.3 mg/L) with 0.3 mg/L undissolved iron. The anions present were chloride (20,208.3 mg/L) and bicarbonate (473.5 mg/L). The pH was 7.31 at 20.4°C. As substantial amounts of water were required for the testing program, constant temperature deaired distilled water was used throughout the program to assure reproducibility of results.

INITIAL SELECTION OF GEOTEXTILE

Filtration properties of the geotextile fabrics were preliminary evaluated by the filter design criteria by Giroud (1988). These filter design criteria are permeability, retention and porosity. The permeability criterion ensures that fluids are allowed to pass through the filter without the buildup of excess pore pressure. The permeability of the sand and the hydraulic gradient of the fluids in the sand adjacent to the filter are significant factors in the permeability required for geotextile filters. Giroud (1988) defines the permeability criterion for noncritical applications as:

$$k_g > i_s k_s \tag{1}$$

where: k_g = the hydraulic conductivity of the geotextile; i_s = the hydraulic gradient in the sand; and k_s= the hydraulic conductivity of the sand.

The more general conservative case equation is:

$$k_g > 10\ i_s k_s \tag{2}$$

As the sand, although fine, contains little fines, the noncritical criterion was used.

The hydraulic conductivity of the geotextiles was measured under compressive stresses expected in the field. For deeply buried drains this was taken to be 500 kPa but tests were conducted to confining stresses of 1300 kPa to evaluate the characteristics of the geotextiles. The hydraulic gradient was varied up to a maximum of 2. As the hydraulic conductivity of the McMurray sand is 0.008 cm/s, the hydraulic conductivity of the geotextiles at a hydraulic gradient of 2 should be a minimum of 0.016 cm/s. This criterion is discussed in more detail by Christopher and Fisher (1992).

The retention criterion prevents significant migration of particles from the sand into the drainage medium. Sand retention with geotextile filters is dependent on the size of the pores in the filter in relation to the grain sizes of the sand. The retention criterion is stated as:

$$O_{95} < \lambda_R\ d_{85} \tag{3}$$

where: O_{95} = the geotextile apparent opening size such that 95% of the openings in the geotextile are smaller than $O_{95;}$ λ_R = a dimensionless coefficient; and d_{85} = the sand particle size such that 85% of the soil by weight is smaller. For the McMurray Formation sand, where the

coefficient of uniformity, Cu, is between 1 and 3, λ_R is calculated as $Cu^{0.3}$ for loose sands and 2 $Cu^{0.3}$ for dense sands (Giroud, 1988). According to these criteria, the O_{95} for a geotextile filter used with the McMurray Formation sand should be less than 0.42 mm for medium dense sand and 0.28 mm for loose sand.

Similarily, Carroll (1983) suggests that:

$$O_{95} < (2 \text{ to } 3)\ d_{85} \tag{4}$$

which requires the O_{95} to be < 0.50 mm to 0.75 mm.

A more comprehensive method to determine soil retention criteria was developed by Luettich, Giroud and Bachus (1992) and discussed by Koerner (1998). As the McMurray sand has less than 10% fines, a d_{10} = 0.093 mm, a Cc = 1.0 and a d'_{50} = 0.18 mm; the O_{95} for medium density sand should be less than 0.38 mm and for loose sand should be less than 0.25 mm. This more stringent criteria was used for the final selection of three geotextiles to be used in a more comprehensive testing program.

The porosity criterion ensures that the filter will function without having a significant number of its openings clogged by sand particles. The porosity criterion is defined as:

$$n \geq 30\% \tag{5}$$

where: n = a minimum porosity for geotextile filters under compressive stresses similar to those encountered in the field.

A durability criterion was also included because the fluid flowing through filters is multiphase consisting of oil and water. To meet the durability criterion, the filter must be chemically compatible with the fluids flowing through the geotextile so that there is no significant change in pore size or reduction of permeability due to interaction between the filter polymers and the fluids.

A number of manufacturers in Canada, USA and Europe were contacted for product information. Only eight manufacturers produced geotextiles which fulfilled the permeability and retention criteria for filters in this application. The properties of these geotextiles were ranked according to the information supplied by each manufacturer (Table 3). Six non-woven, needle-punched (NP) and one needle-punched with net (NPN) geotextile products were finally selected and ordered for testing in durability and filtration-permeability laboratory experiments.

Table 3: Properties of the Seven Selected Geotextile Fabrics
(data provided by the manufacturer)

Geotextile Fabric	**A**	**B**	**C**	**D**	**E**	**F**	**G**
k_n(cm/s)	0.52	0.58	0.49	1.19	0.2	0.50	0.59
Permittivity (s-1)	1.36	2.40	1.86	2.04	0.93	1.87	3.10
Porosity (%)	93	93	78	92	86	88	90
Mass (g/m²)	356	220	800	678	271.2	281.4	175
Thickness (mm)	3.81	2.40	2.66	5.84	2.16	2.67	1.9
O_{95} (mm)	0.212 – 0.125	0.20	0.120	0.125 – 0.09	0.212 – 0.15	0.09	-
Fabric construction	NP	NP	NPN	NP	NP	NP	NP
Fabric type	PET	PET	PET	PET	PP	PP	PP/PET

PET – Polyester; PP – polypropylene; PP/PET – polypropylene/polyester

The testing program is summarized in Table 4.

Table 4: Testing Program on the Selected Geotextile Fabrics

Geotextile Fabric	**A**	**B**	**C**	**D**	**E**	**F**	**G**
Fabric Type	**PET**	**PET**	**PET**	**PET**	**PP**	**PP**	**PP/PET**
Type of Test							
Apparent Opening Size (Fabric only)	X	X	X	X	X	X	X
Compressibility Test (geotextile only)							
- single layer	X				X	X	
- - multi layers	X				X	X	
Gradient Ratio Test (sand/geotextile)	X	X	X	X	X	X	X
Permittivity Test (geotextile only)							
- water			X	X	X		
- heavy oil			X	X	X		

When the seven non-woven geotextile fabrics were received, the actual apparent opening size, AOS, of the fabrics were determined according to the ASTM Standard Test Method D4833 (Table 5).

Table 5: Apparent Opening Sizes of the Seven Selected Geotextiles

Geotextile	Fiber Type	Manufacturer's AOS (mm)	Measured AOS (mm)	Standard Sieve Size
A	PET	0.210	0.412	40
B	PET	0.200	0.300	50
C	PET	0.120	0.110	140
D	PET	0.150	0.150	100
E	PP	0.212 – 0.150	0.110	140
F	PP	0.125 – 0.180	0.300	50
G	PP/PET	0.750 – 1.25	0.300	50

PERMEABILITY AND FILTRATION TESTING

Definition Of Permeability

In order to compare the flow of heavy oil with water, when large variations in viscosity and density exist, the absolute permeability of the geotextile and the different permeants must be considered. For this reason, absolute permeability was used rather than hydraulic conductivity to define the permeability of the geotextile and the permeability of the sand.

The absolute permeability (K) is usually measured in the laboratory using water or oil as the fluid and is calculated using Darcy's equation:

$$K = 10^{12} \cdot \frac{q}{tA} \cdot \frac{L}{\Delta h} \cdot \frac{\mu}{\rho g} \qquad \text{in } \mu m^2 \tag{6}$$

where: q = quantity of flow in m^3; t = time of flow in seconds; A = area normal to flow direction in m^2, L = length of specimen in flow direction in m; Δh = change in head over length L in m; μ = viscosity of fluid in Pa.s; ρ = density of fluid in kg/m^3; g = acceleration due to gravity in m/s^2.

Most geotextile fibers are hydrophobic and oleophilic, therefore the absolute permeability may vary depending on whether water or oil is being used as the permeant. The absolute permeability, (K) can be converted to the hydraulic conductivity (k) using the following conversion factor. A similar calculation can be done using oil properties.

For water at 20° C: $\mu_w = 1$ mPa.s; $\rho_w = 1000$ kg/m^3; and $g \sim 10$ m/s^2

Therefore: $k \text{ in cm/s} = K \times 10^{-3} \text{ in } \mu m^2$ (7)

The minimum hydraulic conductivity of the geotextiles of 0.016 cm/s calculated above (Equation 1) is therefore an absolute permeability of 16 μm^2. This value takes into account the viscosity and density of the fluid flowing through the geotextile.

The problem with using a hydraulic conductivity for fabrics is the dependency of the quantity of flow on the fabric thickness. Therefore, it is possible for a thin geotextile to have similar hydraulic conductivities but have significantly different flow rates. The thickness (t_g) of geotextiles, therefore, is usually taken into account when expressing permeability normal to the fabric by considering the permittivity, Ψ.

Permittivity, $\Psi = k/t_g$ in s^{-1} (8)

In this work, however, flow properties are expressed in terms of absolute permeability in order to compare the flow of water and the flow of oil through the geotextiles. The thickness of the geotextile was similar for both fluids so was not a factor for this comparison.

Gradient Ratio Testing

The purpose of this test was to select suitable geotextile fabrics for further experimental studies, to understand the interaction of the sand-geotextile system under different hydraulic gradient conditions and to determine the permeability of the geotextile fabrics and the clogging and blinding potential of the sand-geotextile system.

A gradient ratio apparatus which is similar to the apparatus specified in the ASTM Standard Test Method D5101 was designed and built (Figure 4). The apparatus is 101 mm in diameter and can accommodate a sand specimen of up to 127 mm in height. It has the capability to vary hydraulic gradients and, by this, flow velocities. The system layout for the test is shown in Figure 5. Deaired, distilled water at a constant temperature was used as the permeant.

The test results showed that the permeability of the sand-geotextile systems for all seven fabrics were greater than the permeability of the sand itself. These measurements indicate that some erosion of fine particles from the sand must have occurred. Therefore all outflow water from the apparatus was directed through a filter to collect any passing particles and the filter was weighed to determine the amount of material passing the geotextile. No material was collected for any of the geotextiles. The eroded fines must have been caught by the geotextiles but this did not significantly reduce the permeabilities of the geotextiles.

Typical results are shown in Figures 6 and 7 for Geotextiles D and G respectively. Geotextile D performance was similar to that of Geotextiles C and E and indicates that the gradient ratio test had stabilized by 24 hours. Geotextile G performance indicated that, especially at high hydraulics gradients, the test had not stabilized in 24 hours and the sand continued to lose fines. Geotextiles A, B and F performed similarly to Geotextile G. The sand in the tests was compacted to a medium density but Geotextiles A, B, F and G were on the borderline for the retention criteria. These four geotextiles were therefore removed from the program and further testing was confined to Geotextiles C, D and E. Both Geotextiles C and D are made of polyester fibers and Geotextile E is made of polypropylene fibers.

CLOGGING OF GEOTEXTILES

As mentioned above some erosion of particles from the sand occurred in all seven gradient ratio tests. These particles became lodged in the geotextiles but did not significantly reduce the permeability of the geotextiles. Mechanical clogging of the geotextiles, therefore, was not considered a problem.

COMPRESSIBILITY OF GEOTEXTILES

In order to ensure that the porosity criterion was satisfied under the in situ stress conditions, the three selected fabrics were compressed by an increase of the vertical stress acting on the geotextiles fabrics. The fabrics were compressed in steps from 2 kPa to 1300 kPa. The compression of the fabrics was measured at the corresponding stress level. The results showed that even under a compressive stress of 500 kPa, all three geotextiles retained a porosity greater than 60%.

PERMEABILITY TESTING WITH WATER AND OIL

A large scale permeability system (Figures 8 and 9) was designed and constructed in order to address the filtration requirements for flowing water and heavy oil. The permeameter cell is 130 mm in diameter and can accommodate a soil specimen of up to 200 mm in height. It has the capability to produce high confining stresses on the sand and geotextile, to vary hydraulic gradients and flow velocities and to accommodate permeants of various types and viscosities. A large number of manometer ports allow changes in hydraulic conductivity of the geotextile and the sand adjacent to the geotextile to be monitored. The equipment can produce a maximum differential fluid head of 400 kPa across the sand-filter system, can accommodate oil or water as the flowing liquids and can achieve a confining stress of up to 1.3 MPa on the sand and geotextile.

The permeability in terms of absolute permeability of the geotextiles was measured in the confining pressure apparatus without a sand sample. Geotextile specimens composed of multiple layers, approximately 10 mm total initial thickness, were tested with water and oil as the permeants. Specimens were soaked in the permeant for 2 days prior to testing to ensure saturation. Absolute permeability was measured under six confining stresses: 1.3, 100, 500, 1300, 100 and 1.3 kPa. A range of hydraulic gradients were used, dependent upon the permeant, but laminar flow conditions were achieved in both the tests with water and oil. Results of the permeability testing are presented in Figures 10 to 16. These figures show the changes in absolute permeability with hydraulic gradient for the six confining stresses used.

Figures 10 and 11 show the normal absolute permeability for Geotextile C when water and oil are the permeants. For both permeants, there is a decrease in permeability with an increase in confining stress as the geotextiles compress. The absolute permeability of water through the geotextile ranges between 170 μm^2 at 1.3 kPa to 20 μm^2 at 1300 kPa and the

absolute permeability of oil through the geotextile ranges from 220 μm^2 at 1.3 kPa to 40 μm^2 at 1300 kPa.. Geotextile C appears to be slightly more permeable to oil than to water.

Similar results were observed with Geotextile D in Figures 12 and 13. This geotextile, which is also polyester, also appeared to be slightly more permeable to oil than to water. The absolute permeability of water through the geotextile ranged from 210 μm^2 at 1.3 kPa to 16 μm^2 at 1300 kPa and the absolute permeability of oil through the geotextile ranged from 270 μm^2 at 1.3 kPa to 22 μm^2 at 1300 kPa.

Figures 14, 15 and 16 show results of the absolute permeability testing for Geotextile E. The absolute permeability of water ranges between 300 μm^2 at 1.3 kPa to 25 μm^2 at 1300 kPa and the absolute permeability of oil ranges between 200 μm^2 at 1.3 kPa to 6 μm^2 at 1300 kPa. This geotextile, which is polypropylene, is considerably more permeable to water than to oil. In the durability tests, Geotextile E swelled after immersion in heavy oil. Specimens of Geotextile E were soaked for 2 days and for 26 days prior to permeability testing to determine if a longer soaking time caused the permeability of the geotextile to oil to decrease even further. The results of these tests, Figures 15 and 16 respectively, are not significantly different. The possible explanation of this effect is that a layer of oil is rapidly attracted to the surface of the highly oleophilic fibers, thus slowing down the flow.

In summary, all three fabrics were highly permeable to both water and oil, but there was a slight difference in absolute permeability between water and oil depending on the fiber type. The polyester fabrics were slightly more permeable to oil and the polypropylene fabric was significantly more permeable to water. The permeability criterion requires a minimum absolute permeability of 16 μm^2 for the geotextile. The two polyester geotextile fabrics comply with this permeability requirement but the polypropylene fabric only had an absolute permeability to oil of approximately 12 μm^2 under a compressive stress of 500 kPa.

CHEMICAL DURABILITY TESTING

The purpose of the chemical immersion testing was to determine the durability of geotextiles to chemical conditions typical of heavy oil. Physical properties were measured on geotextile specimens before and after immersion in typical fluids occurring with heavy oil. The test fluids used in the immersion testing were heavy oil, interstitial water and, as a control fluid, distilled water. The interstitial water was simulated based on a typical water analysis. The specimens were immersed in these fluids for five time periods ranging from zero to 120 days. The effects of chemical-environmental exposure were assessed by measuring change in fiber diameter.

Obvious effects of degradation such as swelling of the fibers, can be determined by measuring the fiber diameter directly or by measuring changes in the length and width of the specimens as well as fabric thickness and mass. Significant swelling of the geotextile fibers will result in a change of the physical properties of the geotextile fabrics, such as strength.

A microscope equipped with a micrometer was used to measure fiber diameters, d_f. Fifty fiber diameters were measured after zero, 15 and 120 days immersion as an indicator test to determine if degradation was occurring at the microscopic level. There was no significant change in the diameter of fibers, Δd_f, from geotextiles C and D after immersion in heavy oil or produced water for 120 days (Table 6). The grey polyester fibers in Geotextile C are the non-woven geotextile while the white polypropylene fibers are a strengthening scrim on the geotextile. Fibers from geotextile E increased in diameter by almost 20% after immersion in oil for 120 days. While the two geotextiles composed of polyester fibers (geotextiles C and D) resisted degradation when exposed to the testing fluids, the results of the fiber diameter testing suggest that the polypropylene fibers (geotextile E) may be susceptible to swelling in heavy oil. Any significant changes in fiber diameter would have an effect on the apparent opening size of the pores in the geotextile filter. This would in turn affect the filtration and permeability properties of the filter material.

No signs of bioclogging of the geotextiles was observed under the microscope after 120 days of immersion. Given the environmental conditions with oil and highly saline water this is an area that requires investigation over longer periods of time.

Table 6: Change in Fiber Diameter after 120 days of Immersion in Produced Fluids

Geotextile	**C grey fibers**	**C white fibers**	**D**	**E**
Polymer type	polyester	polypropylene	polyester	polypropylene
Original d_f (μm)	24.0	21.7	29.7	25.0
Distilled water Δd_f (μm)	-0.7	+1.0	+0.4	+0.7
Produced water Δd_f (μm)	-0.3	-1.5	-1.2	+0.7
Heavy oil Δd_f (μm)	-0.3	-0.3	+1.7	+4.4

SUMMARY AND CONCLUSIONS

An initial study on the filtration properties of seven non-woven, needle punched geotextiles for filtering mixtures of heavy oil and water is reported. The granular material to be filtered was a clean fine, uniform sand.

Gradient ratio tests showed that for four of the geotextiles, A, B, F and G, the sand continued to erode into the fabric during the 24 hours of testing especially at high hydraulic gradients. These geotextiles were on the borderline for the retention criteria with AOS values of 0.300 mm and greater. They were, therefore, rejected and removed from the program.

The three other geotextiles, C, D and E, had gradient ratio test results that stabilized within a few hours. Their AOS values were 0.150 mm and less. Geotextiles C and D are made of polyester fibers and Geotextile E is made of polypropylene fibers.

Permeability testing with water and heavy oil showed that Geotextiles C and D were slightly more permeable to oil than to water. Geotextile E was considerably more permeable to water than to oil.

Chemical durability testing showed that there was no significant change in the diameters of fibers from Geotextiles C and D after immersion in heavy oil or groundwater for 120 days. However the fibers in Geotextile E increased in diameter by almost 20% after immersion in heavy oil for 120 days. This suggests that the polypropylene fibers of Geotextile E are susceptible to swelling in heavy oil. Any significant changes in fiber diameter would have an effect on the apparent opening size of the pores in the geotextile filter. This would in turn affect the filtration and permeability properties of the filter material.

Further evaluation of geotextiles for the filtration conditions for the sand and permeants used in this study should be confined to polyester fabrics with AOS values of 0.150 mm or less.

ACKNOWLEDGEMENTS

The work and interest of former graduate students, C. Penner and E. Wong, are greatly appreciated. Technical cooperation and advice from colleagues, Dr. N. Kerr and Dr.E.A. Richards, were invaluable. Financial assistance and information was received from the Alberta Government and several oil companies.

REFERENCES

Carroll, R.G. Jr. (1983) "Geotextile Filter Criteria", Engineering Fabrics in Transportation Construction, TRR 916, TBR, Washington, DC., pp. 46-53.

Christopher, B.R. and Fisher, G.R. (1992), "Geotextile Filtration Principles, Practices and Problems", J. Geotextiles and Geomembranes, v. 11, n. 4-6, pp. 337-354.

EUB (Alberta Energy and Utilities Board), (2004), Statistical Series (ST) 2004-98, "Alberta's Reserves 2003 and Supply/Demand Outlook 2004-2013", www.eub.gov.ab.ca.

Giroud, J.P. (1988), "Review of Geotextile Filter Criteria", Proceedings of the First Indian Conference on Reinforced Sand and Geotextiles, pp. 1-6.

Koerner, R.M. (1998), "Designing with Geosynthetics", 4th Ed., Prentice Hall, 761 p.

Luettich, S.M., Giroud, J.P. and Bachus, R.C. (1992), "Geotextile Filter Design Guide", J. Geotextiles and Geomembranes, v. 11, n. 4-6, pp. 19-34.

Figure 1. Alberta's three oil sands areas (Modified from EUB, 2004)

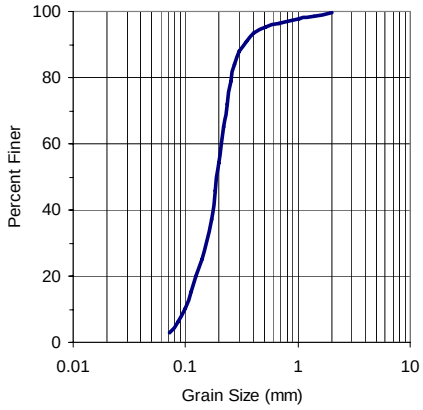

Figure 2. Grain Size Distribution of McMurray Formation Sand

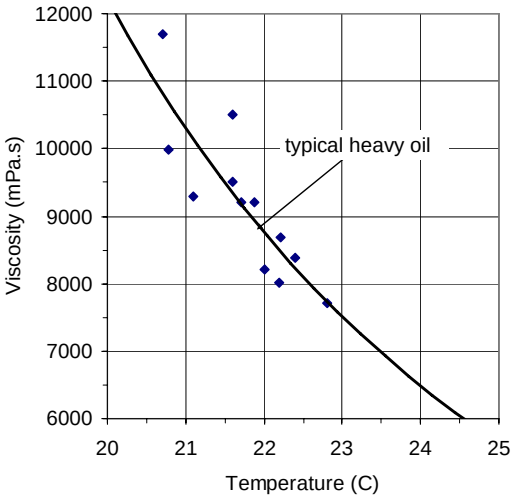

Figure 3. Effect of Temperature on Viscosity of the Heavy Oil

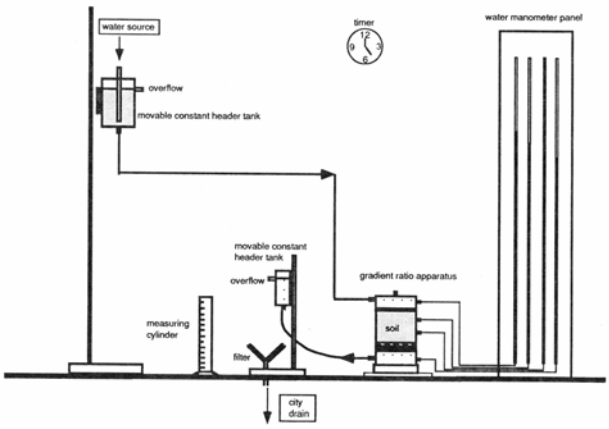

Figure 5. System Layout for Gradient Ratio Test

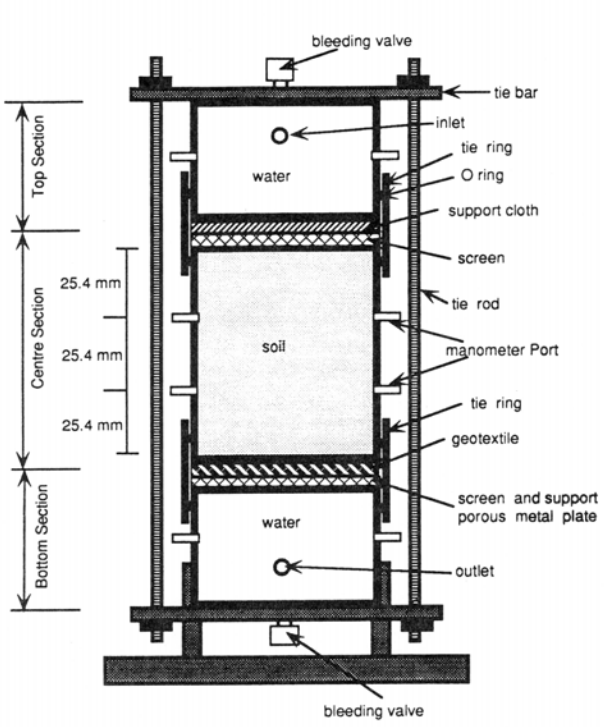

Figure 4. Sectional View of the Gradient Ratio Apparatus

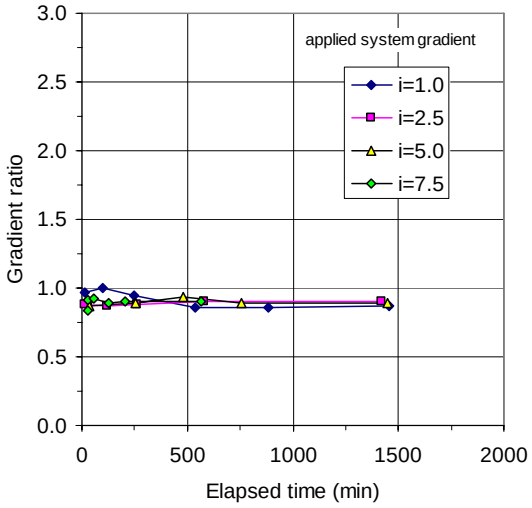

Figure 6. Gradient Ratio for Geotextile D in Gradient Ratio Test

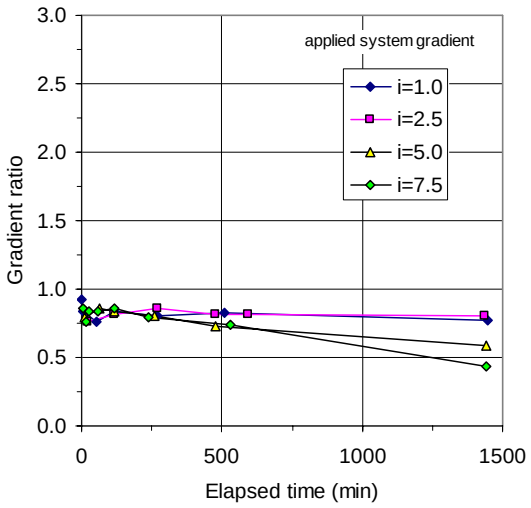

Figure 7. Gradient Ratio for Geotextile G in Gradient Ratio Test

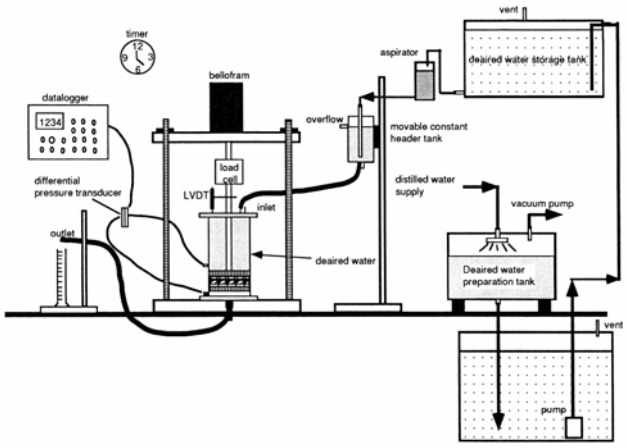

Figure 8. System Layout for Permeability Testing with Water as Permeant

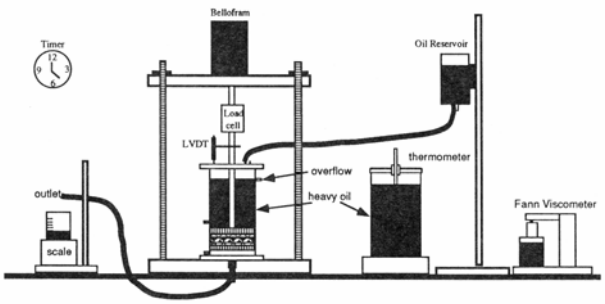

Figure 9. System Layout for Permeability Testing with Heavy Oil as Permeant

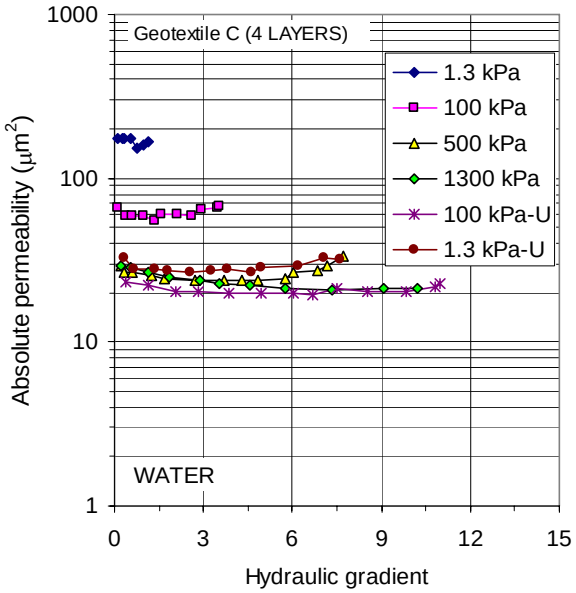

Figure 10. Permeability of Geotextile C to Water

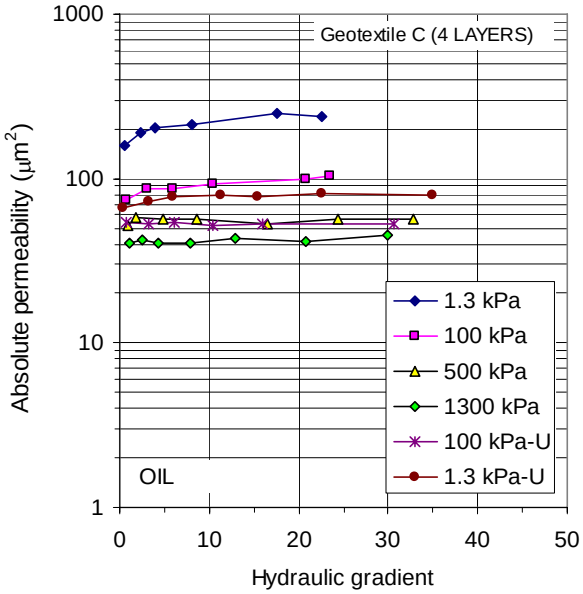

Figure 11. Permeability of Geotextile C to Heavy Oil

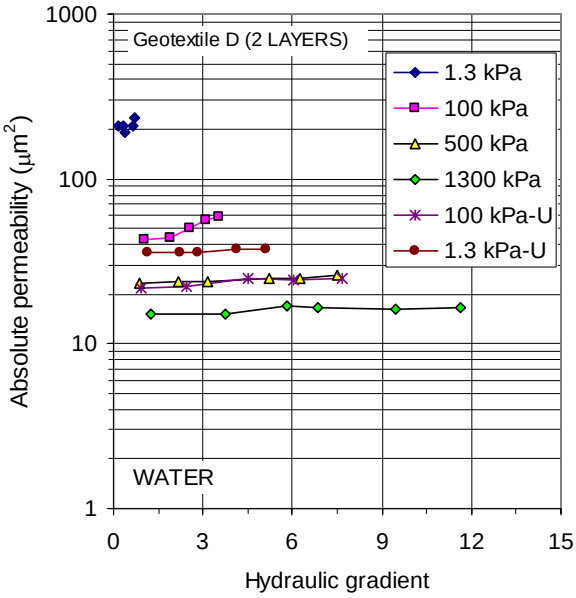

Figure 12. Permeability of Geotextile D to Water

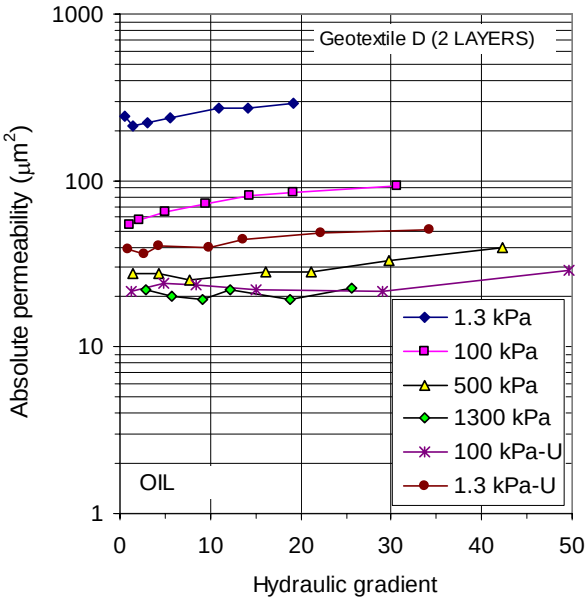

Figure 13. Permeability of Geotextile D to Heavy Oil

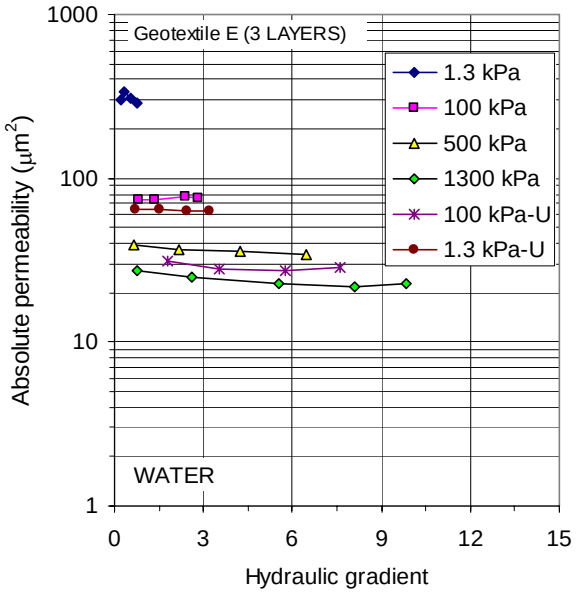

Figure 14. Permeability of Geotextile E to Water

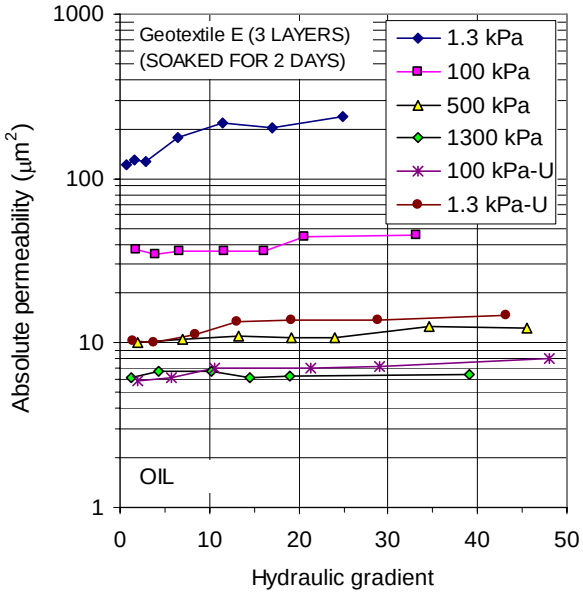

Figure 15. Permeability of Geotextile E to Heavy Oil with Fabric Soaked for 2 Days

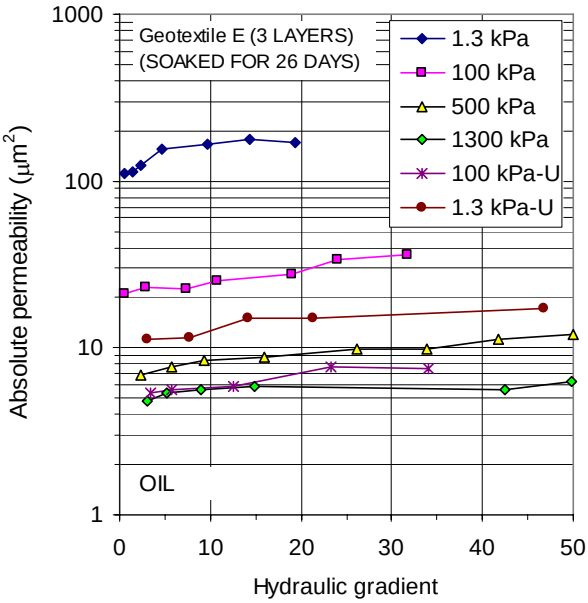

Figure 16. Permeability of Geotextile E to Heavy Oil with Fabric Soaked for 26 Days